Spring 2011

Interfacial effects on dielectric properties of polymer-particle nanocomposites

Sasidhar Siddabattuni

Department: Chemistry

INTERFACIAL EFFECTS ON DIELECTRIC PROPERTIES OF POLYMER-PARTICLE NANOCOMPOSITES

by

SASIDHAR VEERANJANEYULU SIDDABATTUNI

A DISSERTATION

Presented to the Faculty of the Graduate School of the

MISSOURI UNIVERSITY OF SCIENCE AND TECHNOLOGY

In Partial Fulfillment of the Requirements for the Degree

DOCTOR OF PHILOSOPHY

in

CHEMISTRY

2011

Approved
Thomas P. Schuman, Advisor
Fatih Dogan
Jeffrey G. Winiarz
Manashi Nath
K. Chandrashekhara

PUBLICATION DISSERTATION OPTION

This dissertation has been prepared in the form of five manuscripts for publication. Papers included are prepared according to the requirements of the journal to which it is being submitted. A general introduction is added from pages 1-41 for better understanding and as a background for the work done in this dissertation. The first paper, pages 42 through 63 was published in Composite Interfaces, Volume 17, Number 8, pp. 719-731 (2010). The second paper, pages 64 through 89, was submitted to Materials Science and Engineering B. The third paper, pages 90 through 120, was submitted to ACS Nano. The fourth paper, pages 121 through 146, will be submitted to ACS Nano. Finally, the fifth paper, pages 147 to 160, will be submitted to Chemistry of Materials, Rapid Communications.

ABSTRACT

Dielectric materials that are capable of efficiently storing large amounts of electrical energy are desirable for many electronic and power devices. Since the electrical energy density in a dielectric material is limited to $\varepsilon V_b^2/2$, where ε is the dielectric permittivity of the material and V_b is the breakdown strength, increased permittivity and breakdown strength are required for large energy storage density. Interfacial effects can influence the dielectric properties, especially dielectric breakdown resistance in polymer-particle nanocomposites. Several functional organophosphates were used to modify the surface of titania and barium titanate nanofiller particles in order to achieve covalent interface when interacted with polymer and to study the influence the electronic nature of filler surfaces on dielectric properties, in particular the breakdown resistance. Surface modified powders were analyzed by thermogravimetric analysis (TGA) and by X-ray photoelectron spectroscopy (XPS). The dielectric composite films obtained by incorporating surface modified powders in epoxy thermosetting polymer were analyzed by differential scanning calorimetry (DSC), scanning electron microscopy (SEM), impedance spectroscopy, and dielectric breakdown strength measurements. At 30 vol-% filler concentration, a calculated energy density of ~8 J/cm^3 was observed for titania based composites and ~8.3 J/cm^3 for barium titanate based composites involving electron scavenging interface with minimal dielectric losses compared to pure polymer. Covalent interface composites yielded energy density of ~7.5 J/cm^3 for barium titanate based composites at 30 vol.-%. The data indicate that improved dispersion, breakdown strengths and energy densities resulted when electron-poor functional groups were located at the particle surfaces even compared to covalent interface.

ACKNOWLEDGMENTS

I take this opportunity to express my deep sense of gratitude and reverence to my advisor, Dr. Thomas P. Schuman for his constant support, inspiring guidance and encouragement during the course of pursuing my PhD. I extend my gratitude to my committee members, Dr. Dogan, Dr. Winiarz, Dr. Nath and Dr. Chandrashekhara for their invaluable suggestions and support. Special thanks to Dr. Jasinski and Dr. Petrovsky for their time and guidance. The research material is based upon work supported by the National Science Foundation, as part of the Pennsylvania State University-Missouri S&T I/UCRC for Dielectric Studies under Grant No. 0628817, Sub-Award No. 2164-UM-NSF-0812.

I would like to thank Clarissa Wisner, Brian Porter, Eric Bohannan and late Jeff Wight of Materials Research Center at Missouri S&T for running the instruments for my research samples. I must admit the help and co-operation from my current and former lab members, Wang, Dr. Subramani, Olivia and Katie. I would also like to thank all my friends, Ayhan, Tony, Raju, Girish, Xuhui, Moon, Abhishek, Sukhada and everyone of those who have always supported me.

Sincere gratitude and respect to my family members for their love and support while pursuing my endeavors. Last, but not least, my humble salutations to my beloved Lord for being with me and guiding me all the times.

TABLE OF CONTENTS

LIST OF ILLUSTRATIONS

PAPER 5

LIST OF TABLES

SECTION

1. INTRODUCTION

Various mobile electronic devices, stationary power systems, hybrid electric vehicles and pulse power applications require electrical energy storage devices.[1,2] In particular, due to the growing requirements for compact, low-cost electronics and electrical power systems, there is a growing need for capacitors that can accumulate a large amount of energy and deliver it nearly instantaneously,[3] which is generally difficult to achieve with other energy storage technologies like batteries and ultracapacitors. Energy storage devices are characterized by both energy density and power density.

Energy density is the energy stored per unit mass or volume and power density is the power per unit mass or volume. Capacitors store their energy in the form of an electrostatic field rather than in a chemical form. High performance dielectric materials are of primary importance as they are utilized in capacitors which comprise the majority of passive elements in an electronic circuit.[4] Hence, development of high power, high energy density dielectric materials becomes a major enabling technology in the field of electrical energy storage devices.[3] Other general applications of capacitors include their usage in timing, A/D conversion, termination, power filtering, decoupling and dynamic random access memory devices.[5]

1.1. DIELECTRIC MATERIALS

A dielectric material is a nonconducting substance, i.e., an insulator. The term ‘dielectric’ is more often used when considering the effect of alternating electric fields on

the substance while the term ‘insulator’ is more often used when the material is to withstand high electric field.[6,7] Dielectric materials are used to control and store electrical charges and electrical energies and play a key role in modern electronics and electric power systems.[3]

A dielectric capacitor is readily formed by sandwiching a dielectric material between two metal plates as electrodes. An external electric potential is applied between the metal plates. Dielectric materials in capacitors store electrical energy in the form of electric field due to charge separation when the electron distributions around constituent atoms or molecules are polarized. Capacitors permit storing and extracting electrical energy over very short periods, which is often called a charge-discharge operation.[8] Under a given voltage (V), a capacitor can store electric charge (Q) shown as in Equation 1.1.a:

$$Q = CV \tag{1.1.a}$$

The capacitance (C) has units of Farad (F) is a proportionality constant which is a measure of charge per electric potential[9] or the storage capability a material can maintain. One of the simplest configurations of a capacitor is a pair of flat conducting plates with area *A*, separated by a distance *t*, called a “parallel plate capacitor.” In a parallel plate capacitor filled with a dielectric material, the capacitance is given by the Equation 1.1.b:

$$C = \varepsilon_0 \varepsilon_r \frac{A}{t} \tag{1.1.b}$$

where ε_o is the permittivity (or dielectric constant) of free space (8.854×10^{-12} F/m), and ε_r is the relative permittivity of the dielectric material between the electrodes, or dielectric constant. Permittivity is determined by the ability of a material to polarize in response to the electric field.

The energy stored in a capacitor is equal to the work done, W in charging the capacitor that can be released when a load is connected, as expressed in Equation 1.1.c:

$$W = \frac{1}{2} CV^2 \tag{1.1.c}$$

The maximum energy stored, W_{max}, thus depends on the maximum voltage that can be applied without arcing through the dielectric material in the capacitor, called the dielectric breakdown voltage (V_b), as shown in Equation 1.1.d:

$$W_{\max} = \frac{1}{2} CV_b^2 \tag{1.1.d}$$

The maximum energy density, (U_{max}), (energy stored per volume) can be derived from Equation 1.1.d as shown in Equation 1.1.e:

$$U_{\max} = \frac{W_{\max}}{volume} = \frac{\frac{1}{2}CV_b^2}{A\times t} = \frac{1}{2}\frac{\varepsilon_0\varepsilon_r (A/t)V_b^2}{A\times t} = \frac{1}{2}\varepsilon_0\varepsilon_r\left(\frac{V_b}{t}\right)^2 = \frac{1}{2}\varepsilon_0\varepsilon_r E_b^2 \tag{1.1.e}$$

where E_b is the dielectric breakdown strength/resistance. Dielectric breakdown strength of a dielectric material decreases with increase in specimen thickness, operating temperature, frequency and humidity.[7] From Equation 1.1.e, the maximum energy density that can be stored in a linear capacitor is proportional to permittivity of dielectric material and square of the breakdown strength of the dielectric material. For a linear dielectric material the permittivity is constant over entire electric field range. However, for a non-linear dielectric material the permittivity changes at high electric field.

1.1.1. Origin of Dielectric Polarizations. Metals possess free electrons and semiconductors possess free charge carriers (holes or electrons) to conduct electricity when an external electric field is applied. But since dielectric materials are essentially insulators, they do not possess any free electrons or free charge carriers to conduct electricity and therefore the charges associated with their atoms or molecules are only displaced when subjected to electric fields giving rise to polarization.[10, 11]

1.1.2. Types of Dielectric Polarizations. Charge storage capacity in a dielectric material is quantified by a parameter called 'polarization'. Polarization is frequency dependent phenomena and can be broken into several individual mechanisms. The dielectric polarizations are typically described by four major mechanisms: electronic, vibrational, orientation and space charge polarizations, as depicted in Figure 1.1.[12]

Electronic polarization occurs in a neutral atom when the electric field displaces the electron density relative to the nucleus it surrounds, inducing a dipole moment that vanishes as soon as the electric field is removed. Electronic polarization is independent of frequency and thus persists over the entire frequency range. Electronic polarization is common in all dielectric materials.[10, 13]

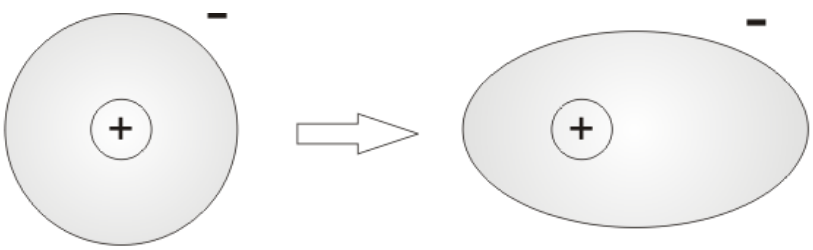

(a) Electronic polarization

(b) Vibrational (displacement) polarization

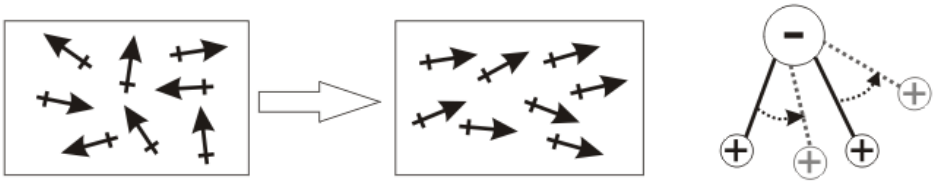

(c) Rotational (dipolar, orientational) polarization

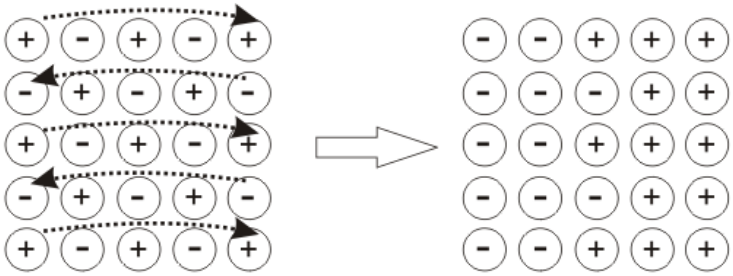

(d) Translational (interfacial, space charge) polarization

Figure 1.1 Mechanisms of dielectric polarizations[12]

Vibrational polarization, also called ionic or displacement polarization, usually occurs in ionic substances. When an electric field is applied to an ionic substance, positive and negative ions are displaced in the opposite directions until the ionic bonding forces stop the process, inducing a dipole moment. This type of polarization is predominant in inorganic crystals, glasses and ceramics and is the principle mechanism for permittivity of inorganic crystals that is observed to be uniform from D.C. through infrared frequencies.[10, 13, 14]

Orientational or rotational type of polarization usually occurs in polar dielectrics, which have permanent dipoles, such as polymeric substances and dipolar ceramics. Under normal conditions, dipoles that are present in polar dielectrics are randomly oriented with zero net dipole moment and polarization. When an external field is applied, the dipoles tend to reorient along the direction of applied field resulting a non-zero net dipole moment and polarization. Orientational polarization occurs from D.C. through microwave frequencies depending on the presence of dipolar bonds and resistance to molecular rotation.[10, 13, 14]

Translational polarization is usually associated with the presence of migrating charges, by electrons or ions, over macroscopic distances in an applied field. They tend to be trapped and accumulate at physical barriers such as defects, voids, impurities, grain or phase boundaries and also at the electrode interfaces where the material has different charge transport properties, e.g., conductivity. The accumulated charges distort the local electric field and gives rise to permittivity. Interfacial polarization is particularly important in heterogeneous or multiphase systems[10] such as polymer-ceramic nanocomposites. Interfacial polarization, involving a long range ion movement, is usually

observed only at lower frequencies, otherwise known as a space-charge or Maxwell-Wagner polarization.[13]

The total polarization of a dielectric material is the sum of the contributions of all polarization mechanisms based on the type of dielectric material. For example, a polar dielectric having ionic bonding and permanent dipoles possess orientational as well as ionic and electronic polarizations, an ionic and non-polar dielectric, e.g., alkali halides, which contain more than one type of bonds but no permanent dipoles, possess both ionic and electronic polarizations.[10]

1.2. TYPES OF DIELECTRIC MATERIALS

Dielectric materials based on their polarity, can be broadly classified into two categories, polar and non-polar, as shown in Figure 1.2. Non-polar dielectrics are made of non-polar bonds and/or molecules and do not possess any net dipole moment in normal conditions, i.e., when no electric field is applied. However, they can acquire temporary dipole moment when placed in electric field that vanishes when the electric field is removed.[10, 15, 16] Examples of such materials are benzene, carbon, N_2, O_2, CH_4, etc. Polar dielectrics, on the other hand, are made of polar atoms or molecules and possess permanent dipole moment with or without the absence of electric field also. But, in the absence of electric field, a polar dielectric has no net dipole moment due to the random orientation of all the polar molecules. Examples of such materials include HCl, NH_3, H_2O, etc.

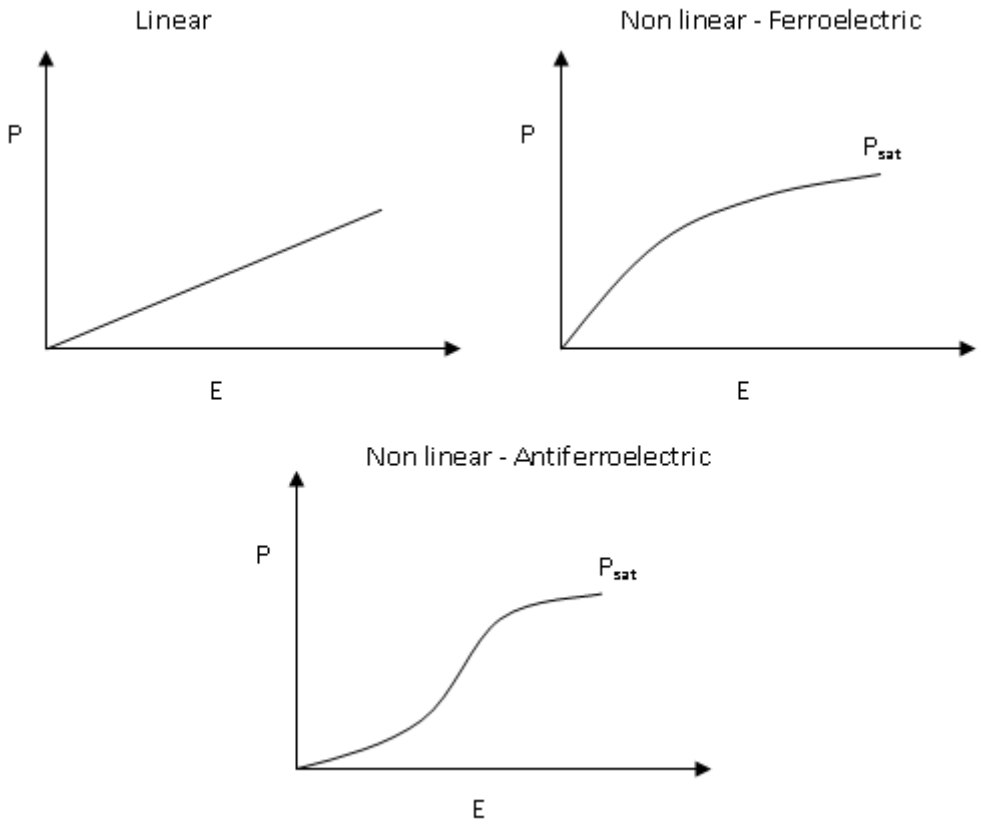

Figure 1.2. Polarization – electric field behaviors of linear and non-linear dielectrics

Dielectric materials can also be classified as linear or non-linear dielectrics based on their polarization-electric field behavior. In most dielectrics, the polarization, P is strictly proportional to the electric field, E, which are called linear dielectrics. In linear dielectrics, dielectric breakdown occurs before dielectric saturation can be observed[17] as shown in Figure 1.3. Materials like titania (TiO_2), aluminum oxide (Al_2O_3), diamond, polymers like polypropylene, polyester, polyimide, polycarbonate, epoxies, etc are some examples of linear dielectrics.

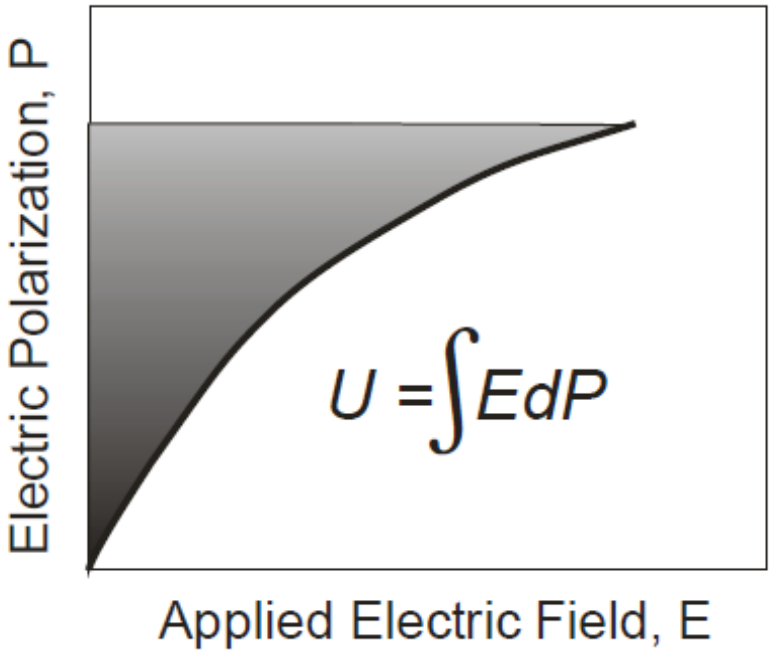

Figure 1.3. P-E curve of a typical ferroelectric material

In some materials, dielectric polarization can become so large that non-linear effects and dielectric saturation or polarization saturation become observable. Ferroelectric materials like barium titanate ($BaTiO_3$) and antiferroelectric materials like sodium niobate ($NaNbO_3$) are some examples of non-linear dielectrics. Though maximum energy density is calculated as shown in Equation 1.1.e, for non-linear dielectrics, energy density stored depends on dielectric saturation behavior of material and can be calculated from the area of P-E curve[3] (shaded area as shown in Figure 1.3), expressed as shown in Equation 1.2.a.

$$U_{measured} = \int EdP \tag{1.2.a}$$

1.2.1. Ceramic Dielectrics. Ceramic materials, which are inorganic in nature, are widely used dielectric materials for capacitor applications. In certain type of ceramic dielectrics, there is a finite net polarization even when the electric field is removed, e.g., ferroelectric materials or ferroelectrics. Some special features of ferroelectrics are non-linear P versus E curves which gives rise to ferroelectric hysteresis, spontaneous polarization and reversibility of polarization.[10] Because of the ability to maintain high concentrations of electrical charge due to high polarization, ferroelectrics show high values of dielectric constant and are very good candidates for many capacitor applications. Barium titanate is a well-known ferroelectric material extensively used in capacitor production, because of both its inherent dielectric response and the ability to tailor this response through the addition of various additives, many of which form a solid solution within the barium titanate crystal lattice.[18]

1.2.2. Polymer Dielectrics. Polymeric materials dielectrics, which are organic in nature, are extensively used especially as electrical insulators for their low cost, ease of manufacture, light weight, availability and good electrical insulating properties.[19] Polyethylene, polypropylene, epoxies, silicones, polyimides etc. are some examples of polymeric dielectrics. Most polymers have low dielectric constant, in the range of 2 – 5. Polypropylene and epoxies are two most widely used polymeric dielectrics in the electronics industry.[20-22] Compared with conventional polymeric dielectrics, there are several ferroelectric polymers which can have dielectric constants, above 10, because of their polar backbone.[23] For example, pure polyvinylidene fluoride (PVDF) polymer has a dielectric constant of around 11 at 1kHz and 25 °C.[24,25] Poly(vinylidene fluoride-trifluoroethylene) (P(VDF-TrFE) copolymer can have a relatively high dielectric constant

of about 40 at room temperature after irradiation treatment.[26] Polyvinylidene fluoride-trifluoroethylene-chlorotrifluoroethylene (P(VDF-TrFE-CTrFE) terpolymer can have dielectric constant of about 60 at 1kHz and 33 °C.[27, 28] However, their large dielectric loss (>10% above 100 kHz) limits their use, especially in high frequency applications (>100 kHz) that require fast charge/discharge cycles.

1.3. DIELECTRIC MATERIALS IN ALTERNATING FIELDS

The permittivity of a dielectric material is constant in D.C. fields when there is not significant dielectric saturation and decreases with increasing DC fields when there is dielectric saturation present.[29] Under A.C. fields, permittivity of a dielectric material can strongly depend on the frequency of the applied field, where permittivity increases with increasing strong A.C. fields and can be expressed as a complex number with a real part and imaginary part[10, 30] as shown in equation 1.3.a:

$$\varepsilon^* = \varepsilon' - j\varepsilon'' = \varepsilon_0\varepsilon_r - j\varepsilon'' \qquad \textbf{(}1.3.a\textbf{)}$$

where ε' and ε'' are the real and imaginary parts of the complex permittivity, ε^* and $j = \sqrt{-1}$. The magnitudes of ε' and ε'' depend on the frequency of the applied electric field as illustrated in Figure 1.4.[31] The real part of the permittivity, i.e., the dielectric constant mentioned in Equation 1.1.b, indicates the ability of the material to store energy from applied electric field. The imaginary part of the permittivity is called dielectric loss. For an energy storage device like a capacitor, dielectric loss has to be obviously as low as possible.[32]

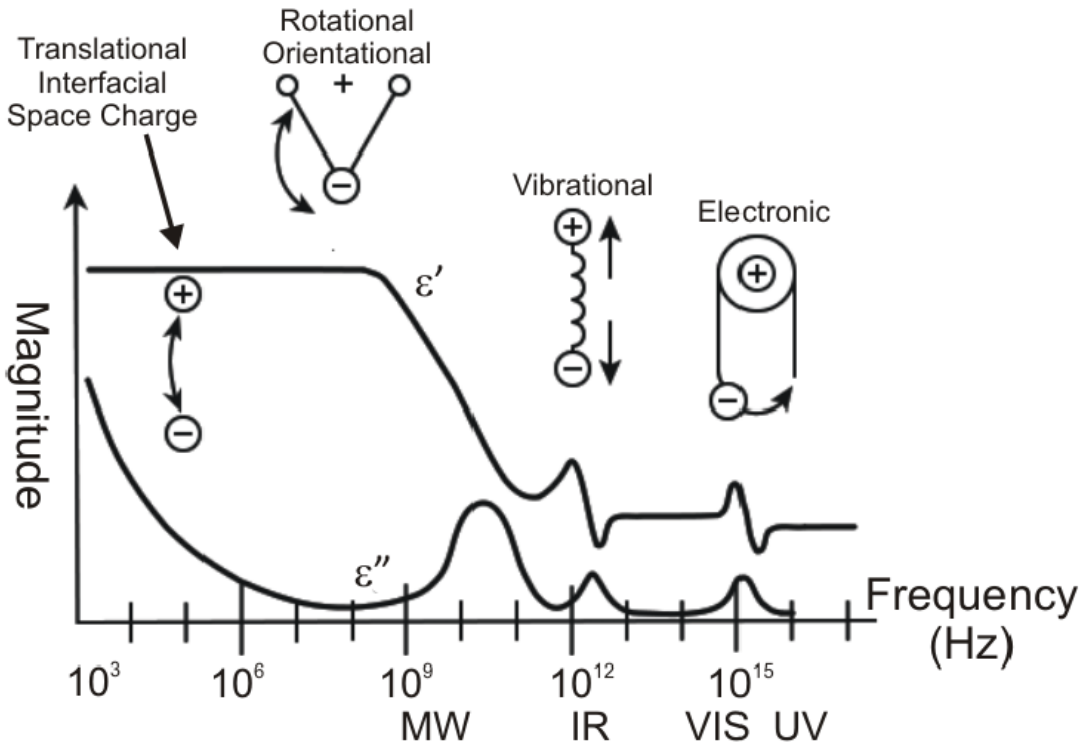

Figure 1.4. Frequency dependency of real and imaginary parts of complex permittivity[31]

The ratio of imaginary part to the real part of the permittivity is defined as dissipation factor (DF) as shown in Equation 1.3.b, which is also known as a loss tangent as it is related to the dielectric loss.[30]

$$\text{Dissipation factor (DF)} = \tan\delta = \frac{\varepsilon''}{\varepsilon'} \qquad (1.3.b)$$

In general, dielectric loss results from the sum of distortional, dipolar, interfacial and conduction losses. The distortional loss is related to electronic and ionic polarization mechanisms. The interfacial loss originates from an excessive polarized interface induced

by, e.g., the fillers in the composites and specifically the movement of ions or rotation of the atoms or molecules in the alternating fields. Conduction loss is attributed to the D.C. electrical resistive conductivity of the materials, representing the flow of charge through the dielectric materials.[33, 34] In general, dielectric loss increases with increase in temperature, humidity, voltage and frequency of the applied voltage.[10]

1.4. POLYMER/CERAMIC NANOCOMPOSITES

From Figure 1.5, the current state-of-the-art for pulsed power capacitor materials has energy storage densities of approximately 1 – 3 $J.cm^{-3}$ and state-of-the-art power electronic capacitors have energy storage densities one order of magnitude lower than pulsed power capacitors, which utilize either ceramic or polymer dielectric materials.[35-37] Future pulsed-power and power electronic capacitors will require dielectric materials with ultimate energy storage densities of >30 $J.cm^{-3}$, operating voltages of >10 kV and millisecond-microsecond charge/discharge times with reliable operation near the dielectric breakdown limit.[36] The Department of Defense (DoD) goal for a packaged capacitor is 10 $J \cdot cm^{-3}$ considering the loss in energy density that occurs when the dielectric is incorporated in a packaged component. The goal for dielectric materials is to be able to store approximately 30 $J \cdot cm^{-3}$ at an applied field of around 4 $MV.cm^{-1}$.[3, 8, 35] Table 1.1 shows a recent literature compilation of energy densities from various research groups in the area of polymer-ceramic nanocomposites.[32]

Inorganic (I) ceramic materials usually have large permittivity, but they are limited by relatively small breakdown strengths, poor procecessability and mechanical properties due to high sintering temperature and porosity. On the other hand, polymers,

which are organic (O) usually have higher breakdown strength, excellent mechanical properties and processability but suffer from smaller permittivity.[38-40]

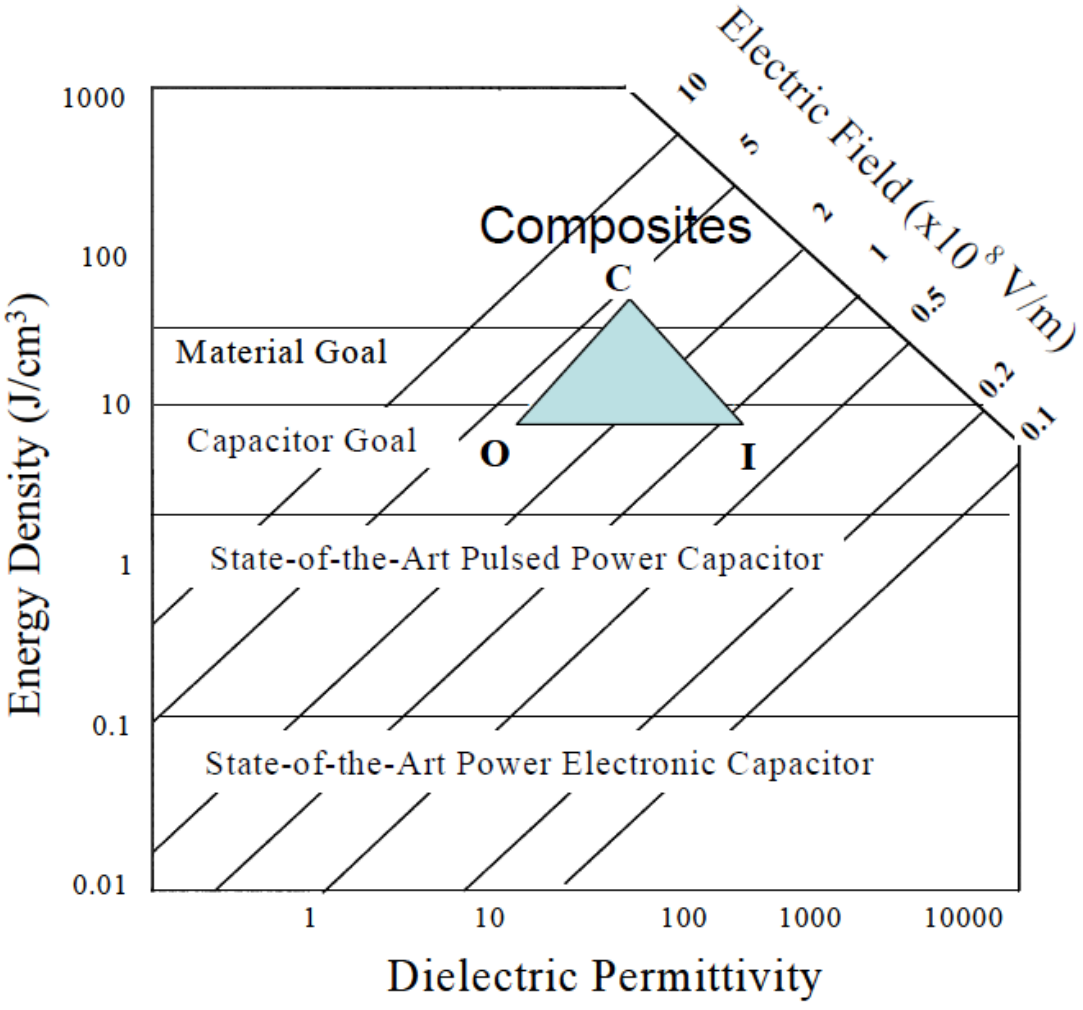

Figure 1.5. Comparison of dielectric materials performance with targeted goals for future applications.[35]

Table 1.1. Compilation of energy densities from literature of polymer-ceramic composites[32]

Comparable Dielectric Systems Found in Literature	**ε_r**	**DBS (V/μm)**	**Energy Density ($J \cdot cm^{-3}$)**
PVDF-HFP + 50vol% Phosphonic acid modified BT (loss ~3%)	35	215	~ 7
PvDF-HxFP+50vol% Phosphonic acid modified BT	37	210	6.10
Ether Bisphenol Epoxy Resin	10	332	4.88
Polycarbonate+50vol% phosphonic acid modified BT	20	210	3.90
Polyimide+60 vol% BT	30	168	3.75
Polystyrene+60 vol% nanoBT	45	120	2.87
PvDF-TrFE-CTFE+20 wt% BT	48	115	2.80
Polyimide + 40vol% BT	20	168	2.50

Miniaturization and the current need for high-power density, high voltage capacitors and power-storage devices has stimulated a new field of research interest in polymer nanocomposites as composite dielectrics (C).[41-46] By incorporating high permittivity inorganic nanoparticles into a polymer matrix with low dielectric loss and high breakdown strength, one may be able to develop new composite materials that have improved dielectric properties, dielectric strength, permittivity and dielectric losses, and retain unique attributes of polymers.

The most distinctive feature of polymer nanocomposites in comparison with conventional microcomposites is the participation of interfacial surface area between the nanoparticles and the polymer matrix. The smaller the size of the embedded

nanoparticles, the larger the surface area to volume ratio, which leads to larger interfacial regions.[47, 48] For filler nanoparticles with modest loadings, the surface area associated with the internal interfaces becomes dominant in nanocomposites compared to microcomposites.[49] The properties of these interface areas may differ substantially from those of both the base polymer matrix and the nanoparticle material.[49, 50] From literature, polymer nanocomposites with metal oxide nanoparticle fillers exhibited enhanced electrical breakdown strength and voltage endurance compared to their unfilled or micrometer sized particle filled counterparts.[49, 50] In addition, convincing theoretical arguments have been made suggesting that large inclusion-matrix interfacial areas should afford greater polarization levels, dielectric response, and breakdown strength.[36, 51-53]

1.4.1. Role of Interface. Incorporation of nanoparticles into polymer matrix for developing nanocomposites, which has produced interesting results in last few years, has led researchers to investigate mechanisms for the improved dielectric properties. Researchers have emphasized the critical role of the interfacial region and present hypotheses for multiscale phenomena operating in polymer nanocomposites dielectrics.[49,50] Figure 1.6 shows the physical description of the interfacial region in polymer nanocomposites.[49] In thermoplastics, the interfacial polymer can exhibit changes in crystallinity, group mobility, chain conformation, molecular weight, and chain entanglement density. There is an additional complication of changes in cross link density, in thermosets, due to small molecule migration to or from the interface.

The interfacial region has a direct impact on the dielectric properties of the composites. Therefore it is important to study the interfacial region. A multi-core model was proposed,[49, 50, 54] which tries to capture the charge behavior and structure of the

interfacial region. The metal oxide nanoparticle has a surface charge, which creates a Stern layer at the 2D interface, which is screened by a charged layer in the polymer. The next layer is a diffuse double layer of charge with around 10nm of radial depth in a resistive medium (polymer). Since the diffusion double layer is a region of mobile charge, both the dispersion of nanoparticles and the resulting dielectric properties in the polymer nanocomposites have significant influence.

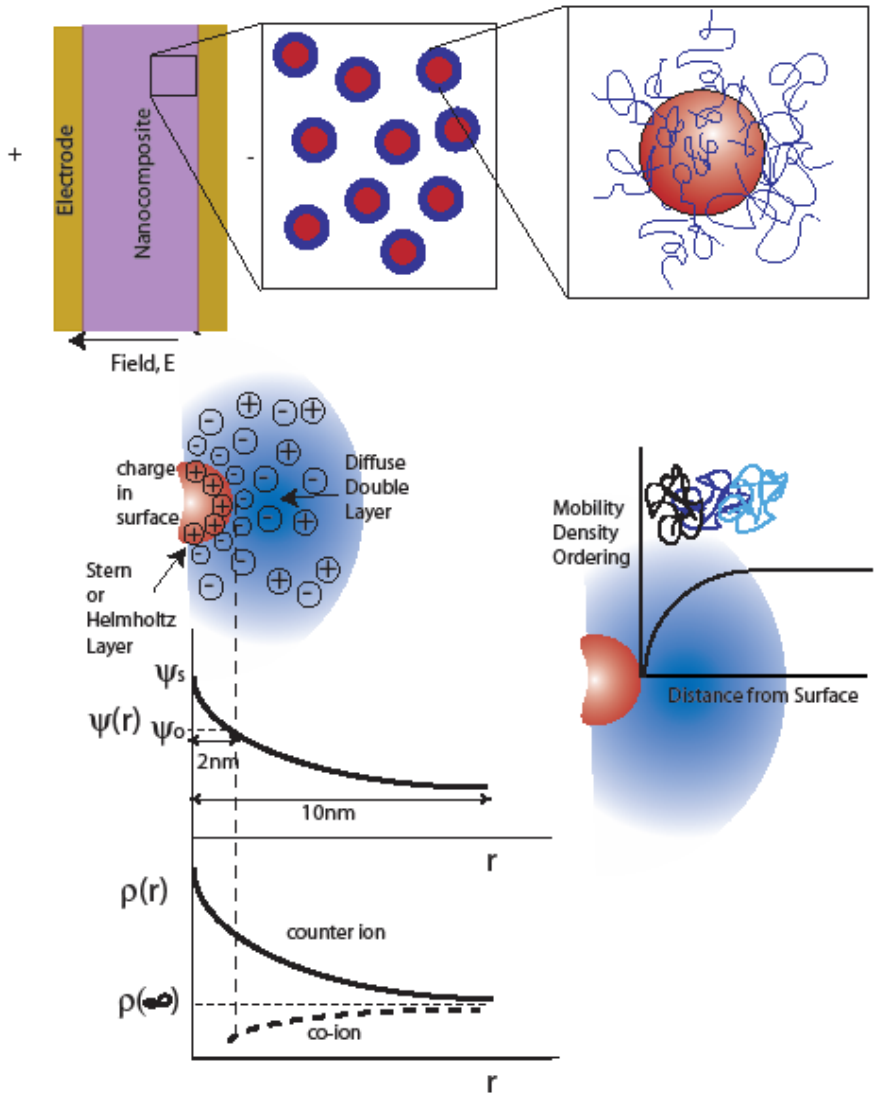

Figure 1.6. Physical depiction of the interface region in polymer nanocomposites[50]

Based on the interfacial structure, hypotheses to explain the impact of interfacial region on the dielectric properties are summarized as following:[49]

- There is a change in polymer structure (free volume, mobility, etc.) and local charge distribution because of the nanoparticle surface.
- The interfacial region becomes more dominant, as the size of the filler is reduced. The density and perhaps the depth of trap sites are altered due to the change in local structure which affects the carrier mobility and energy.
- The carriers are accelerated over shorter distances and have reduced energy if they are trapped more often and same is the case for carriers that are scattered. As a result, the dielectric life time of the polymer is increased.
- The voltage required for charge injection is increased as the homocharge resulting from carrier trapping mitigates the electric field at the electrodes. Thus the voltage required for the short term breakdown is also increased. The breakdown strength becomes the function of the rate of measurement (A.C., D.C., or impulse) as the charge takes time to build up.
- As the nanocomposites have larger interfacial area, it increases the probability for scattering. Scattering may become the primary mechanism for the increase in the breakdown strength of nanocomposites during impulse test conditions, since significant shielding homocharge cannot be accumulated in such a short time.

Because interfacial area is so large, while some of the above mechanisms may operate in micron sized filler filled polymer composites, they are then overshadowed by the large defects the micron scale fillers introduce and the field enhancements they create.

Microcomposites exhibit Maxwell-Wagner interfacial polarization, which is generally finite in nanocomposites and depends on filler concentration and filler material.[49, 50] Electroluminescence, photoluminescence, thermally stimulated currents, X-ray secondary emission spectroscopy and electron paramagnetic resonance provided experimental evidence to suggest the working of the hypothesis.[49, 55]

1.4.2. Surface Modification of Nanoparticles. As the properties of polymer nanocomposites are often influenced by the interfacial region, control of interface becomes very important. Failure to control the interface results in aggregation or agglomeration of nanoparticles in polymer matrix, which leads undesirable properties due to poor film quality and inhomogeneities.[43, 56] Thus, proper dispersion of nanoparticles in polymer nanocomposites plays an important role in polymer nanocomposites. Without proper dispersion and distribution of filler particles in polymer, the high surface area of nano-sized particles is compromised and the aggregates can act as defects, which limits properties.[57]

The most common method to achieve proper dispersion is to modify the surface of nanoparticles. The first aspect of modifying the surface of nanoparticles is to attain stabilization of particles against agglomeration to accomplish homogeneous nanocomposites. The second aspect is to render the guest material (nanoparticle filler) compatible with host material (polymer). The third interest in nanoparticles modification is to enable their self-organization.[58]

Surface modification of nanoparticles can be obtained by using suitable surfactants that yield an adsorptive interface or by grafting organic groups on the surface of metal oxide nanoparticles, e.g., using phosphates, phosphonates or silanes as coupling agents or dispersants which yields stable and complex organic oxide interface.[59, 60]

1.5. ROLE OF VOLUME FRACTION

Previous studies have shown that as the volume fraction of the high permittivity component, nano particle fillers, is increased, the effective permittivity of the nanocomposites also increases.[61-63] However, increasing the volume fraction of the nanoparticles typically decreases the apparent dielectric breakdown strength of the nanocomposite due to the enhancement of the local electric field in the host material[56, 64] and nanocomposites with large volume fractions of nanoparticles typically exhibit porosity that is detrimental to their dielectric performance. Therefore, the role of volume fraction of high permittivity nanoparticles on the dielectric properties (permittivity, loss and breakdown strength) is important and should be rationally chosen in order to maximize the stored electrical energy density.

Many mixing models like parallel model, series model, Lichteneckers rule exist which are able to predict electrical properties based on the dc conductivity/resistivity and work best for dilute composites at low volume fractions.[65] Another popular method of predicting the properties of composites is percolation theory, which is based on the assumption that the properties will change when the second phase is totally connected, i.e., percolated, from one side of the composite to the other.[66] The volume fraction at which percolation occurs is called the ‘percolation threshold.’ Percolation threshold depends on many factors, including the connectivity of the phases, the size of each phase,

the shape of each phase and the wetting behavior of the phases. Percolation models allow for a large, orders of magnitude, change of properties over a very small concentration range.[67]

As a mixing system, composites filled with inorganic fillers are ideal objects from the point of view of percolation theory. When the concentration of fillers is low, the composites will behave more like the insulating matrix. Once the volume fraction of fillers nears the percolation threshold, for example, 16% or 19% considering impurities, the electrical properties of the composites can be obviously changed by the channels formed in which charge carriers connect inorganic fillers.[68] The percolation threshold for a 2-dimentional system is accurately predicted as 50% by effective medium theory and the predicted percolation threshold for 3-dimentional system is at 33% by effective medium theory.[68, 69]

1.6. DIELECTRIC BREAKDOWN

The dielectric material will suddenly begin to conduct current if the voltage across it becomes too high. This phenomenon is called ‘dielectric breakdown’[70] and the maximum voltage that can be applied without breaking is called ‘dielectric breakdown strength’. In solid dielectrics, electrical breakdown usually results in permanent damage.

1.6.1. Dielectric Breakdown Mechanisms. The breakdown in a dielectric material is controlled by several mechanisms shown in Figure 1.7.[71, 72] Under a variety of field stresses, the breakdown suffered by dielectric materials presents a very strong time dependent relationship and can be divided into five or more kinds by breakdown speed. Electrical, thermal and electromechanical breakdown mechanisms are known as the

short-term breakdown mechanisms and the others are long term breakdown or degradation mechanisms.[73]

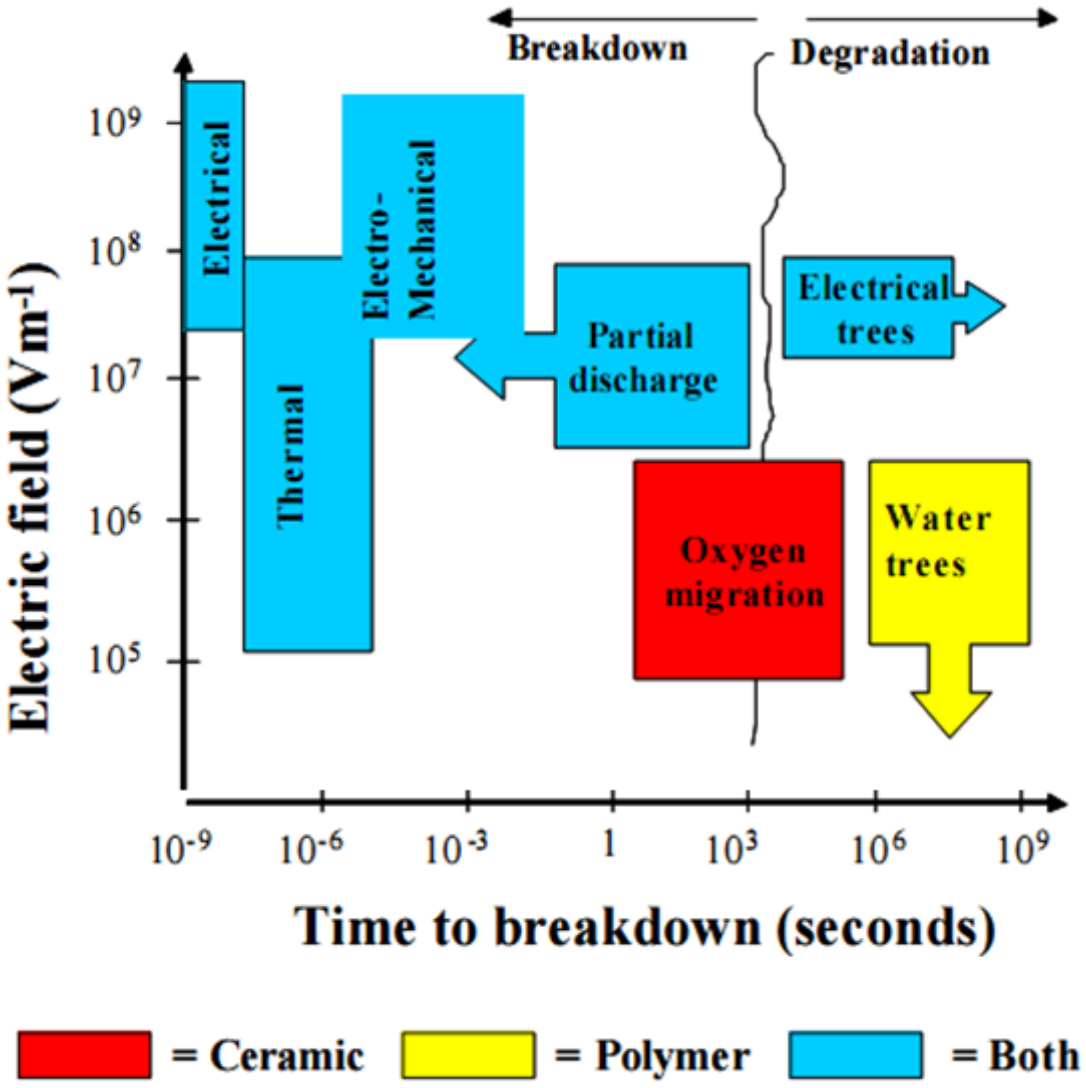

Figure 1.7. Schematic depicting times and electric fields at which various electrical breakdown mechanisms are operative[72]

Electrical breakdown in polymers and composite dielectrics is limited by high field carrier injection and charge trapping electrode-dielectric interface.[72] Thermal breakdown, expected to occur at lower fields than electrical breakdown, is dependent on the ratio of electrical to thermal conductivity of dielectrics and is also limited by charge transportation mechanisms at high temperatures.[74] Electromechanical breakdown is controlled by mechanical properties of dielectric material under high electrical stress and structural parameters.[75] Generally large changes in dielectric breakdown strength at temperatures approaching glass transition temperature are attributed to be related to electromechanical breakdown mechanism. Where gas is present inside any voids in the dielectric material, gas gets ionized leading to breakdown or discharge within the void under high electric fields leading to the phenomenon known as partial discharge breakdown. The discharge damages the structure of the materials and voids or cracks becomes larger, which can be considered as degradation, which erodes the dielectric resulting in breakdown.[72] Discharge may also take place in surface of the dielectric if the surface is contaminated by dirt, water or any other impurities.

Various factors influence the dielectric breakdown event, which include temperature; defects and inhomogenity of material; thickness, area and volume of the material; duration of time for which the dielectric is subjected to electric field; surface conditions and the method of placing the electrodes; area of the electrodes; composition of the electrodes; moisture (humidity) and other contaminations; aging and mechanical stress.[10]

1.6.2. Analysis of Dielectric Breakdown Strength Measurements. The dielectric breakdown strength data of polymer nanocomposite films were obtained by using high voltage generator and point contact method. The maximum voltage which the film withstands before the failure took place was recorded as the dielectric breakdown voltage.

The breakdown data obtained were analyzed using a Weibull probability failure analysis method which has been frequently adopted for the investigation of dielectric breakdown strength of different materials system in this field.[76-82] Weibull analysis is based on an empirical failure probability (P_f), which is typically described using three parameters:

$$P_F(E) = 1 - \exp[-\{(E-\gamma)/\alpha\}^{\beta}] \qquad (1.6.a)$$

where α is a scale parameter, β is a shape parameter that shows the dispersion of values of E, and γ is a threshold parameter below which value of E no failure occurs. For the analysis of breakdown results of nanocomposites, γ was set to zero. The failure probability can now be expressed as:

$$\log[-\ln\{1-P_F(E)\}] = \beta \log E - \beta \log \alpha \qquad (1.6.b)$$

The above probability is equated to with a median ranked positioning which is expressed as:

$$P_F(i,n) = (i - 0.5)/(n + 0.25) \quad (1.6.c)$$

where i is the index (1, 2, 3, … n) and n is the sample size. The measured n breakdown values (E) are reordered in ascending order and then the probability failure for each E is given from the positioning equation. A linear fitting of log{-ln(1-P)} versus log E gives the parameters α and β. The breakdown field for the data set is found to be $E_b = \alpha$ when the probability failure is 63.2% i.e., 1-1/e.

1.7. DIELECTRIC SPECTROSCOPY

Dielectric constant and dielectric loss data can be obtained by dielectric spectroscopy. Dielectric spectroscopy can provide useful information on the dielectric properties of the specimen using the parameters, e.g., capacitance, dissipation factor, etc., which it can measure. Prior to the measurement, polymer nanocomposite films which were applied on copper sheets are electroded using silver paint to create a thin conductive sheet so as to produce a sample as a parallel plate capacitor.

Dielectric spectroscopy depends on the polarization that is induced in the dielectric material due to the effect of an external electrical stress. Various polarization mechanisms were discussed earlier in Section 1.1. Each polarization mechanism, either a relaxation or resonance process, is centered around its particular characteristic frequency, which is the reciprocal of the characteristic time of the process and therefore separable in frequency.[83]

The interaction of electric field with matter is of fundamental importance in basic and applied science. Many aspects of dielectric response, especially in the non-linear

processes, are more easily understood in terms of the response to time dependent signals. However, there exists a very powerful alternative approach which offers a very considerable theoretical and practical advantage, provided that a linear system is studied, which is the determination of the response to harmonic excitation, i.e., sinusoidal waves.[84, 85]

The mathematical basis for the treatment of the frequency (ω) domain response rests on the fourier transformation of a given function of time G(t), defined by the Fourier transform:[84]

$$F[G(t)] = \psi(\omega) = (2\pi)^{-\frac{1}{2}} \int_{-\infty}^{\infty} G(t) \exp(-i\omega t) dt \qquad (1.7.a)$$

The Fourier transform gives the frequency spectrum ψ(ω) of the time-dependent function G(t) - the amplitudes, phases and frequencies of the sinusoidal waves which make up the given time signal. The inclusion of *i* in the above expression means that any transformed term will be complex, i.e., possess both real component and imaginary component, which therefore indicates that any resulting expressions will take into account the phase behavior of the response of the specimen[86] as well as the ratio of the amplitudes.

1.8. INSTRUMENTATION AND CHARACTERIZATION

1.8.1. Thermogravimetric Analysis. A thermal analysis instrument, Netzsch STA 409, with a single sample in controlled environment (compressed air) was used for TGA measurements. Change in weight of the sample was measured from ambient to 800 °C at 10 °C/min ramp rate. Thermogravimetric analysis (TGA) can be used to characterize any material that exhibits a weight change decomposition, oxidation and dehydration. In this research, TGA was used to investigate the weight loss of the surface modified filler particle surfaces in comparison to unmodified filler particle surfaces. Weight loss data obtained was then used with surface area per weight of the unmodified particles to calculate the number of groups per square area.

1.8.2. X-ray Photoelectron Spectroscopy. X-ray Photoelectron Spectroscopy (XPS) is a sensitive non-destructive analysis technique employed to investigate the elemental composition and surface chemistry characteristics on filler particles surfaces. XPS analysis was performed on KRATOS AXIS 165 XPS spectrometer. Magnesium X-ray source was used to excite the sample surface. The resultant photoelectrons that are detected provide a fingerprint of the elements contained on the surface and also provide chemical binding information based on the energy of the peaks. XPS scans were performed on powder samples of 1 cm^2 mounted onto copper stubs with double-sided conductive adhesive tape and introduced into the XPS chamber via a turbo-pumped antechamber.

1.8.3. Differential Scanning Calorimetry. The differential scanning calorimetry (DSC) was used to glass transition temperatures of pure polymer and polymer nanocomposites, at 5 vol.-% as glass transition process involve heat-related events. A TA instruments DSC was used to obtain glass transition temperatures. In DSC studies, a sample of ~10mg was placed in a hermetic DSC sample pan. During initial cycle, the sample and reference were heated from ambient to 100 °C at a rate of 10 °C/min before quenching to ambient using liquid nitrogen. After preliminary thermal annealing cycle, sample and reference were heated from ambient to 150 °C at a rate of 10 °C/min. Nitrogen purging was applied during all DSC measurements. Glass transition temperatures were reported using inflection point of the transition.

1.8.4. Scanning Electron Microscopy. The dispersion quality of nano particles in epoxy polymer matrix was investigated using scanning electron microscopy (SEM). The Hitachi S-4700 Field Emission SEM, equipped with a single crystal tungsten electron gun was used to obtain images. Sample films were freeze fractured in liquid nitrogen and small piece of freeze fractured films were mounted on Aluminum sample mount, 0 - 90˚ using carbon tape in such a way to see the cross-section of samples for observing dispersion quality in the nanocomposites. The samples were Au-Pd sputter coated for 90secs as the samples are non-conductive dielectrics. Cu tape was used for electrical grounding. Accelerating voltage of 5 kV, 4-5mm working distance and high resolution mode were employed for taking images at high magnifications using secondary electron detector.

1.8.5. Dielectric Breakdown Measurement. Dielectric breakdown strength measurements were made by applying D.C. voltage across the polymer and polymer nanocomposite films using a Spellman SL 30 high voltage generator with a fixed ramp rate of 200 $V \cdot sec^{-1}$ until the point of film failure. A pin electrode was applied by light spring tension to the surface of the composite, which served as the electrical ground. The Spellman electrode was connected beneath the copper substrate and the sample immersed in Fluorinert FC-40 to displace air as the breakdown strength is sensitive to moisture and oxygen near the test device and thus must be minimized to truly test the materials property. The voltage when the failure took place was recorded as the breakdown voltage.

1.8.6. Electrical Impedance Measurement. The frequency dependent capacitance and loss tangent of a capacitor were measured using Solartron 1260 impedance analyzer connected to a Solartron 1296 dielectric interface at frequency range of 1 Hz to 1 MHz at ambient temperature and from 0.01 Hz to 1 MHz at 100 °C (for temperature dependent dielectric response) with voltage amplitude of 1 V operated in an equivalent parallel circuit. The measurements were based on measuring the current (amplitude and phase) in the material with respect to an ac electric field, which is a periodic function in the form of sinusoid. The data collected was analyzed using Zview® software. Parallel-plate capacitors were fabricated by depositing circular (31.67 mm^2) silver top electrodes onto the nanocomposite films.

1.9. OBJECTIVES OF THE RESEARCH

The dielectric properties of nanocomposites have been found to be better in comparison to microcomposites and neat polymers. Various proposed models with some experimental evidence have attributed this property enhancement to the interfacial effects related to filler-polymer interactions in nanocomposites. In this regard, this thesis has focused on finding the ways to enhance the energy storage capacity of polymer nanocomposites by concentrating on interfacial interactions between polymer and filler particle surfaces within an applied field. The main objectives of this research are:

- To modify the surface of nano-sized particles ceramic particles with bifunctional organophosphate coupling agents so as to achieve a covalent interface when used within an epoxy polymer matrix composites.
- To study the influence of covalent interface on electrical properties, especially dielectric breakdown strength of polymer nanocomposite dielectrics compared to physically adsorbed interface based nanodielectrics and neat polymer.
- To study the influence of electronic nature of surface functionalized filler particles on dielectric properties of their composites in epoxy. The electron donating and electron accepting functional groups were used as surface modifying reagents, attached via an organophosphate ligand on to the surface of filler particles.
- To enhance the energy density of polymer nanocomposites by compromising the decrease in dielectric breakdown strength with increase in permittivity at higher filler particle volume concentration.

REFERENCES

[1] H. Nalwa, *Handbook of Low and High Dielectric Constant Materials and Their Applications*, Academic press: London, UK (1999).

[2] T. Osaka and M. Datta, *Electrical Storage Systems for Electronics*, Gordan and Breach: Amsterdam, The Netherlands (2001).

[3] B. Chu, X. Zhou, K. Ren, B. Neese, M. Lin, Q. Wang, F. Bauer and Q. M. Zhang, "A Dielectric Polymer with High Electric Energy Density and Fast Discharge Speed," *Science*, Vol. 313, No. 5785, Pp. 334-336 (2006).

[4] K. W. Paik, S. D. Cho, J. G. Hyun, S. Lee, H. Kim and J. Kim, "Epoxy/$BaTiO_3$ ($SrTiO_3$) Composite Films for High Dielectric Constant and Low Tolerance Embedded Capacitors Fabrication in Organic Substrates," *IEEE International Symposium on Advanced Packaging Materials*, Pp. 227-232 (2005).

[5] R. R. Tummala, E. J. Rymaszewski and A. G. Klopfenstein, (Eds) *Microelectronics Packaging Handbook*, Part 1-3, Chapman and Hall: New York (1997).

[6] Dominick V. Rosato, N. R. Schott, Donald V. Rosato and M. G. Rosato, *Plastics Engineering Manufacturing and Data Handbook*, Vol. 2, Kluwer Academic Publishers: Boston (2001).

[7] N. Kumar, *Electrical Engineering Materials*, Tata McGraw-Hill: New Delhi (2007).

[8] W. J. Sarjeant, R. E. Dollinger, J. Zirnheld, F. W. MacDougall and H. Goldberg, "Capacitors – Past, Present and Future: A Trans-national Perspective," *IEEE 22nd International Power Modulators Symposium*, Pp. 209-212 (1996).

[9] M. Mansfield and C. O'Sullivan, *Understanding Physics*, 2nd Ed., John Wiley & Sons: West Sussex, UK (2011).

[10] P. Maheshwari, *Electronic Components & Processes*, New Age International Publishers: New Delhi, India (2007).

[11] A. A. Zaky and R. Hawley, *Dielectric Solids*, Dover Publications Inc.: New York (1970).

[12] D. W. Hess and K. W. Jensen, *Microelectronics Processing: Chemical Engineering Aspects*, ACS Publication: Washington DC (1989).

[13] T. W. Dakin, "Conduction and Polarization Mechanisms and Trends in Dielectrics," *IEEE Electrical Insulation Magazine*, Vol. 22, No. 5, Pp. 11-20 (2006).

[14] R. Arora and W. Mosch, *High Voltage Insulation Engineering: Behaviour of Dielectrics – Their Properties & Applications*, 1st Ed., New Age International Publishers: New Delhi, India (1995).

[15] A. Kumar, *Introduction to Solid State Physics*, Prentice-Hall of India: New Delhi, India (2010).

[16] H. C. Sharma, R. Kharb and R. Sharma, *Comprehensive Physics for Engineers*, 4th Ed., Laxmi Publications: New Delhi, India (2005).

[17] F. Seitz and D. Turnbull, *Solid State Physics*, Vol. 4, Academic Press: New York (1957).

[18] B. Jaffe, W. R. Cook, Jr. and H. Jaffe, *Piezoelectric Ceramics*, Academic Press: London & NY (1971).

[19] R. Bartnikas, (Ed) *Engineering Dielectrics*, Vol. 2-B, American Society for Testing & Materials (1987).

[20] Y. Rao and C. P. Wong, "Material Characterization of a High-Dielectric-Constant Polymer-Ceramic Composite for Embedded Capacitor for RF Applications," *Journal of Applied Polymer Science*, Vol. 92, Pp. 2228-2231 (2004).

[21] C. W. Reed and S. W. Chichanowski, "The Fundamentals of Ageing in HV Polymer-Film Capacitors," *IEEE Transactions on Dielectrics and Electrical Insulation*, Vol. 1, Pp. 904 (1994).

[22] M. Rabuffi and G. Picci, " Status Quo and Future Prospects for Metallized Polypropylene Energy Storage Capacitors," *IEEE Transactions on Plasma Science*, Vol. 30, Pp. 1939 (2002).

[23] H. S. Nalwa, *Ferroelectric Polymers*, Marcel Dekker: New York (1995).

[24] S. Yano, "Dielectric Relaxation and Molecular Motion in Poly(vinylidene fluoride)," *Journal of Polymer Science Part A-2: Polymer Physics*, Vol. 8, Pp. 1057-1072 (1970).

[25] H. Kakutani, "Dielectric Absorption in Oriented Poly(vinylidene fluoride)," *Journal of Polymer Science Part A-2: Polymer Physics*, Vol. 8, Pp. 1177-1186 (1970).

[26] Q. M. Zhang, V. Bharti and X. Zhao, "Giant Electrostriction and Relaxor Ferroelectric Behavior in Electron-Irradiated Poly(vinylidene fluoride-trifluoroethylene) Copolymer," *Science*, Vol. 280, Pp. 2101-2104 (1998).

[27] T. C. Chung and A. Petchsuk, "Synthesis and Properties of Ferroelectric Fluoroterpolymers With Curie Transition at Ambient Temperature," *Macromolecules*, Vol. 35, Pp. 7678-7684 (2002).

[28] Z. Yu, C. Ang, L. E. Cross, A. Petchsuk and T. C. Chung, "Dielectric and Electroactive Strain Properties of Poly(vinylidene fluoride-trifluoroethylene-chlorotrifluoroethylene) Terpolymers," *Applied Physics Letters*, Vol. 84, Pp. 1737-1739 (2004).

[29] R. C. Buchanan, (Ed) *Ceramic Materials for Electronics*, Marcel Dekker: New York (2004).

[30] K. C. Kao, *Dielectric Phenomena in Solids*, Elvesier Academic Press: California & London (2004).

[31] Application Note 1217-1, "Basics of Measuring the Dielectric Properties of Materials," Hewlett Packard Literature Number 5091-3300E, Pp. 6 (1992).

[32] P. Barber, S. Balasubramanian, Y. Anguchamy, S. Gong, A. Wibowo, H. Gao, H. J. Ploehn and H.-C. Zur Loye, "Polymer Composite and Nanocomposite Dielectric Materials for Pulse Power Energy Storage," *Materials*, Vol. 2, 1697-1733 (2009).

[33] G. J. Johnson, *Solid State Tesla Coil*, Chap. 3 Lossy Capacitors (2001), available at www.eece.ksu.edu/~gjohnson/.

[34] O. E. Gouda, A. M. Thabet and H. H. El-Tamaly, "How to Get Low Dielectric Losses in Binary and Multi-mixtures Dielectrics at High Frequency," *39th International Universities Engineering Conference*, Vol. 3, Pp. 1237-1240 (2004).

[35] M. Lanagan, "Glass Ceramic Materials for Pulsed Power Capacitors," *NSF Center for Dielectric Studies Meeting*, Albuquerque, NM, May (2004).

[36] N. Guo, S. A. DiBenedetto, P. Tewari, M. T. Lanagan, M. A. Ratner and T. J. Marks, "Nanoparticle, Size, Shape, and Strength of Metal Oxide – Polyolefin Nanocomposites: Experiment and Theory," *Chemistry of Materials*, Vol. 22, 1567-1578 (2010).

[37] M. Lanagan, "High Power Capacitors and Energy Storage," presented at *Materials Day*, University Park, Penn State University, April 14 (2008).

[38] J. Y. Li, L. Zhang and S. Ducharme, "Electric Energy Density of Dielectric Nanocomposites," *Applied Physics Letters*, Vol. 90, Pp. 132901 (2007).

[39] C. Muralidhar, "The Off-Valency Additive Effect and its Influence on the Curie Peak of the Barium Titanate ($BaTiO_3$)/Polyvinylidene Fluoride (PVDF) Composite," *Japanese Journal of Applied Physics*, Vol. 27, No. 2, Pp. 1349-1350 (1988).

[40] Y. Xiaojun, Y. Zhimin, M. Changhui and D. Jun, "Dependence of Dielectric Properties of BT Particle Size in EP/BT Composites," *Rare Metals*, Vol. 25, Pp. 250 (2006).

[41] Y. Cao, P. C. Irwin and K. Younsi, "The Future of Nanodielectrics in the Electrical Power Industry," *IEEE Transactions on Dielectrics and Electrical Insulation*, Vol. 7, Pp. 797 (2004).

[42] F. Ciuprina, I. Plesa, P. V. Notingher, T. Tudorache and D. Panaitescu, "Dielectric Properties of Nanodielectrics with Inorganic Fillers," CEIDP Annual Report Conference on *Electrical Insulation and Dielectric Phenomena*, Pp. 682-685 (2008).

[43] P. Kim, S. C. Jones, P. J. Hotchkiss, J. N. Haddock, B. Kippelen, S. R. Marder and J. W. Perry, "Phosphonic acid-modified Barium Titanate Polymer Nanocomposites with High Permittivity and Dielectric Strength," *Advanced Materials*, Vol. 19, Pp. 1001-1005 (2007).

[44] S. Ramesh, B. A. Shutzberg, C. Huang, J. Gao and E. P. Giannelis, "Dielectric Nanocomposites for Integral Thin Film Capacitors: Materials Design, Fabrication and Integration Issues," *IEEE Transactions on Advanced Packaging*, Vol. 26, Pp. 17 (2003).

[45] Y. Bai, Z.-Y. Cheng, V. Bharti, H. S. Xu and Q. M. Zhang, "High-Dielectric-Constant Ceramic-Powder Polymer Composites," *Applied Physics Letters*, Vol. 76, Pp. 3804 (2000).

[46] S. Liang, S. R. Chong and E. P. Giannelis, "Barium Titanate/Epoxy Composite Dielectric Materials for Integrated Thin Film Capacitors," In *Proceedings of 48th Electronic Components and Technology Conference,* Pp. 171 (1998).

[47] T. J. Lewis, "Interfaces: nanometric dielectrics," *Journal of Physics D: Applied Physics,* Vol. 38, Pp. 202 (2005).

[48] J. K. Nelson and Y. Hu, "Nanocomposite dielectrics – properties and implications," *Journal of Applied Physics D: Applied Physics,* Vol. 38, Pp. 318 (2005).

[49] M. Roy, J. K. Nelson, R. K. MacCrone, L. S. Schadler, C. W. Reed, R. Keefe and W. Zenger, "Polymer Nanocomposite Dielectrics – The Role of the Interface," *IEEE Transactions on Dielectrics and Electrical Insulation,* Vol. 12, Pp. 629 (2005).

[50] R. C. Smith, C. Liang, M. Landry, J. K. Nelson and L. S. Schadler, "The Mechanisms Leading to the Useful Electrical Properties of Polymer Nanodielectrics," *IEEE Transactions on Dielectrics and Electrical Insulation,* Vol. 15, Pp. 187-196 (2008).

[51] S. K. Saha, "Observation of Giant Dielectric Constant in an Assembly of Ultrafine Ag Particles," *Physical Reviews B,* Vol. 69, 125416/1-4 (2004).

[52] J. K. Nelson, L. A. Utracki, R. K. MacCrone and C. W. Reed, "Role of Interface in Determining the Dielectric Properties of Nanocomposites," *IEEE Conference on Electrical Insulation and Dielectric Phenomena,* Pp. 314-317 (2004).

[53] J. Li, "Exchange Coupling in P(VDF-TrFE) Copolymer Based All-Organic Composites with Giant Electrostriction," *Physical Review Letters,* Vol. 90, 217601/1-4 (2003).

[54] T. Tanaka, M. Kozako, N. Fuse and Y. Ohki, "Proposal of a Multicore Model for Polymer Nanocomposite Dielectrics," *IEEE Transactions on Dielectrics and Electrical Insulation,* Vol. 12, Pp. 669-681 (2005).

[55] J. K. Nelson, "Overview of Nanodielectrics: Insulating Materials of the Future," *IEEE Electrical Insulation Conference and Electrical Manufacturing Expo,* Pp. 229-235 (2007).

[56] L. J. Gilbert, T. P. Schuman and F. Dogan, "Dielectric Powder/Polymer Composites for High Energy Density Capacitors," *Advances in Electronic and Electrochemical Ceramics: Proceedings of the 107th Annual Meeting of the American Ceramic Society*, Wiley, Baltimore, Maryland, USA (2005).

[57] P. M. Ajayan, L. S. Schadler and P. V. Brawn, *Nanocomposite Science and Technology*, Wiley-VCH: Weinheim, Germany (2003).

[58] M.-A. Neouze and U. Schubert, "Surface Modification and Functionalization of Metal and Metal Oxide Nanoparticles by Organic Ligands," *Monatshefte fur Chemie*, Vol. 139, No. 3, Pp. 183-195 (2008).

[59] M. Hosokawa, K. Nogi, M. Naito and T. Yokoyama, (Ed) *Nanoparticle Technology Handbook*, Elvesier: Oxford, UK (2007).

[60] T. P. Schuman, S. Siddabattuni, O. Cox and F. Dogan, "Improved Dielectric Breakdown Strength of Covalently-Bonded Interface Polymer-Particle Nanocomposites," *Composite Interfaces*, Vol. 17, No. 8, Pp. 719-731 (2010).

[61] N. Jayasundere and B. V. Smith, "Dielectric Constant for Binary Piezoelectric 0-3 Composites," *Journal of Applied Physics*, Vol. 73, No. 5, Pp. 2462-2466 (1993).

[62] Y. Rao, J. Qu, T. Marinis and C. P. Wong, "A Precise Numerical Prediction of Effective Dielectric Constant for Polymer-Ceramic Composite Based on Effective Medium Theory," *IEEE Transactions on Advanced Packaging Technologies*, Vol. 23, No. 4, Pp. 680-683 (2000).

[63] J. P. Calame, "Finite Difference Simulations of Permittivity and Electric Field Statistics in Ceramic-Polymer Composites for Capacitor Applications," *Journal of Applied Physics*, Vol. 99, 084101 (2006).

[64] C. Huang, Q. Zhang, "Enhanced Dielectric and Electromechanical Responses in High Dielectric Constant All-Polymer Percolative Composites," *Advanced Functional Materials*, Vol. 14, No. 5, Pp. 501-506 (2004).

[65] J. G. Head, N. M. White and P. S. Gale, "Modification of the Dielectric Properties of Polymeric Materials," *5th International Conference on Dielectric Materials, Measurement and Applications*, Issue. 27-30, Pp. 61-64 (1988).

[66] D. S. McLachlan, M. Blaskiewicz and R. E. Newnham, "Electrical Resistivity of Composites," *Journal of American Ceramic Society*, Vol. 73, No. 8, Pp. 2187-2203 (1990).

[67] J. R. Kokan, R. A. Gerhardt, R. Ruh and D. S. McLachlan, "Dielectric Spectroscopy of Insulator/Conductor Composites," Pp. 341-346 in *Materials Research Society Symposium Proceedings*, Vol. 500, Electrically Based Microstructural Characterization II, Edited by R. A. Gerhardt, M. A. Alim and S. R. Taylor, *Materials Research Society*, Pittsburgh, PA (1998).

[68] R. Zallen, *The Physics of Amorphous Solids*, John Wiley & Sons: New York (2004).

[69] S. Kirkpatrick, "Percolation and Conduction," *Reviews of Modern Physics*, Vol. 45, No. 4, Pp. 574-588 (1973).

[70] C. Mukherjee, K. Bardhan and M. Heaney, "Predictable Electrical Breakdown in Composites," *Physical Review Letters*, Vol. 83, No. 6, Pp. 1215-1218 (1999).

[71] M. Lanagan, "High Power Capacitors and Energy Storage," presented at *Materials Day*, University Park, Penn State University, April 14 (2008).

[72] L. A. Dissado and L. C. Fothergill, *Electrical Degradation and Breakdown in Polymers*, Peter Peregrins Ltd.: London, UK (1992).

[73] S. Li, G. Yin, G. Chen, J. Li, S. Bai, L. Zhong, Y. Zhang and Q. Lei, "Short-term Breakdown and Long-term Failure in Nanodielectrics," *IEEE Transactions on Dielectrics and Electrical Insulation*, Vol. 17, No. 5, Pp. 1523-1535 (2010).

[74] J. J. O'Dwyer, *The Theory of Dielectric Breakdown of Solids*, Oxford University Press: London, UK (1964).

[75] J. Claude, Y. Lu and Q. Wang, "Effect of Molecular Weight on the Dielectric Breakdown Strength of Ferroelectric Poly(vinylidene fluoride-chlorotrifluoroethylene)s," *Applied Physics Letters*, Vol. 91, Issue. 21, 212904 (2007).

[76] S. Ul-Haq and G. R. G. Raju, "Weibull Statistical Analysis of Area Effect on the Breakdown Strength in Polymer Films," *2002 Annual Report Conference on Electrical Insulation and Dielectric Phenomena*, Pp. 518-521 (2002).

[77] G. Raju, A. Katebian and S. Z. Jafri, "Breakdown Voltages of Polymers in the Temperature Range 23° - 250° C," *IEEE Transactions on Dielectrics and Electrical Insulation,* Vol. 10, No. 1, Pp. 117-127 (2002).

[78] J. Prendergast, E. O'Driscoll and Ed Mullan, "Investigation into the Correct Statistical Distribution for Oxide Breakdown Over Oxide Thickness Range," *Microelectronics Reliability,* Vol. 45, Pp. 973-977 (2005).

[79] E. Tuncer, D. R. James, I. Sauers, A. R. Ellis and M. O. Pace, "On Dielectric Breakdown Statistics," *Journal of Physics D: Applied Physics,* Vol. 39, Pp. 4257-4268 (2006).

[80] E. Tuncer, I. Sauers, D. R. James, A. R. Ellis, M. P. Paranthaman, T. Aytug, S. Sathyamurthy, K. L. More, J. Li and A. Goyal, "Electrical Properties of Epoxy Resin Based Nanocomposites," *Nanotechnology,* Vol. 18, No. 2, 025703 (2007).

[81] E. Tuncer, I. Sauers, D. R. James, A. R. Ellis, M. P. Paranthaman, A. Goyal and K. L. More, "Enhancement of Dielectric Strength in Nanocomposites," *Nanotechnology,* Vol. 18, No. 32, 325704 (2007).

[82] P. Kim, "Surface Modification of Nanoparticles for Polymer/Ceramic Nanocomposites and Their Applications," Georgia Institute of Technology, December (2008).

[83] T. Liu, J. Fothergill, S. Dodd and U. Nilsson, "Dielectric Spectroscopy Measurements on Very Low Loss Cross-linked Polyethylene Power Cables," *Journal of Physics: Conference Series,* Vol. 183, 012002 (2009).

[84] A. K. Jouscher, *Dielectric Relaxation of Solids*, Chelsea Dielectric Press: London, UK (1983).

[85] C. Zou, "The Effect of Humidity and Surface Functionalization on the Dielectric Properties of Nanocomposites," University of Leicester, July (2007).

[86] D. Q. M. Craig, *Dielectric Analysis of Pharmaceutical Systems,* Taylor and Francis: London, UK (1995).

PAPER

1. IMPROVED DIELECTRIC BREAKDOWN STRENGTH OF COVALENTLY-BONDED INTERFACE POLYMER-PARTICLE NANOCOMPOSITES

Thomas P. Schuman,[*,1] Sasidhar Siddabattuni,[1] Olivia Cox,[1] and Fatih Dogan[2]

[1]Missouri University of Science and Technology (formerly the University of Missouri-Rolla), Chemistry Department, 400 W. 11th Street, Rolla, MO 65409 (USA), Phone: 573-341-6236, Fax 573-341-6033, E-mail: tschuman@mst.edu; USA

[2] Missouri University of Science and Technology, Materials Science and Engineering Department, 1400 N. Bishop Avenue, Rolla, MO 65409 (USA), Phone: 573-341-7130, E-mail: doganf@mst.edu, USA

Running title: Covalent Interface Composite Breakdown Strength
Keywords: Breakdown strength, Crosslinking, Dielectric properties, Nanocomposite, Interfaces, Covalent, Glass transition temperature

ABSTRACT

Interfacial covalent bonding is an effective approach to increase the electrical resistance of a polymer-particle composite to charge flow and dielectric breakdown. A bifunctional tether reagent bonded to an inorganic oxide particle surface assists with particle dispersion within a thermosetting epoxy polymer matrix but then also reacts covalently with the polymer matrix. Bonding the particle surface to the polymer matrix resulted in a composite that maintained the pure polymer glass transition temperature, compared to modified or unmodified particle dispersions that lacked covalent bonding to the polymer matrix, which depressed the polymer glass transition to lower temperatures. The added interfacial control, directly bonding the particle to the polymer matrix, appears to prevent conductive percolation across particle surfaces that results in a reduced Maxwell-Wagner relaxation of the polymer-particle composite and a reduced sensitivity to a dielectric breakdown event. The inclusion of 5 vol.-% particles of higher permittivity produce a composite of enhanced dielectric constant and, with surface modification to permit

surface crosslinking into the polymer, a polymer-particle composite with a Weibull Eo dielectric breakdown strength of 25 percent greater than that of the pure polymer resulted. The estimated energy density for the crosslinked interface composite was improved 260% compared to the polymer alone, 560% better than a polymer-particle composite synthesized using bare particles, and 80% better than a polymer-particle composite utilizing bare particles with a dispersant.

1.1. INTRODUCTION

Capacitors are used to store and release electrical energy. The ability of a parallel plate capacitor to store energy may be calculated using Equation 1:

$$J = \int_0^{E_{max}} \varepsilon_o \, \varepsilon(E) \, E \, dE \qquad [1]$$

where J is the energy density (J/m^3), E is the applied electric field (V/m), ε_o is the permittivity of free space (F/m) and ε is the relative permittivity or dielectric constant. For a linear dielectric material (ε independent of field), the energy density of an infinite parallel plate capacitor can be derived (Equation 2).

$$J = {}^1\!/_2 \, \varepsilon_o \, \varepsilon' \left({}^{E_o}\!/_d \right)^2 \qquad [2]$$

where and ε' is the relative permittivity or dielectric constant, E_o is the maximum applied voltage, and d is the distance between the electrode plates. Applications that require high power storage density and reliability, such as pulse power applications, must possess high dielectric constant and dielectric layers as thin as possible that withstand high applied fields.

A composite dielectric design is based on dispersing non-conductive, e.g., ceramic, materials of high dielectric constant into polymer of lower dielectric constant, relying on the polymer for electrical resistance and the included phase to raise composite permittivity [1-9]. However, the interfaces created when dispersing a high surface energy particle into a low surface energy polymer both make uniform dispersion of the particles problematic and generate interfaces that can conduct charge. While the dispersion of particles directly into the polymer typically results in a decrease in breakdown strength beginning at quite low volume concentrations [1], some researchers have found that composite breakdown strength can be improved by the inclusion of particles where the particles are resistive and of low dielectric constant [2,3]. Also, the addition of surfactants such as phosphate esters can improve the dispersion and film quality that results in improved breakdown strengths compared to ceramic-particle composites without dispersants [1].

Surface complexation using phosphonate, sulfonate, silane, and carboxylate was recently reported [10,11]. Phosphonic acids have been reported to bond to TiO_2, ZrO_2, and In-Sn oxide surfaces and are thought to couple through heterocondensation with metal hydroxides or surface metal (crystal-defect) ions [12-14]. Modification of the particle surfaces with organo-phosphonates resulted in improved particle dispersion and breakdown strengths, while the high dielectric constant particles and poly(vinylidene difluoride) increased the dielectric permittivity, resulting in improved energy density [10]. Other surface groups that were examined appeared to not be as useful for tethering organic groups to the barium titanate particle surface since they have lower surface adsorption densities [11]. In producing a surface modified particle, only one side of the

interface is controlled by coupling leaving the remaining interface to be controlled by wetting and adsorption of the polymer chains, which is variable in structure [15]. The surface bond between the acid moiety and the metal oxide particle creates a stable, salted organic oxide interface.

We propose the use a bifunctional reagent, e.g., 2-aminoethyl dihydrogen phosphate, that can not only bond to an inorganic oxide particle surface to assist particle dispersion but also to react covalently with the polymer matrix. The added interfacial control appears to prevent conductive percolation across particle surfaces that results in a reduced Maxwell-Wagner (MW) relaxation of the polymer-particle composite and a reduced sensitivity to dielectric breakdown [16]. The increases in dielectric constant and breakdown strength compared to the pure polymer resulted in a dielectric capacitor of enhanced energy density.

1.2. METHODS

The chemicals and reagents were obtained from the following sources and were used without further purification. Epoxy resin Epon 828 was obtained from Hexion. The polyamide resin used was a moderately low molecular weight, liquid, blend of the commercial Ancamide 2353 and Ancamine 2205 used at a 3:1 ratio and activated with 5 vol.-% Ancamine K-54 that were each obtained from Air Products. Mirror-polished copper sheet (Electronic grade 110 alloy, 0.8125 mm thick, #8 finish) was purchased from McMaster Carr that was supplied with a protective plastic peel ply and cut to a 25 cm2 size upon receipt. The ply was removed just prior to film application onto the polished copper. Titanium dioxide, anatase in structure, of average particle size 32nm was obtained from Alfa Aesar. The dispersant BYK-w-9010 (a proprietary copolymer

mixture with acidic groups) was provided by Byk-Chimie. 2-Ethylhexyl phosphoric acid ester (EHP) was obtained from Akzo Nobel and 2-aminoethyl dihydrogen phosphate (AEP) was obtained from Acros Organics. Water was distilled-deionized and of 1 M□-cm-1 resistance. ACS grade toluene was obtained from Fisher Scientific.

In a typical surface modification reaction, the titanium dioxide was dispersed in water and degassed by sonication while under aspirator-reduced pressure for 15 min. For 2-ethylhexyl phosphoric acid ester, the process was performed in toluene solvent. The phosphate was added to the titanium oxide dispersion and magnetically stirred at reflux for 5 hr. The dispersion was then recovered by filtration followed by re-dispersion, and degassing into fresh water and filtration, repeated twice.

Characterization of the powders, modified and unmodified, were analyzed by thermogravimetric analysis (TGA) and by X-ray photoelectron spectroscopy (XPS). TGA (Netzsch STA409) was used to measure the weight of organophosphate incorporated on the surface of particles and then used with surface area per weight of unmodified particles to calculate the number of groups per square area. Sample weight loss was measured from ambient to 700 □C at 10 □C/min in air. XPS (KRATOS model AXIS 165 XPS spectrometer) was utilized for determining the chemical composition of the particle surfaces. A Mg K□ anode with a photon energy of h□= 1253.6 eV was operated at 225 W. Adventitious carbon for the C1s orbital at a binding energy of 285.2 eV was used to correct for charging. The system pressure during XPS analysis was ca. 1 x 10–9 Torr. The Cu 2p3/2 (932.7 eV) and Au 4f7/2 (84.0 eV) orbitals were employed as standards from sputter-cleaned foils to calibrate the XPS binding energy (BE) range.[17] XPS scans were performed on powder samples of 1 cm2 mounted onto copper stubs with

double-sided conductive adhesive tape and introduced into the UHV via a turbo-pumped antechamber. Crystal diffraction patterns from the particles was obtained using an XDS 2000 WAXS diffractometer using a copper source from 5 to 120 degrees at a 2 degrees per minute scan rate.

Composite films were made by dispersing particles to obtain a 5 vol.-% concentration in the composite into polyamide resin via a ball-milling process overnight (~16-18 hr). A separate dispersant, the w-9010, was added only to a bare particle dispersion of titania in polyamide as an experimental control for comparison of a dispersed particle against a bare particle with no added dispersant and against a self-dispersing (surface modified) particle, where the particle uses bound surface groups to aid its dispersion. The ball-milled dispersion was sieved into a clean, pre-weighed jar through a coarse stainless steel screen to remove ball media. Epoxy resin, in amount stoichiometric to the amount of polyamide amine, was added to the dispersion and the uncured, liquid composite stirred for 5 min. Films of the uncured, liquid composite were applied to freshly exposed, polished copper plate at a 0.09 mm film thickness. Composites were allowed to initially cure overnight in a dust-free vented cabinet, followed by completing the polymer matrix crosslinking process by baking in a forced-air conventional oven at 80 □C for 24 hr followed by 100 □C for 6 days.

Composites were characterized by differential scanning calorimetry (DSC), scanning electron microscopy of the freeze-fractured cross section interfaces, electrical impedance and dielectric breakdown strength. Film thicknesses were measured with a Mitutoyo 0293-340 micrometer and subtracting the thickness of the copper sheet.

Glass transition temperatures were assessed in a Perkin Elmer DSC after a preliminary thermal anneal stage (10 □C • min-1, from ambient to 100 □C, quenched to ambient using liquid nitrogen) by scanning temperature from ambient to 150 □C versus an air-sealed pan. Glass transition temperatures are reported using the inflection point of the transition.

Parallel-plate capacitors were fabricated by depositing circular (31.67 mm2) silver (Pelco® colloidal silver liquid, Ted Pella Inc.) top electrodes onto the nanocomposite thin films. Frequency-dependent capacitance was measured on a Solartron 1260 impedance analyzer connected with a Solartron 1296 dielectric interface (Solartron Analytical, Hampshire, England) at frequency range of 1 Hz to 1 MHz at 22 □C and from 0.01 Hz to 1 MHz at 100 □C with voltage amplitude of 1 V and analyzed by Zview® software. Reported relative dielectric constant used for energy density calculation was calculated according to capacitance measured at 10 kHz.

Dielectric breakdown strength measurements were made by applying D.C. voltage across the films using a Spellman SL 30 high voltage generator (Spellman High Voltage Electronics Corporation, New York, USA), with a fixed ramp rate of 200 V • sec-1 until the point of film failure. A pin electrode was applied by light spring tension to the surface of the composite, which served as the electrical ground. The Spellman electrode was connected beneath the copper substrate and the sample immersed in Fluorinert FC-40 (Acros Scientific) to displace air.

1.3. RESULTS AND DISCUSSION

EHP or AEP ligand (~2 wt.-% of particles) was added to a degassed dispersion of particles, which was stirred and refluxed for 5 hours to modify the particle surfaces. Gao

et al. assumed a theoretical surface area of 24 $Å^2$ per group while Kim observed phosphonate surface densities of ~15 $Å^2$ per group [10,12-14,18,19] describing the phosphono groups as self-assembled, uniform monolayers on the metal oxide surface. TGA measurements showed surface group densities of about 24 to 46 $Å^2$ per group calculated from weight loss and surface area, which were similar in site density to those previously reported. XPS measurements indicated the introduction of phosphorous for EHP samples and, for the amino containing ligand modification (AEP), phosphorous and nitrogen (see Table 1.1).

The ligands form metal oxide phosphate esters at the metal oxide surface. The transition of the phosphorous group from free to bound is indicated by the binding energies of phosphorous and oxygen groups through XPS. A P2p photoelectron binding energy (134.3 eV) and O1s photoelectron binding energies (531.2 eV and 532.4 eV) with a peak area ratio of 0.5:1 were observed and compared to the aminoethylphosphate on the surface of titania. The nitrogen group of the pure AEP shows nearly entirely protonated amine (area 4068), binding energy 401.7 eV [20]. Free amine was observed at 400.0 eV (peak area 565). For the AEP titania, the percentages of free to complexed amine were nearly reversed, where 80% was observed to be free amine (400.0 eV) and 20% protonated amine (401.7 eV).

The amount of protonated amine in the free AEP powder also explained a lower than expected oxygen ratio of 0.5:1 that was observed rather than the expected 0.33:1 [19], if one oxygen atom is assigned as complexing with the nitrogen and the third species (complexed oxygen) is fitted as a third photoelectron emission peak between the current two assigned peaks. The XPS analysis of the powder then indicated that nearly

all the nitrogen and nearly all of one fourth the phosphate oxygen atoms (532.0 eV, area 6260) of the phosphatewere complexed together; one fourth of the AEP oxygen atoms are phosphonyl oxygen (P=O, 531.1 eV, area 7940); and, slightly more than one half of the phosphate oxygen atoms are bonded oxygen (as P-O-C ether or hydroxyl group, 533.0 eV, area 10770).

AEP titania showed a P2p binding energy of 133.5 eV and O1s binding energies of 531.2 eV and 532.4 eV, in addition to a new O1s binding energy at 530.0 eV that corresponds to underlying TiO_2 [19]. The trends of change in O1s binding energy from the free to bound phospho group are similar to the findings of Spencer et al. that indicated coordinate covalent bonding of the phospho group with the metal oxide surface [19]. In our case, the AEP bonding to titania appears mostly bidentate, which was assessed through the observed oxygen peak area ratio (2.13) of O1s peaks at 531.2 eV(area 5305) to 532.4 eV (area 2486), respectively. Based on XPS results, the amine of the AEP titania particles should have but a small percentage that is surface complexed (20%) and thus is mostly a free amine and expected to be reactive upon exposure to an epoxy group of the epoxy resin.

Composites were made by dispersing the surface-modified particles into the liquid polyamide portion of the two-part thermoset epoxy without using a separate dispersant. The epoxy polyamide itself served as a comparative control sample. Two other control composite samples were made using unmodified particles, i.e., bare titanium dioxide particles, that were dispersed into the polyamide resin, one sample without an added dispersant and a separate control was made where the titanium oxide particles were dispersed into the polyamide in the presence of 1 wt.-% of the particles of added

commercial phosphate ester dispersant [1]. Others have discussed surface modification and its relevance to dispersion quality and dielectric properties, in particular breakdown strength [4,5,11,16]. Blum et al. have studied how particle curvature, surface adsorption and composition influence the polymer free volume observed as changes in glass transition temperature and deuterium NMR relaxation [15,21,22]. Interfacial adsorption has also been shown to affect polymer chain density and mobility at the interface [21-23]. We suspected that the interface effects on free volume could influence the dielectric breakdown resistance and have previously evidenced that greater free volume for polymers of identical structure reduces electrical breakdown resistance.

Glass transition temperatures (T_g) are related to the free volume of polymer chains as described by the Williams-Landel-Ferry theory [24]. Polymer nanometer-sized particle composites typically show a decreased glass transition temperature, which is related to the curvature of the particles increasing the free volume of polymer chains [25]. For example, pure epoxy polymer showed a glass transition temperature of about 99 °C, while unmodified nanoparticle composites showed a depressed T_g inflection point, about 95 °C. The T_g of the unmodified TiO_2 epoxy composite with dispersant was even lower, 85 °C, possibly due to some plasticization of the epoxy polymer by unadsorbed, free dispersant (see Table 1.2).

Either bare particles or bare TiO_2 nanoparticles dispersed using an added dispersant into epoxy polymer was observed to increase the free volume of the polymer chains as shown by a depressed polymer T_g. The EHP modified particles, which do not allow covalent bonding from the particle surface to the matrix polymer but only provide adsorptive interactions, similarly resulted in a decreased T_g of the polymer composite, 83

°C. The decrease in glass transition temperature seemed to result from a combination of nanoparticle curvature effect and a plasticizing effect similar to bare particles with a dispersant since T_g was not similarly depressed for a micrometer-sized particle TiO_2 composite. Plasticizing, e.g., by a solvent or free dispersant in the matrix, or weak adsorption of a polymer chains also result in increased free volume and depressed polymer T_g.

Polymer crystallinity has contiguous space between crystal planes that permit the relatively scatter free acceleration of an electron in an electric field and that decrease electrical breakdown resistance [26]. An increased free volume of the chains at the interface may be similar in effect as increased crystallinity, which increases the mean free path length of an accelerated electron and decreases breakdown strength [26] despite the polymer matrix is non-crystalline. A weakly adsorbed interface could also explain an increased free volume [15,21,22], which would also reduce electromechanical strength [24]. However, when amino groups were present on the surface, capable of covalently reacting with the epoxy polymer matrix, it could crosslink the polymer-particle interface to locally retain the bulk T_g and free volume of the native epoxy polymer. The slight decrease in T_g for the AEP modified particle composite could be residual particle curvature effects or, given the relatively large size of the particle compared to polymer radius of gyration and/or a surface-limited crosslinking reaction, could be a slightly reduced crosslink density compared to the bulk epoxy.

The surface modifications also appear to provide for some improved dispersion and composite cohesion compared to bare particles, as exemplified by reduced particle pull out on cross sectioning. Dispersion has been shown to be important in the dielectric

breakdown performance and the ability of dispersants to improve dielectric breakdown voltage despite that a dispersant impurity in the polymer causes a sharp decrease in breakdown voltage of the polymer [1,28]. The composite was better dispersed when the particle dispersion in polyamide and epoxy resin were blended with high shear mixing.

While glass transition temperature indicated the effect of surface modification on the polymer chain mobility, impedance spectroscopy measured the influence of the modifying groups on the particle surface's electrical properties. Of particular interest was the Maxwell-Wagner relaxation (MW) loss at low frequency [16,29]. The samples were tested for dynamic impedance at 100 °C to enhance composite conductivity signal and reduce low frequency signal noise (Figure 1 and 2). Dielectric constant varied little as a function of temperature though samples displayed higher dielectric constant and loss at near-D.C. polarization frequencies.

Unmodified particle composites displayed higher dielectric losses over the entire frequency spectrum compared to surface modified filler samples. Unmodified particle composites showed especially large dielectric losses at low polarization frequencies compared to the modified samples, which corresponds to a MW or free charge conductivity loss. The EHP sample also showed significant MW relaxation at low frequency, which may indicate the presence of remaining loose charges at the adsorbed polymer-EHP interface. The amino phosphate modified particle composites showed lower dielectric losses over the 10^{-2} to 10^{6} Hz polarization frequency range compared to all other adsorbed interface composites and dielectric loss of less than 1% from 100 to 10^{6} Hz. However, the AEP titania composites had slightly greater dielectric losses compared to the neat epoxy samples, which showed the least loss of samples tested.

The dielectric constants of the composites were 9.5±1.6, which is similar to a κ ~8.6 that was expected for a composite of 95 vol.-% epoxy of κ ~3.9 and of TiO_2 filler of κ ~100 at a 5 vol.-% concentration. The variance in dielectric constant for the samples could be simply due to errors in the thickness measurement of the thin films. The dielectric constants demonstrate the premise that addition of a higher dielectric constant powder into a polymer of lower dielectric constant produces a composite of enhanced permittivity compared to that of the polymer alone in accordance with simple mixing rules [1,6,10].

Dielectric breakdown strength was measured by stepwise DC polarization until failure. Figure 3 shows the Weibull distributions of dielectric breakdown strengths of the composites. The measurements were reproduced using multiple samples and thus show the Weibull E_o expected over multiple measurements. In general, samples that displayed larger low frequency (MW) loss produced the lowest dielectric breakdown resistance, e.g., composites containing unmodified particles. The effect of dispersion was demonstrated by the unmodified sample with dispersant w-9010, which had a much improved breakdown resistance in comparison with the unmodified sample and no added dispersant.

The modified particle composites show enhanced dielectric breakdown voltages compared to the unmodified particle composites. The EHP modification displayed an E_o slightly lower than the original epoxy with significant overlap in their Weibull distributions. On the other hand, the AEP modified particle composites displayed some dielectric breakdown voltages similar to, but many values greater than, the pure epoxy polymer.

The unmodified particle surfaces display the extreme case of a poorly adsorptive interface, relying on weak interfacial contacts that provide poor cohesion, dispersion, and control, e.g., of surface groups and charge. One can look at the shared interface as two-sided, one half controlled by the particle surface and the other by the polymer surface, each side responsive toward the other resulting in the final interfacial structure. Like other reported surface modified particles [10,12-14,18,19] and surface modified particle composites [4,5,10,29], the EHP binds to the particle surface but presents an adsorptive interface toward the polymer, leaving a weak polymer adsorption interaction, greater free volume, and lower breakdown strengths. Controlling the particle surface alone thus appears less resistant to dielectrical breakdown than controlling both the particle and polymer sides of the interface through a bifunctional group.

On the other hand, the bifunctional AEP modification can covalently react with the thermoset epoxy, crosslinking the polymer to the particle surface. As such, the organo phosphate systems are analogous to silane reactions for glass fiber reinforced composites but silanes are less reactive to many metal oxides and have a complex, diffuse structure [20]. Covalent reactions are also probably important for controlling charge mobility, observed as a reduced MW relaxation, and for resisting a dielectric breakdown event. The improved interfacial bonding could localize interfacial electrons and ions in bonding interactions to provide deeper, more stable potential energy states, reduced leakage current and mobility, reduced dielectric loss, resulting in fewer resistive heating failures and a reduced likelihood of cascade failure under electrical load. The reactive agent for coupling the particle to the matrix is critically important for preventing a major

mechanism of composite failure, interfacial disbonding [30] and from our results appears important for preventing electrical breakdown failure of composite dielectrics.

All of the composites tested had a higher dielectric constant compared to the pure polymer. Only the EHP or AEP surface modified titania composites had breakdown strengths similar to or greater than the pure epoxy, respectively (see Table 1.2). Both of the unmodified particle composites, with or without a dispersant, had less energy density compared to the pure polymer due to a loss of breakdown strength. On the other hand, the EHP modified particle composite produced a 1.4 fold increase in calculated energy density compared to the pure epoxy film despite a minimal loss of breakdown strength compared to pure polymer. In this case, the increase in energy density due to dielectric constant overcomes the smaller loss of energy density due to breakdown strength. The AEP composite showed, at a 5 vol.-% particle concentration, an energy storage density of 3.3 $J \cdot cm^{-3}$, a 2.6 fold increase compared to the epoxy matrix alone through the concurrent improvement of dielectric constant and breakdown strength compared to the pure polymer. The AEP composite performance is a 5.6 fold improvement compared to 0.5 $J \cdot cm^{-3}$ calculated energy density for the bare particle composite of identical volume filler concentration.

1.4. CONCLUSIONS

Surface modification to bond the particle surface to the polymer matrix reduced the Maxwell Wagner relaxation loss, maintained the innate matrix glass transition temperature compared to unmodified particle dispersions. The surface modification provided stable dispersion, and increased electrical breakdown resistance. Interfacial covalent bonding is another approach that increases resistance to charge flow and

dielectric breakdown. The inclusion of the particles of higher permittivity produced a composite of enhanced dielectric constant and, with surface modification to permit surface crosslinking with the polymer, a polymer-particle composite of dielectric breakdown strength similar to or greater than that of the pure polymer resulted. The estimated energy density for the covalent interface composite was improved 267% compared to the polymer alone, 560% better than a composite utilizing bare particles, and 83% better than a composite utilizing bare particles with a dispersant.

1.5. ACKNOWLEDGEMENTS

This material is based upon work supported by the National Science Foundation, as part of the Center for Dielectric Studies under Grant No.0628817, Sub-Award No. 2164-UM-NSF-0812 and through the U.S. DOEd GAANN award number P200A040065. The authors thank Jeff Whyte for XPS measurements and Clarissa Wisner for electron microscopy imaging at the Materials Research Center at the Missouri University of Science and Technology, and Michael Lanagan of Pennsylvania State College for helpful discussion.

1.6. REFERENCES

1 L. J. Gilbert, T. P. Schuman and F. Dogan, in: *Ceramic Transactions (Advances in Electronic and Electrochemical Ceramics)*, F. Dogan, P.N. Kumta (Eds.), Vol. 179, p. 17. Wiley, N.Y. (2006).

2 Y. Cao, P. C. Irwin and K. Younsi, The Future of Nanodielectrics in the Electrical Power Industry, *IEEE Transactions on Dielectrics and Electrical Insulation*, **2004**, *11*, 797.

3 Y. Murata, Y. Murakami, M. Nemoto, Y. Sekiguchi, Y. Inoue, M. Kanaoka, H. Hozumi and M. Nagao, Effects of nano-sized MgO-filler on electrical phenomena under DC voltage application in LDPE, *IEEE Transactions on Electrical Insulation and Dielectric Phenomena*, **2005**, *12*, 158.

4 D. Ma, R. W. Siegel, J-I Hong, L. S. Schadler, E. Martensson and C. Onneby, "Influence of nanoparticle surfaces on the electrical breakdown strength of nanoparticle-filled low-density polyethylene, *J. Mater Res. Soc.*, **2004**, *19*, 857.

5 D. Ma, T. A. Hugener, R. W. Siegel, A. Christerson, E. Martensson, C. Oenneby and L. S. Schadler, Toward polyethylene nanocomposites with controlled properties, *Nanotechnology*, **2005**, *16*(6), 724.

6 Y. Rao and C. P. Wong, Novel Polymer-ceramic Nano-composite based on high dielectric constant epoxy formula for embedded capacitor application, *J. Appl. Polym. Sci.*, **2004**, *92*, 2228.

7 S. Ramesh, B. A. Shutzberg, C. Huang, J. Gao and E. P. Giannelis, Dielectric nanocomposites for integral thin film capacitors: materials design, fabrication and integration issues, *IEEE Trans. Adv. Packag.*, **2003**, *26*, 17.

8 S. Ogitani, S. A. Bidstrup-Allen and P. A. Kohl, Factors influencing the permittivity of polymer/ceramic composites for embedded capacitors, *IEEE Tran. Adv. Packag.*, **2000**, *23*, 313.

9 Y. Bai, Z.-Y. Cheng, V. Bharti, H. S. Xu, and Q. M. Zhang, High dielectric constant ceramic powder polymer composites, *Appl. Phys. Lett.*, **2000**, *76*, 3804.

10 P. Kim, S. C. Jones, P. J. Hotchkiss, J. N. Haddock, B. Kippelen, S.R. Marder, and J.W. Perry, Phosphonic acid-modified barium titanate polymer nanocomposites with high permittivity and dielectric strength, *Adv. Mater.*, **2007**, *19*, 1001-1005.

11 Y. Yin and A.P. Alivisatos, Colloidal nanocrystal synthesis and the organic-inorganic interface, *Nature*, **2005**, *437*, 664.

12 W. Gao, L. Dickinson, C. Grozinger, F. G. Morin and L. Reven, Self-assembled monolayers of alkylphosphonic acids on metal oxide surfaces, *Langmuir*, **1996**, *12*, 6429.

13 P. H. Mutin, G. Guerrero and A. Vioux, Organic–inorganic hybrid materials based on organophosphorus coupling molecules: from metal phosphonates to surface modification of oxides, *J. Mater. Chem.*, **2005**, 15, 3761.

14 C. M. Knobler and D. K. Schwartz, Langmuir and self-assembled monolayers, *Curr. Opin. Colloid Interface Sci.*, **1999**, *4*, 46.

15 F. D.. Blum,. B. R.. Sinha, and F. C. Schwab, Density profile of terminally adsorbed polymers, *Macromolecules*, **1990**, *23*, 3592.

16 T. J. Lewis, Interfaces: nanometric dielectrics: Cluster on dielectrics at meso and nano scales, *J. Phys. D: Appl. Phys.*, **2005**, *38*, 202.

17 M. P. Seah, Post-1989 calibration energies for X-ray photoelectron spectrometers and the 1990 Josephson constant, *Surf. Interface Anal.*, **1989**, *14*, 488.

18 R. Helmy and A. Y. Fedeev, Self-assembled monolayers supported on TiO_2: Comparison of $C_{18}H_{37}SiX_3$ (X = H, Cl, OCH_3), $C_{18}H_{37}Si(CH_3)_2Cl$, and $C_{18}H_{37}PO(OH)_2$, *Langmuir*, **2002**, *18*, 8924.

19 a) M. Textor, L. Ruiz, R. Hofer, A. Rossi, K. Feldman, G. Hähner and N.D. Spencer, Structural chemistry of self-assembled monolayers of octadecylphosphoric acid on tantalum oxide surfaces, *Langmuir*, **2000**, *16*, 3257; b) R. Hofer, M. Textor, N.D. Spencer, Alkyl Phosphate Monolayers, Self-Assembled from Aqueous Solution onto Metal Oxide Surfaces, *Langmuir*, **2001**, *17*, 4014.

20 H. Ishida, A Review of Recent Progress in the Studies of Molecular and Microstructure of Coupling Agents and Their Functions in Composites, Coatings, and Adhesive Joints, *Polymer Composites*, **1984**, *5*, 107.

21 F. D. Blum, W.-Y. Lin and C. E. Porter, Dynamics of adsorbed poly(methyl acrylate) and poly(methyl methacrylate) on silica, *Colloid and Polymer Science*, **2003**, *281*(3), 197.

22 B. Zhang, F. D. Blum, Thermogravimetric Study of Ultra-thin PMMA Films on Silica: Effects of Tacticity, *Macromolecules*, **2003**, *36*(22), 8522.

23 K. Akabori, K. Tanaka, T. Nagamura, A. Takahara, T. Kajiyama, Thermal molecular motion in polystyrene thin and ultrathin films by dynamic viscoelastic measurement, *Journal of Central South University of Technology*, **2007**, *14(1)*, 346.

24 G.S. Grest and M.H. Cohen, Liquids, glasses, and the glass transition: A free-volume approach, *Adv. Chem. Phys.*, **1981**, *48*, 455.

25 P. J. Dionne, R. Ozisik and C. R. Picu, Structure and dynamics of polyethylene nanocomposites, *Macromolecules*, **2005**, *38*, 9351.

26 Y. Tanaka, N. Ohnuma, K. Katsunami and Y. Ohki, Effects of crystallinity and electron mean-free-path on dielectric strength of low density polyethylene, *IEEE Transactions on Electrical Insulation*, **1991**, *26*(2), 258.

27 J. Claude, Y. Lu, K. Li and Q. Wang, Electrical storage in poly(vinylidene fluoride) based ferroelectric polymers: correlating polymer structure to electrical breakdown strength, *Chem. Mater.*, **2008**, *20*, 2078.

25 J.P. Calame, Finite difference simulations of permittivity and electric field statistics in ceramic-polymer composites for capacitor applications, *J. Appl. Phys.*, **2006**, *99*, 084 101.

29 M. Roy, J. K. Nelson, R. K. MacCrone, L. S. Schadler, C. W. Reed, R. Keefe and W. Zenger, Evidence for the role of the interface in polyolefin nanocomposites, *IEEE Transactions on Dielectrics and Electrical Insulation*, **2005**, *12*(4), 629.

30 S.-L. Bai, M. Wang and X.-F. Zhao, Interfacial debonding behavior of a rigid particle filled polymer composite, *Composite Interfaces*, **2003**, *10*, 243.

Table 1.1. Characterization of surface modified titania powders

Powder	TGA Organic weight loss		XPS (atomic percent)				
	Loss Wt.-%	Surface area $Å^2$- $ligand^{-1}$	C 1s	Ti 2p	O 1s	N 1s	P 2p
TiO_2 anatase	0.0	-	47.99	12.32	39.69	0.0	0.0
EHP	1.9	46	24.52	17.93	54.34	0.0	3.21
AEP	1.4	24	21.07	21.23	54.53	1.16	2.02

Table 1.2. Characterization data for pure polymer compared with 5 vol.-% particle-polymer composites.

Sample	T_g (°C)	Permittivity ε' (at 10 kHz)	Dielectric Loss (at 10 kHz)	E_o ($V \cdot \mu m^{-1}$)	Energy Density [b] ($J \cdot cm^{-3}$)
Pure Polymer	99	3.9	< 0.007	240	0.9
TiO_2 (w/o dispersant) [a]	95	9.8	< 0.011	110	0.5
TiO_2 (w/ dispersant) [a]	85	9.2	< 0.01	193	1.8
EHP TiO_2 [a]	83	10.4	< 0.013	220	2.2
AEP TiO_2 [a]	97	8.1	< 0.01	302	3.3

[a] TiO_2 nanoparticles were 30–40 nm in diameter. [b] Calculated energy density, average relative permittivity and dissipation factors measured at 10 kHz breakdown strength and Weibull distribution intercept (E_o) were used.

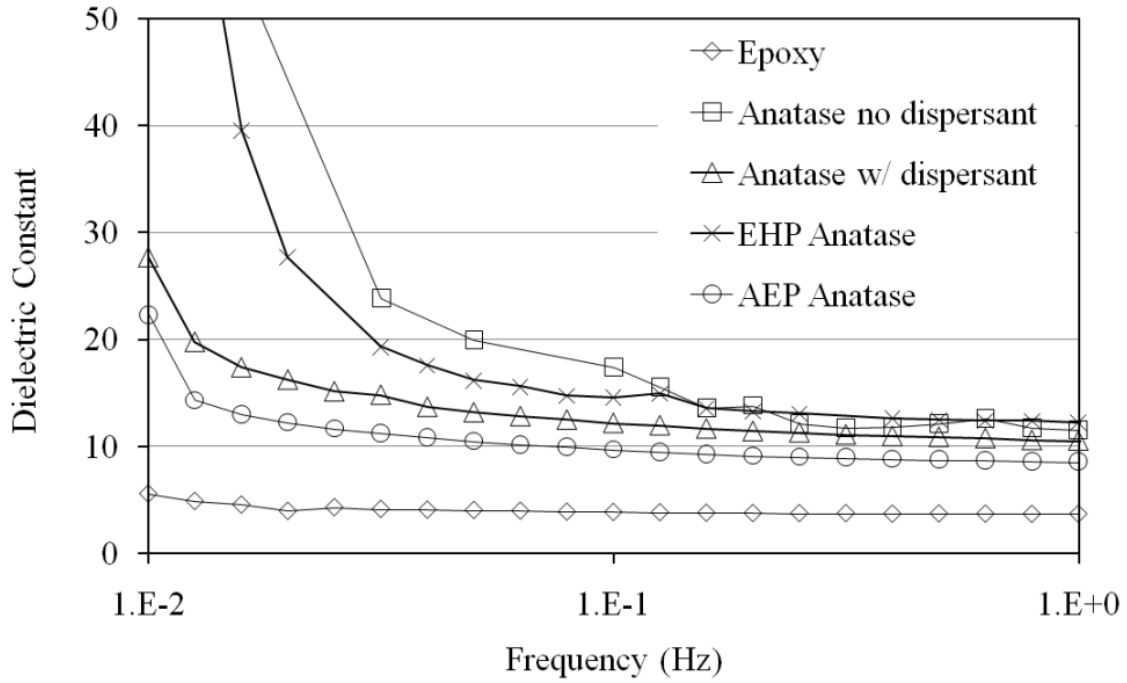

Figure 1. Frequency dependent dielectric constant of pure polymer and 5 vol.-% TiO_2 epoxy dielectric composites, measured at 100 °C.

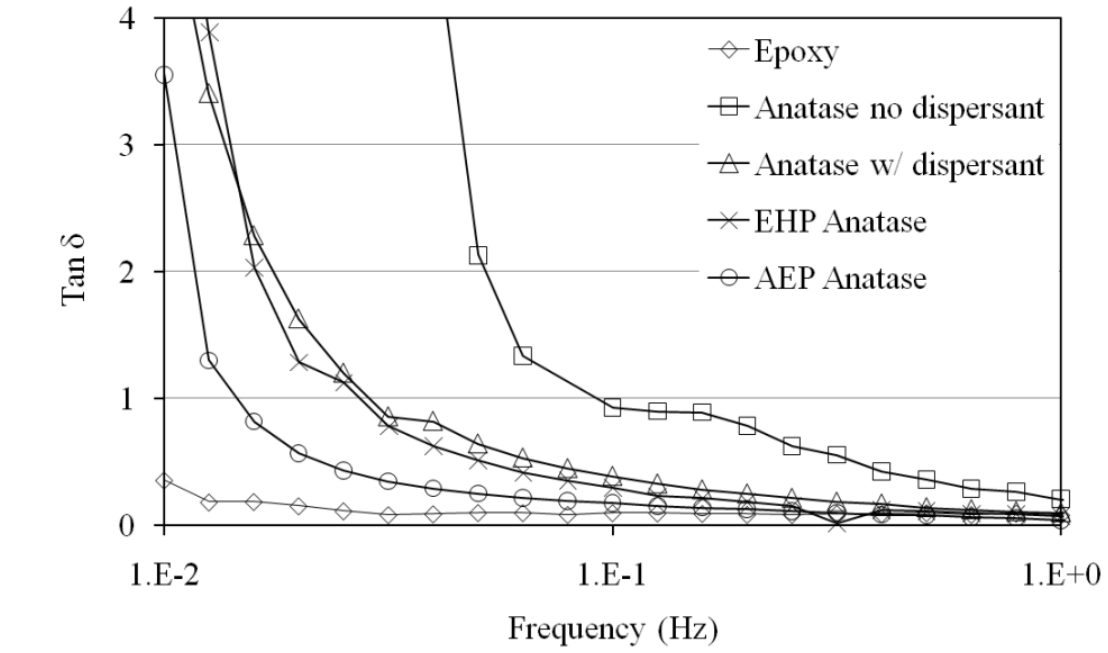

Figure 2. Frequency dependent dielectric loss response of pure polymer and 5 vol.-% TiO_2 epoxy dielectric composites, measured at 100 °C.

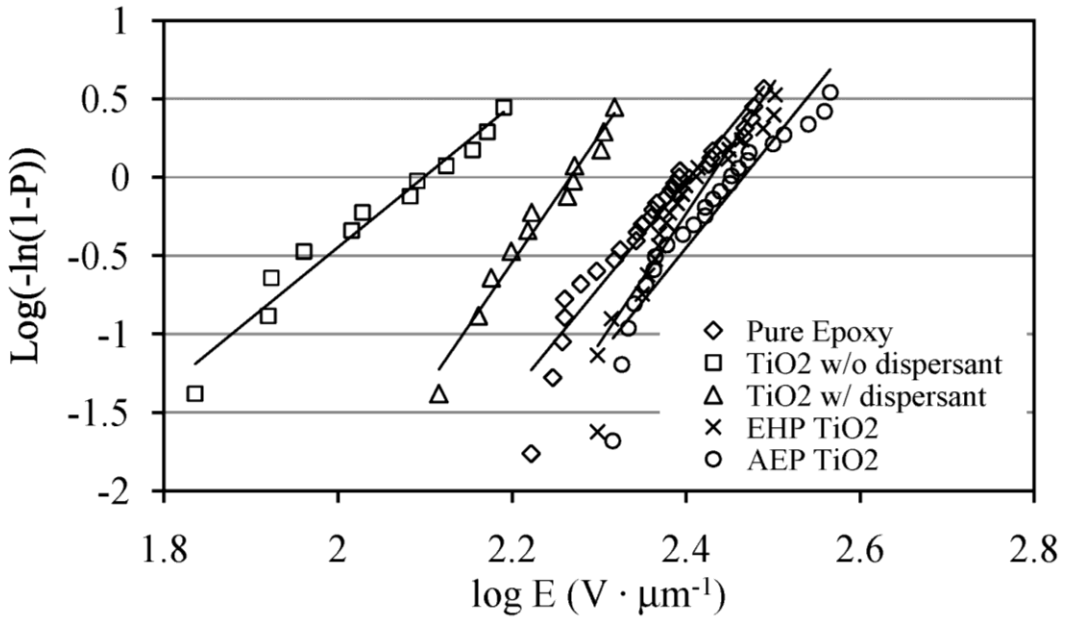

Figure 3. Weibull plot of dielectric breakdown measurements for 5 vol.-% TiO_2 nanoparticle-epoxy composite films.

2. DIELECTRIC PROPERTIES OF INTERFACE CONTROLLED POLYMER NANOCOMPOSITES

Sasidhar Siddabattuni[a], Thomas P. Schuman[a, *], Fatih Dogan[b]

[a] *Missouri University of Science and Technology (formerly the University of Missouri-Rolla), Chemistry Department, 400 W. 11th Street, Rolla, MO 65409 (USA)*
[b] *Missouri University of Science and Technology, Materials Science and Engineering Department, 1400 N. Bishop Avenue, Rolla, MO 65409 (USA)*
[*] *Address all correspondence to this author. Email: tschuman@mst.edu*

ABSTRACT

Interfacial coupling is an effective approach to improve a polymer-particle composite dielectric film resistance to charge flow and dielectric breakdown. A bi-functional interfacial coupling agent added to the inorganic oxide particles' surface assists dispersion into the thermosetting epoxy polymer matrix and upon composite cure reacts covalently with the polymer matrix. The composite attains the glass transition temperature of pure polymer, a reduced Maxwell-Wagner relaxation of the polymer-particle composite, and a reduced sensitivity to dielectric breakdown compared to particle epoxy composites that lacked interfacial coupling between the composite filler and polymer matrix. The energy density of a covalent interface nanoparticle barium titanate in epoxy composite at a 5 vol-% particle concentration was significantly improved compared to the pure polymer dielectric film. The interfacially bonded, dielectric composite film of permittivity ~7.3 and of 30 microns thickness achieved a calculated energy density of 5.1 J/cm^3 compared to 1.3 J/cm^3 for a neat polymer film.

Keywords: A. Polymer-matrix composites (PMCs); B. Electrical properties; B. Interfacial strength; A. Nano particles; B. Surface treatments

Abbreviations: barium titanate (BT); 2-aminoethyl dihydrogen phosphate (AEP); hydrogen peroxide (HP); dielectric breakdown strength (DBS)

2.1. INTRODUCTION

Dielectric materials that are capable of efficiently storing electrical energy are desirable for many electronic and electric systems. Since the electric energy density (U) in a linear dielectric material is limited to equation $U=kE_b^2/2$, where k is the dielectric constant or permittivity of the material and E_b is the breakdown strength, both a larger permittivity and greater breakdown strength improve electric energy storage [1]. While solid ceramic materials like barium titanate (BT) have large permittivity, they are limited by a relatively low breakdown resistance due to poor processability of large parts due to high sintering temperature resulting in porosity defects and poor mechanical integrity. On the other hand, polymers usually have higher breakdown strength, excellent mechanical properties and improved processability but suffer lower permittivity [2].

Numerous efforts have been ongoing to combine the polymers of high dielectric strength with nanoparticles of high permittivity to enhance the electric energy density of a resulting nanocomposite. The approach is appealing for two reasons. Firstly, large interfacial areas in a nanocomposite could promote interfacial exchange coupling through a dipolar interface layer and lead to enhanced polarization and polarizability in polymer matrix near the interface [3,4]. Secondly, the use of nanoscale particles makes it possible to reduce the thickness of the dielectric composite film. Enhanced polarization and reduced film thickness are beneficial for energy density [5].

However, the influence of the particle interface is often underestimated. Interfaces that can conduct charge are created when dispersing high surface energy ceramic

particles into a low surface energy polymer, which can produce low breakdown resistance and also make uniform dispersion of the particles problematic. The addition of surfactants such as phosphate esters can improve dispersion and film quality that results in improved breakdown strengths compared to ceramic-particle composites without dispersants [6]. Surface complexation using phosphonate, sulfonate, silane, and carboxylate was recently tested by Schuman, et al. and other researchers [6,7]. Phosphonic acids have been reported to bond to TiO_2, ZrO_2, and In-Sn oxide surfaces and are thought to couple through heterocondensation with metal hydroxides or surface metal (crystal-defect) ions [8-10].

Modification of the particle surfaces with organo-phosphonates has resulted in improved particle dispersion and breakdown strengths. Examples include the embedding of high dielectric constant particles into poly(vinylidene difluoride) (PVDF) increasing the dielectric permittivity but reducing the breakdown strength compared to PVDF, resulted in an energy density of about 6.1 J/cm^3 at 50 vol-% at a film thickness of about 3.84 microns [7]. The energy density was greater than the current state-of-the-art biaxially oriented polypropylene high energy density capacitors (3.5-4 J/cm^3). The surface bond between the organophosphorous moiety and the metal oxide particle creates a stable, complexed organic oxide interface [6-10]. In producing a surface modified particle, only one side of the interface was controlled by coupling leaving the remaining interface to be controlled by wetting and adsorption of the polymer chains, which is variable in structure [11].

In the present work, we applied a bi-functional reagent, 2-aminoethyl dihydrogen phosphate (AEP) to modify the surface of BT nanoparticles for dispersion and covalent

reactivity with the epoxy polymer matrix properties to achieve high energy density nanocomposites of low volume concentration (5%). AEP not only bonds with particle surfaces, placing organic groups at the particle surface to assist with dispersion, but also reacts covalently with an epoxy polymer matrix. The covalent interface improves breakdown strength and energy density. In general, commercial BT nanoparticles are aggregated and show poor dispersion in organic media. To improve the dispersion of BT nanoparticles in polymer matrix, surface modification is essential and is usually achieved by adsorptive surfactants or polymer coatings [12-14]. In this work we anticipated that the AEP may increase interfacial strength compared to native BT; however, we found that nano particulate BT lacked surface reactivity to the phosphate groups and thus was difficult to form chemical bonds with the surface modifying agents. We therefore synthesized surface hydroxyl groups on BT nanoparticles using aqueous hydrogen peroxide (HP) solution [15] so as to improve the reactivity of BT nanoparticles towards a subsequent organophosphate treatment and composite interfacial strength against dielectric breakdown.

2.2. EXPERIMENTAL

In a typical surface modification reaction, nanoparticle BT (Sigma Aldrich, 30-50 nm particle size and 14 m^2/g average surface area) was dispersed in water (distilled and deionized) and degassed by sonication while under aspirator-reduced pressure for 15 min. AEP (Acros Organics)(~ 2 wt.-% of particle mass) was added to the BT filler dispersion and magnetically stirred at reflux for 5 hr. The dispersion was then recovered by micro filtration followed by re-dispersion in fresh water and filtration, repeated twice. Surface activation of BT was achieved prior to surface modification by refluxing 10 g BT powder

in 100 mL 50 wt.-% HP solution (Acros Organics) for 2 hours at 110 °C, which was cooled to 90 °C to add AEP and magnetically stirred for 2 hours. The dispersion was then recovered by filtration followed by re-dispersion in fresh water and filtration twice. Commercially available BYK-w-9010 (Byk-Chemie)(a proprietary copolymer mixture with acidic groups) was used as an adsorptive dispersant for comparison.

The powders, modified and unmodified, were analyzed by thermogravimetric analysis (TGA) and by X-ray photoelectron spectroscopy (XPS) as described before [6]. Composite films were prepared and then characterized by differential scanning calorimetry (DSC), electrical impedance and dielectric breakdown strength as described before [6].

2.3. RESULTS AND DISCUSSION

TGA measurements showed significant organic layer mass loss (2.2%, onset 180 °C) only for BT particles involving HP treatment before AEP modification (Fig. 1). The AEP mass loss, obtained after removing mass losses assigned to HP treatment and adsorbed water, corresponds to a surface group density of about 25 $Å^2$ per group that was calculated from mass loss and particle surface area, which was similar in method and calculated site density to those previously reported for surface modification of metal oxides [7-14]. Mass loss results showed poor reactivity of as received BT particles and provided strong evidence that high and robust surface coverage by AEP ligand were achieved on BT particles when HP treatment was utilized as part of the surface modification.

High resolution XPS spectra of HP treated BT indicated the generation of hydroxyl groups on the surface of BT nanoparticles (See Supplementary Information in Appendix).

Hydroxylation improved the reactivity for organophosphate modification compared to as received BT. XPS measurements indicated the introduction of phosphorous and nitrogen for AEP ligand modification (Table 2.1). It has been reported that the P(2p) spectra consists of $2p_{3/2}$ and $2p_{1/2}$ peaks, whose intensity ratio is 1.9:1.0 as theoretically determined by spin-orbit splitting [16-18]. The XPS scan of the P(2p) region (Fig. 2) of AEP modified HP treated BT (AEP HP BT) powder shows an asymmetric peak that was fitted as a spin-doublet at 133.6eV and 135.5eV, corresponding to $2P_{1/2}$ and $2P_{3/2}$ peaks, which is in good agreement with the results previously reported [16,19].

XPS characterization also clearly indicated the formation of AEP layers on the surface of extensively washed HP treated BT. The nitrogen group of the pure AEP (Fig. 3) showed nearly entirely protonated amine (85%, 401.7eV) but some free amine (15%, 400.0 eV). Based on XPS results, the amine of the AEP HP BT particles showed 58% protonated amine, binding energy 400.7eV and 42% free amine, binding energy 399.5eV and expected to be reactive upon exposure to an epoxy group of the epoxy resin. AEP bonding to BT appears mostly bidentate, which was assessed through the observed oxygen peak area ratio (2.06) of O1s peaks at 530.0 eV to 531.8 eV (Fig. 3c). An analogous free amine peak for AEP modified, as-received BT was not detectable.

Glass transition temperatures (T_g) are directly related to the free volume of polymer chains as described by the Williams-Landel-Ferry theory [20]. We suspect that interfacial effects on free volume influence the dielectric breakdown resistance and have previously evidenced that greater free volume for polymers reduces electrical breakdown resistance [6,21,22]. Polymer nanometer-sized particle composites typically show a decreased T_g, which can be caused by particle radius of curvature increasing the free

volume of polymer chains [6]. A decrease in T_g compared to pure epoxy could be due to particle curvature effects or, given the relatively large size of the particle compared to polymer radius of gyration and/or a surface-limited crosslinking reaction, could be a locally reduced crosslink density and broadened glass transition. For example, pure epoxy polymer showed a T_g of about 99 °C, while unmodified nanoparticle composites showed a depressed T_g inflection point, from about 91 to 93 °C (Table 2.2 and Fig. 4), a fairly large decrease. A weakly adsorbed interface could also explain an increased free volume [6,11] and would also reduce electromechanical strength [20].

However, amino groups present on the surface, capable of covalently reacting with the epoxy polymer matrix, should be reactive to and crosslink into the polymer-particle interface. Interfacial bonding restricts interfacial chain motion, reducing free volume locally to be similar to bulk polymer free volume and, therefore, bulk T_g of the native epoxy polymer, which is evident by an increase in T_g to 97°C for AEP HP BT composite. We observed similar T_g increases in interfacially bonded titania composites [6] and decreases in T_g for adsorbed interfaces. The T_g of AEP as-received BT (without HP surface activation) was similar to that of unmodified particle composites. XPS further supported the poor reactivity of as-received BT toward AEP by the relative absence of nitrogen or phosphate signals and, consequently, poorly reactive to the epoxy matrix.

While glass transition temperature indicated the effect of bifunctional ligand surface modification on the polymer's free volume and chain mobility, impedance spectroscopy measured the influence of the particle interface on electrical properties. Of particular interest was the Maxwell-Wagner relaxation (MW) loss at low frequency [6,23]. The samples were tested for dynamic impedance at 100 °C to thermally enhance composite

conductivity and thereby increase the signal to noise ratio (See Fig. 5 and Supplementary Information in Appendix). Dielectric constant varied little as a function of temperature although samples displayed higher dielectric constant as a result of MW loss at near-D.C. polarization frequencies. The AEP HP BT particle composites showed lower dielectric loss compared to all other adsorbed interface composites, even less than that of pure polymer, at low polarization frequencies (Fig. 5). Unmodified particle composites showed especially large dielectric losses at low polarization frequencies compared to the modified samples (Table 2.2), which corresponds to a MW or free charge relaxation loss.

The measured dielectric constants complied with a Lichtenecker mixing rule where addition of a higher dielectric constant powder into a polymer of lower dielectric constant produces a composite of enhanced permittivity [7,24]. A larger dielectric constant of the AEP HP BT compared to unmodified or AEP as-received BT was attributed to the generation of hydroxyl groups on the surface of BT by HP treatment and better surface modification, through interfacial exchange coupling that leads to enhanced interfacial polarizability near the interface [3,4]. Surprisingly, AEP HP BT composites also had lower MW loss. AEP as-received BT had a dielectric constant similar to unmodified BT with surfactant, supporting a poor reactivity of the as-received BT to the coupling agent.

Dielectric breakdown strength (DBS) was measured by applying stepwise increasing DC polarization until failure. Figure 6 shows the Weibull distributions of dielectric breakdown strengths of the composites. The measurements were merged from multiple sample results and thus show a statistical E_o. The effect of dispersion alone was represented by the unmodified, as-received BT with dispersant composite, which had a much improved breakdown resistance in comparison with the unmodified BT composite

but no added dispersant (see also ref [24]). Previous research studies on composites with nanometer sized BT for electrical insulation applications have reported a range of results from slight degradation to a significant improvement in the DBS characteristics of composites when compared to an unfilled polymer dielectric film material [24-27]. Nanometer size BT filled epoxy composites with an added dispersant generated a DBS greater than pure epoxy (Table 2.2).

Composites made from AEP HP surface modified BT particles, where a covalent interface between the polymer matrix and the coupling agent was produced, resulted in large increase in Weibull E_o. Chemically bonding the polymer to the particle surface produced a calculated energy density of around 3.63 J/cm^3 for a film of 70 μm thickness. The AEP HP BT composite DBS was nearly twice that of pure polymer of similar film thickness. The energy density of AEP as-received BT obtained was similar to that of pure polymer, which was attributed to the poor chemical reactivity of the AEP coupling agent to the as-received BT surface.

Energy storage density in a linear dielectric is proportional to the product of the dielectric constant and square of the DBS. One approach to increase energy density is to increase the dielectric constant [28]. Previous studies suggest that the volume fraction of the high dielectric constant nanoparticles has to be increased above a certain threshold (usually 30%) to effectively increase nanocomposite dielectric constant while volume fractions greater than 50 vol.-% decreases the effective dielectric constant of the nanocomposite due to increased porosity [29]. However, an increasing volume fraction of the nanoparticles typically decreases the apparent DBS of the nanocomposite owing to

the MW loss, conductivity, and a local enhancement of the electric field [24,29-31]. Higher volume concentrations also reduce the composite adhesion and flexibility. Since energy density increases with the square of the DBS, it is essential that the material has a reliable, high DBS [28]. DBS is determined by both intrinsic and extrinsic factors but there is general consensus that, except for very thin films deposited on the substrate, the DBS in practical terms is limited by defects introduced during film manufacture. Our study of DBS for varied thickness (Fig. 7 and supplementary information in Appendix) to reduce film defects demonstrated further increases in breakdown strengths and thus energy densities for AEP HP BT composites in epoxy at 5 vol-% particle composite. At a film thickness of 30 microns, the dielectric films achieved breakdown strength of 406 calculated energy density of around 5.1 J/cm^3.

2.4. CONCLUSIONS

Surface modification using a coupling agent to bond the particle surface into the polymer matrix reduced the Maxwell Wagner relaxation loss and raised the matrix glass transition temperature compared to unmodified particle dispersions. Hydrogen peroxide treatment was utilized before surface modification to greatly improve the reactivity of BT compared to untreated particles. Enhanced surface modification provided better dispersion, glass transition temperature, MW loss, dielectric constant, and greatly improved DBS. Interfacial covalent bonding increased composite resistance to charge flow and dielectric breakdown. The inclusion of the particles of higher permittivity produced a composite of enhanced dielectric constant and, with surface modification to permit interfacial cross-linking into the polymer, a polymer-particle composite of dielectric breakdown strength greater than the neat polymer film or surface unmodified

particle-polymer composites resulted. The calculated energy density for a covalent interface composite was improved 275% compared to the polymer alone. A composite film of 30 microns achieved a calculated energy density of around 5.1 J/cm^3 at 5 vol-% BT filler concentration.

2.5. ACKNOWLEDGEMENTS

This material is based upon work supported by the National Science Foundation, as part of the Pennsylvania State University-Missouri S&T I/UCRC for Dielectric Studies under Grant No. 0628817, Sub-Award No. 2164-UM-NSF-0812. The authors acknowledge the assistance of Jeff Wight for XPS measurements and Eric Bohannan for TGA & DSC measurements obtained at the Materials Research Center at the Missouri University of Science and Technology.

2.6. REFERENCES

[1] J.Y. Li, L. Zhang, S. Ducharme, Electric energy density of dielectric nanocomposites, Appl. Phys. Lett. 90 (13) (2007) 132901/1-132901/3.

[2] Y. Xiaojun, Y. Zhimin, M. Changhui, D. Jun, Dependence of dielectric properties on BT particle size in EP/BT composites, Rare Met. 25 (6) (2006) 250-254.

[3] Q.M. Zhang, H.F. Li, M. Poh, F. Xia, Z.Y. Cheng, H.S. Xu, C. Huang, An all-organic composite actuator material with a high dielectric constant, Nature 419 (694) (2002) 284-287.

[4] J. Y. Li, Exchange Coupling in P(VDF-TrFE) Copolymer Based All-Organic Composites with Giant Electrostriction, Phys. Rev. Lett. 90 (21) (2003) 217601/1-217601/4.

[5] A.V. Bune, V.M. Fredkin, S. Ducharme, L.M. Blinov, S.P. Palto, A.V. Sorokin, S.G. Yudin, A. Zlatkin, Two-dimensional ferroelectric films, Nature 391 (1998) 874-877.

[6] T.P. Schuman, S. Siddabattuni, O. Cox, F. Dogan, Improved Dielectric Breakdown Strength of Covalently-Bonded Interface Polymer-Particle Nanocomposites, Compos. Interf. 17 (8) (2010) 719-731.

[7] P. Kim, S.C. Jones, P.J. Hotchkiss, J.N. Haddock, B. Kippelen, S.R. Marder, J.M. Perry, Phosphonic acid-modified barium titanate polymer nanocomposites with high permittivity and dielectric strength, Adv. Mater. 19 (7) (2007) 1001-1005.

[8] W. Gao, L. Dickinson, C. Grozinger, F.G. Morin, L. Reven, Self-assembled monolayers of alkylphosphonic acids on metal oxides, Langmuir 12 (26) (1996) 6429-6435.

[9] P.H. Mutin, G. Guerrero, A. Vioux, Hybrid materials from organophosphorus coupling molecules, J. Mater. Chem. 15 (35-36) (2005) 3761-3768.

[10] C.M. Knobler, D.K. Schwartz, Langmuir and self-assembled monolayers, Curr. Opin. Colloid Interface Sci. 4 (1) (1999) 46-51.

[11] F.D. Blum, B.R. Sinha, F.C. Schwab, Density profile of terminally adsorbed polymers, Macromolecules 23 (12) (1990) 3592-3598.

[12] U. Paik, V.A. Hackley, S.C. Choi, Y.G. Jung, The effect of electrostatic repulsive forces on the stability of $BaTiO_3$ particles suspended in non-aqueous media, Colloids Surf. A 135 (1-3) (1998) 77-88.

[13] J. Rudolph, Z. Patzsch, W.H. Meyer, Interaction of acrylic diblock copolymers with aluminium oxide surfaces, Colloids Surf. A 86 (FM3) (1994) 299-309.

[14] S. Bhattacharjee, M.K. Paria, S.H. Maiti, Polyvinyl butyral as a dispersant for barium titanate in a non-aqueous suspension, J. Mater. Sci. 28 (23) (1993) 6490-6495.

[15] S.-J. Chang, W.-S. Liao, C.-J. Ciou, J.-T. Lee, C.-C Li, An efficient approach to derive hydroxyl groups on the surface of barium titanate nanoparticles to improve its chemical modification ability, J. Colloid Interface Sci. 329 (2) (2009) 300-305.

[16] Y. Chen, L.-R. Guo, W. Chen, X.-J. Yang, B. Jin, L.-M. Zhang, X.-H. Xia, 3-mercaptopropylphophonic acid modified gold electrode for electrochemical detection of dopamine, Bioelectrochemistry 75 (1) (2009) 26-31.

[17] M.Y. Tsai, J.C. Lin, Surface characterization and platelet adhesion studies of selfassembled monolayer with phosphonate ester and phosphonic acid functionalities, J. Biomed. Mater. Res. 55 (4) (2001) 554-565.

[18] T.M. Willey, A.L. Vance, C. Bostedt, T. van Buuren, R.W. Meulenberg, L.J. Terminello, C.S. Fadley, Surface structure and chemicalswitching of thioctic acid adsorbed onAu (111) as observed using near-edge X-ray absorption fine structure, Langmuir 20 (12) (2004) 4939-4944.

[19] M.L. Jespersen, C.E. Inman, G.J. Kearns, E.W. Foster, J.E. Hutchison, Alkanephosphonates on hafnium-modified gold: a new class of self-assembled organic monolayers, J. Am. Chem. Soc. 129 (10) (2007) 2803-2807.

[20] G.S. Grest, M.H. Cohen, Liquids, glasses, and the glass transition: A free-volume approach, Adv. Chem. Phys. 48 (1981) 455-525.

[21] P. Barber, S. Balasubramanian, Y. Anguchamy, S. Gong, A. Wibowo, H. Gao, H.J. Ploehn, H.C. Loye, Polymer composite and nanocomposite dielectric materials for pulse power energy storage, Materials 2 (4) (2009) 1697-1733.

[22] D. Ma, R.W. Siegel, J.I. Hong, L.S. Schadler, Influence of nanoparticle surfaces on the electrical breakdown strength of nanoparticle-filled low-density polyethylene, J. Mater. Res. 19 (3) (2004) 857-863.

[23] M. Roy, J.K. Nelson, R.K. MacCrone, L.S. Schadler, C.W. Reed, R. Keefe, W. Zenger, Polymer nanocomposite dielectrics - The role of the interface, IEEE Trans. Dielectr. Electr. Insul. 12 (4) (2005) 629-643.

[24] L.J. Gilbert, T.P. Schuman, F. Dogan, Dielectric powder/polymer composites for high energy density capacitors, in: F. Dogan, P.N. Kumta (Eds), Ceramic Transactions (Advances in Electronic and Electrochemical Ceramics), Wiley, NewYork, 176, 2006, 17-26.

[25] E. Tuncer, I. Sauers, D.R. James, A.R. Ellis, M.P. Paranthaman, T. Aytug, S. Sathyamurthy, K.L. More, J. Li, A. Goyal, Electrical properties of epoxy resin based nanocomposites, Nanotechnology 18 (2) (2007) 25703-25708.

[26] E. Tuncer, I. Sauers, D.R. James, A.R. Ellis, R.C. Duckworth, Nanodielectric System for Cryogenic Applications: Barium Titanate filled Polyvinyl Alcohol, IEEE Trans. Dielectr. Electr. Insul. 15 (1) (2008) 236-242.

[27] J.K. Nelson, Y. Hu, Nanocomposite dielectric-properties and implications, J. Phys. D: Appl. Phys. 38 (2) (2005) 213-222.

[28] D. Stephen, An inside-out approach to storing electrostatic energy, ACS Nano 3 (9) (2009) 2447-2450.

[29] P. Kim, N.M. Doss, J.P. Tillotson, P.J. Hotchkiss, M.J. Pan, S.R. Marder, J. Li, J.P. Calame, J.W. Perry, High energy density nanocomposites based on surface modified $BaTiO_3$ and a ferroelectric polymer, ACS Nano 3 (9) (2009) 2581-2592.

[30] C. Huang, Q. Zhang, Enhanced dielectric and electromechanical responses in high dielectric constant all-polymer percolative composites, Adv. Funct. Mater. 14 (5) (2004) 501-506.

[31] Y. Shen, Y. Lin, C.W. Nan, Interfacial effect on dielectric properties of polymer nanocomposites filled with core/shell-structured particles, Adv. Funct. Mater. 17 (14) (2007) 2405-2410.

Table 2.1. The characterization of atomic percent composition at the surface of modified BT powders as measured by XPS.

Powder	XPS (atomic percent)					
	C (1s)	Ba (3d)	Ti (2p)	O (1s)	N (1s)	P (2p)
BT	28.48	8.5	13.18	46.35	3.5	0
HPwashBT	28.05	7.59	12.08	52.01	0	0
AEPBT	24.57	7.49	11.98	51.81	0.55	3.59
AEP.HPwash.BT	36.18	6.05	8.06	49.53	3.22	6.96

Table 2.2. Electrical characterization data of the epoxy polymer compared with the BT polymer composites at a 5 vol.-% filler concentration.

Dielectric film (~70 μm thickness)	T_g	Permittivity	Dielectric Loss		Breakdown Strength	Energy Density
	(°C)	ε′ (at 10 kHz)	at 1 kHz	at 10 kHz	($V \cdot \mu m^{-1}$)	($J \cdot cm^{-3}$)
pure polymer	99	3.9	0.014	0.022	277	1.3
BT (w/o 9010)	94	6.1	0.033	0.034	240	1.6
BT (w/ 9010)	95	6.8	0.018	0.026	310	2.9
HP.BT (w/ 9010)	92	6.9	0.024	0.043	235	1.7
AEP.BT	93	6.7	0.017	0.024	225	1.5
AEP.HP.BT	97	7.3	0.014	0.022	335	3.6
AEP.HP.BT (30 μm)	–	6.9	0.016	0.019	406	5.1

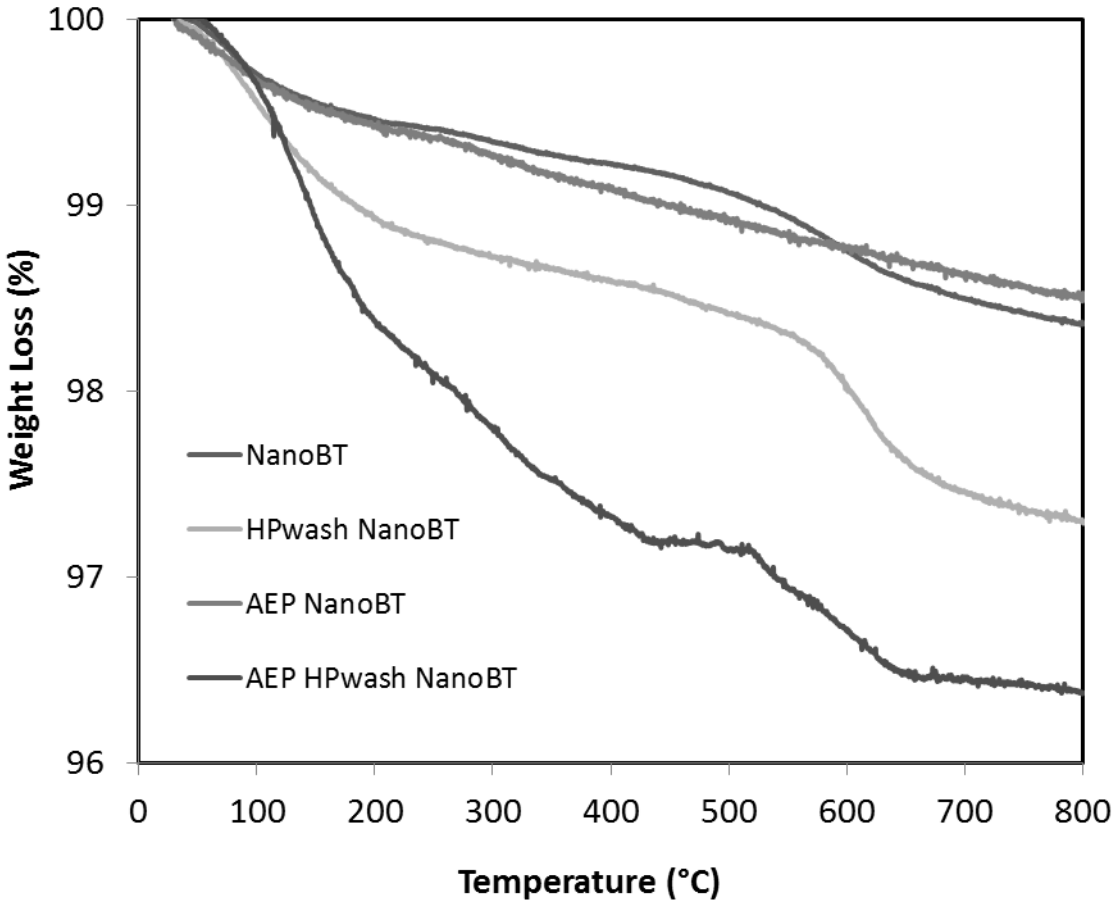

Figure 1. Thermogravimetric analysis curves of surface modified and unmodified BT particles showing significant organic weight loss compared to as-received nanopowder $BaTiO_3$ (BT) for only AEP modified HP treated BT particles.

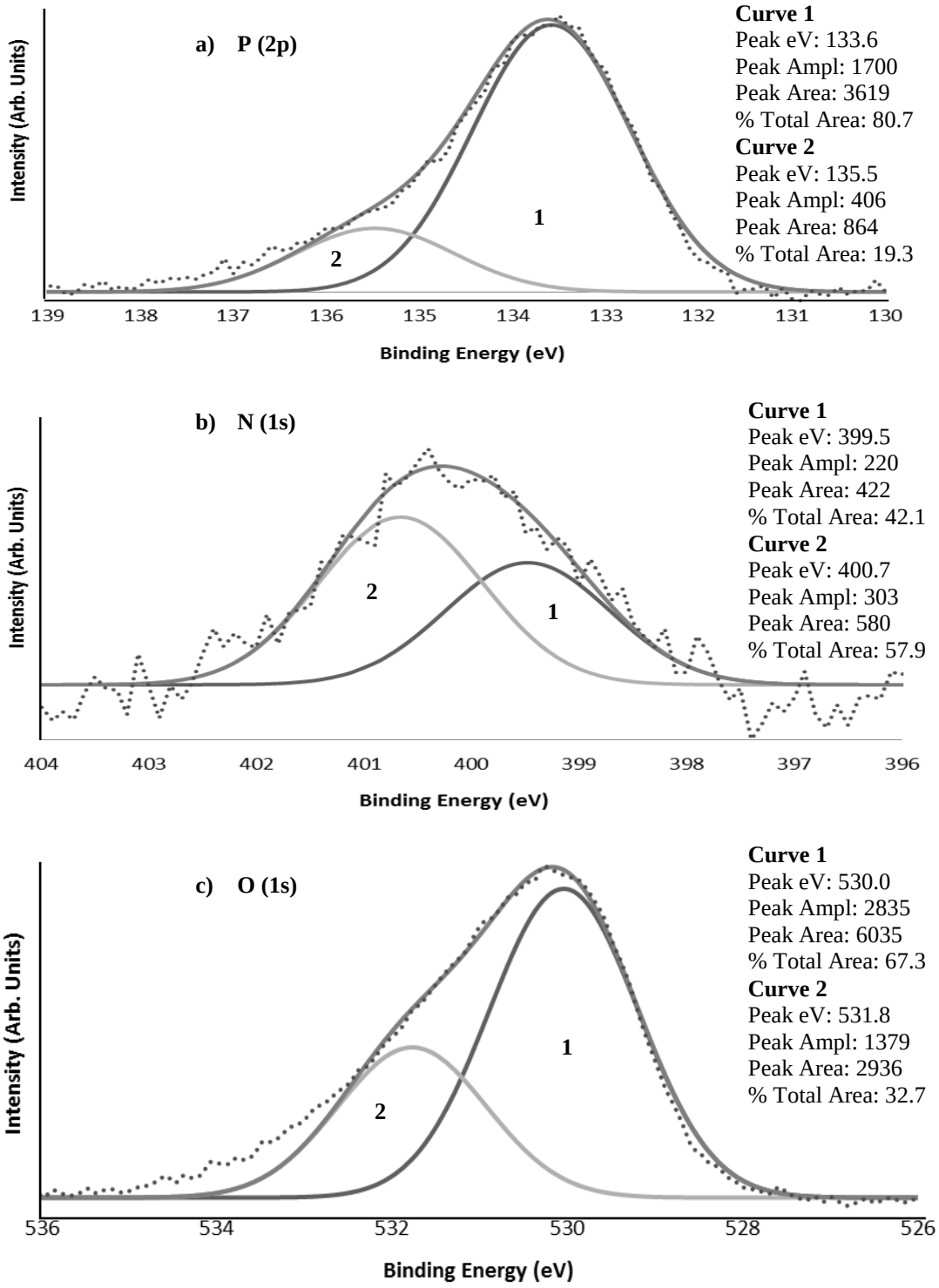

Figure 2. XPS spectra of: a) P(2p), b) N(1s) and c) O(1s) regions of AEP HP BT. Dotted line shows the raw data points that are plotted with continuous line deconvoluted and fitting summation curves.

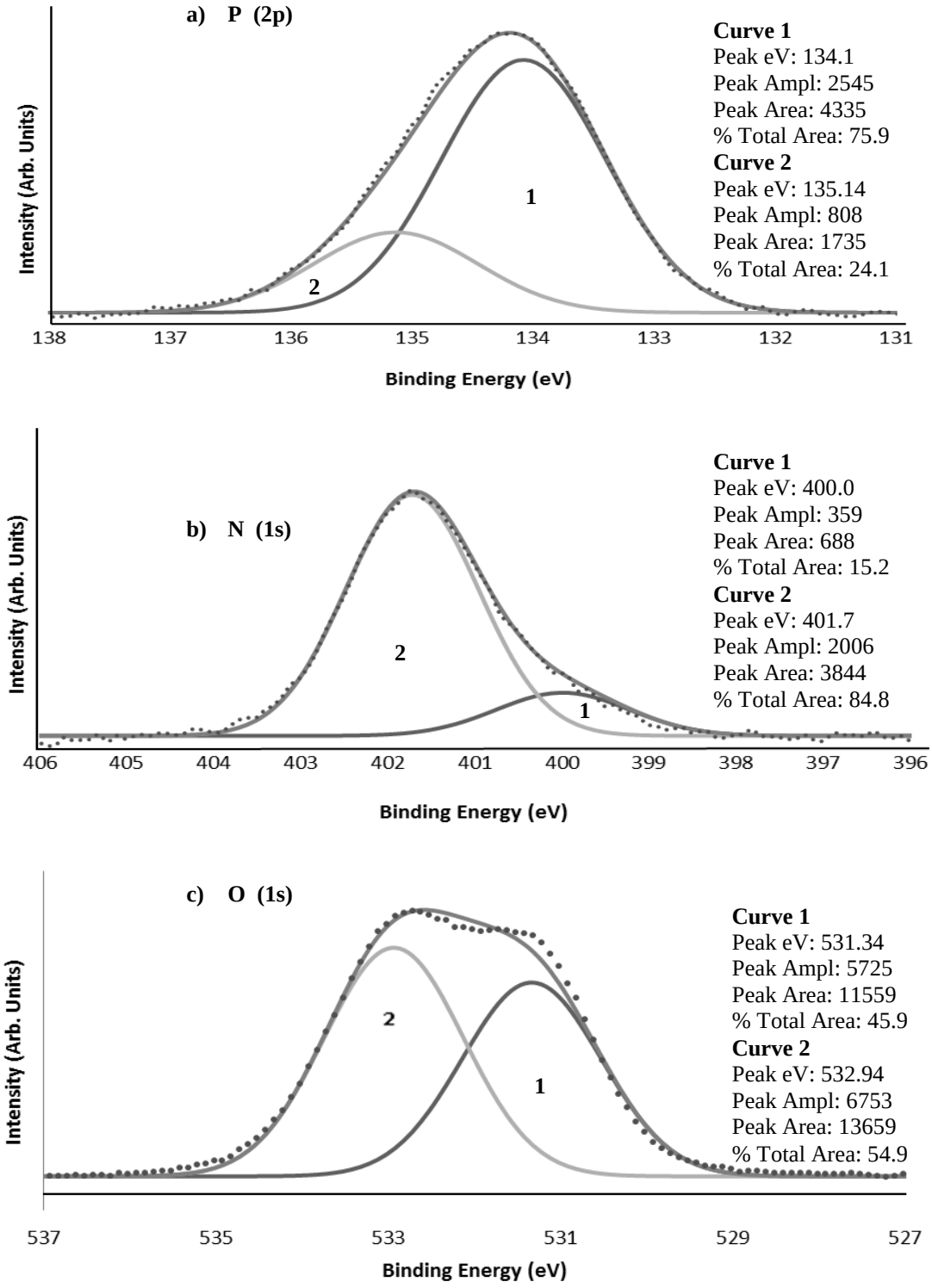

Figure 3. XPS spectra of: a) P(2p), b) N(1s) and c) O(1s) regions of aminoethylphosphate (AEP). Dotted line shows the raw data points that are plotted with continuous line deconvoluted and fitting summation curves.

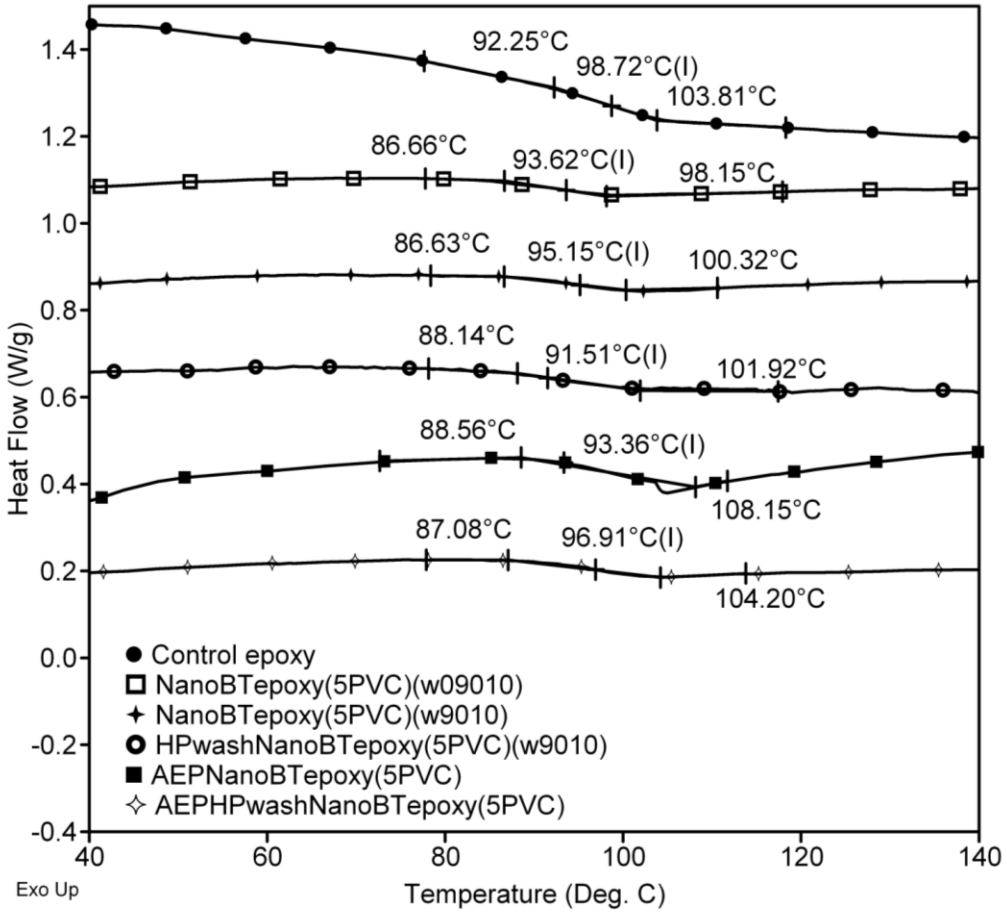

Figure 4. DSC plot of the epoxy polymer in comparison to the 5 vol.-% BT-epoxy composites. W/O9010 and W/9010 in the legend indicates as-received BT composites synthesized without and with a dispersant, respectively. HP and AEP refer to hydrogen peroxide and aminoethylphosphate treatments of BT powder, respectively, made before synthesis of the dielectric composite.

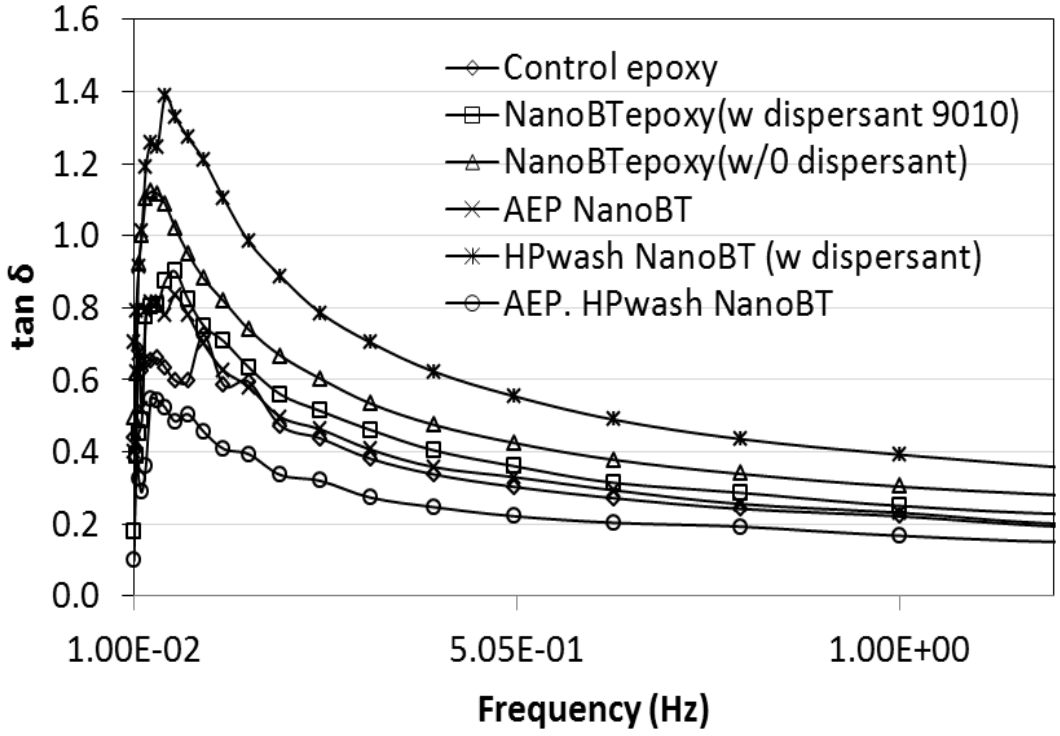

Figure 5. Frequency dependent dielectric loss response of pure polymer and 5 vol.-% BT-epoxy dielectric composites, measured at 100 °C.

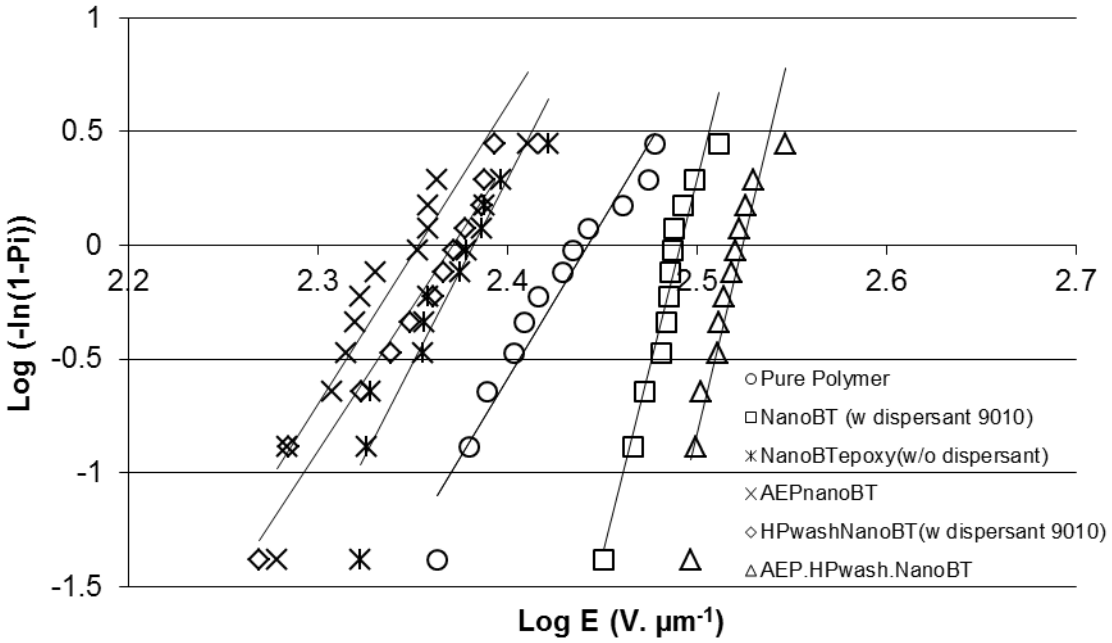

Figure 6. Weibull plot of dielectric breakdown measurements for epoxy polymer 5 vol.-% BT epoxy composite dielectric films.

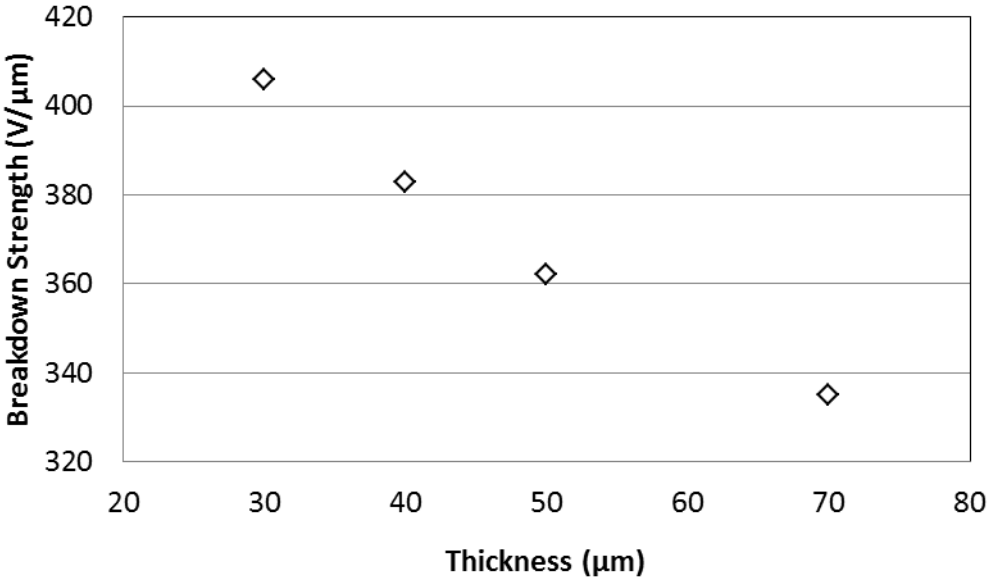

Figure 7. Dielectric breakdown measurements plotted as a function of film thickness measurements of AEP HP BT composite dielectric samples.

APPENDIX
SUPPLEMENTARY INFORMATION

This document shows XPS comparison plots of as-received nanoBT and HP treated nanoBT (**Section 1**), dielectric constant versus frequency plot of dielectric nanocomposites measured at 100 °C (**Section 2**), and a table showing film thickness variation study of AEP HP NanoBT epoxy dielectric (**Section 3**).

1. High resolution XPS comparison plots of as-received nanoBT and HP treated nanoBT

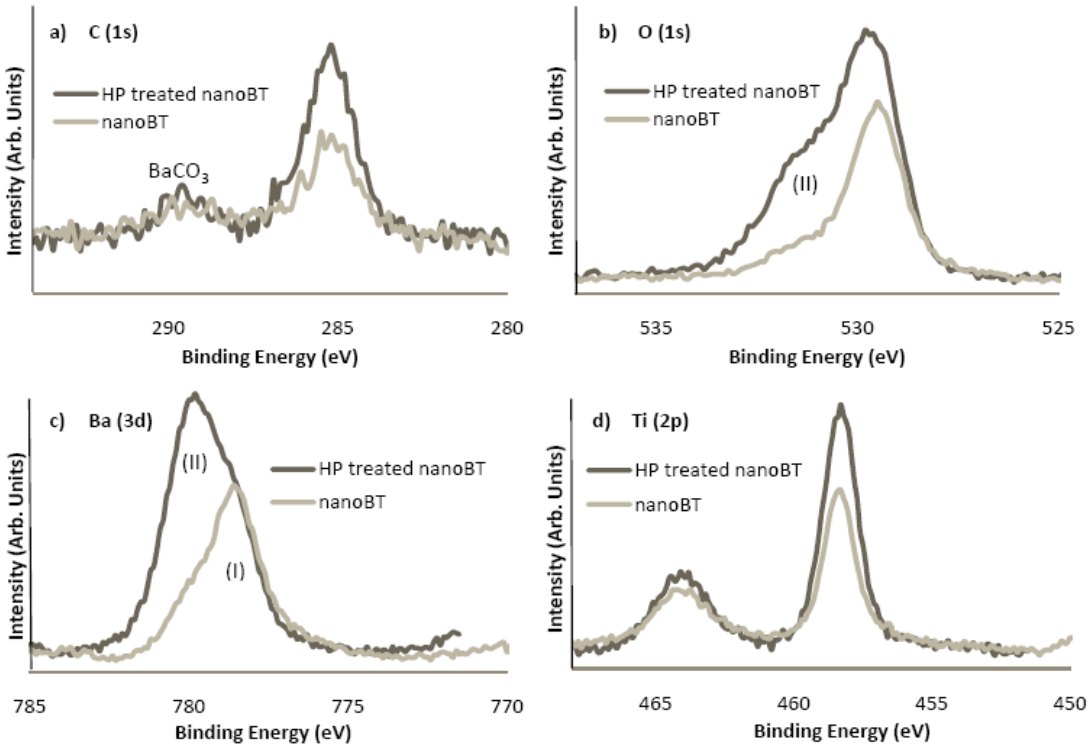

Figure 1. Comparative plots of the: a) C (1s), b) O (1s), c) Ba (3d) and d) Ti(2p) XPS spectra between hydrogen peroxide (HP) treated nanoBT and as-received nanoBT. The label 'I' was assigned to the perovskite structure while 'II' was assigned to surface oxide/hydroxide species. Assignment that shows a reduction of surface barium carbonate is labeled in the C(1s) spectrum.

Generation of hydroxyl groups by treating the surface of BT nanoparticles with aqueous hydrogen peroxide solution was evident from the XPS scan of the O(1s) region for HP treated nanoBT compared to as-received nanoBT. The main photoemission centered on 529.5 eV was assigned to oxygen in the $BaTiO_3$ lattice, which is in good agreement with the literature [1,2]. A broadened high binding energy shoulder associated with the main peak was assigned as hydroxyls or strongly chemisorbed H_2O (531.5 eV, Fig. 1b), which is in good agreement from previous studies [1] and XPS of bulk [3,4] and single crystal [5] $BaTiO_3$. The high resolution XPS spectra of the Ba(3d) region shows two components at 778.5 eV and 780 eV, which indicated the existence of barium in two different chemical environments [3]. The low energy component was assigned to the perovskite structure and the high energy emission that increased in intensity after peroxide treatment could be assigned as either $BaCO_3$ or $Ba(OH)_2$. While both $BaCO_3$ and $Ba(OH)_2$ environments possess binding energies of ~780.0 eV, we assigned the 780.0 eV emission to $Ba(OH)_2$ by corroborating the C(1s) region (C(1s) ~ 289.5 eV, see Fig. 1a) against the Ba(3d) region (Fig. 1c), which indicated a decrease in the $BaCO_3$ signal upon peroxide treatment. Thus, hydroxyl groups that were generated on the surface of nanoBT by HP treatment appear to be associated with surface barium rather than surface titanium groups since the high resolution XPS spectrum of the Ti(2p) region (Fig. 1d) appeared unchanged after HP treatment.

References:

1. Wegmann M, Watson L, Henry A. XPS analysis of submicrometer barium titanate powder. J Am Ceram Soc 2004; 87(3): 371-377.

2. Kumar S, Raju VS, Kutty TRN. Investigations on the chemical states of sintered barium titanate by X-ray photoelectron spectroscopy. Appl Surf Sci 2003; 206(1-4): 250-261.
3. Battye FL, Hochst H, Goldmann A. Photoelectron studies of the $BaTiO_3$ and $SrTiO_3$ valence states. Solid State Communications 1976; 19(3): 269-271.
4. Nakamatsu H, Adachi H, Ikeda S. Electronic structure of the valence band for perovskite-type titanium double oxides studied by XPS and DV-Xa cluster calculations. J Electron Spectrosc Relat Phenom 1981; 24(2): 149-159.
5. Pertosa P, Michel-Calendini F. X-Ray Photoelectron Spectra, Theoretical Band Structures, and Densities of States for $BaTiO_3$ and $KNbO_3$. Phys Rev B 1978; 17(4): 2011-2020.

2. Dielectric constant versus frequency plot of dielectric nanocomposites measured at 100 °C

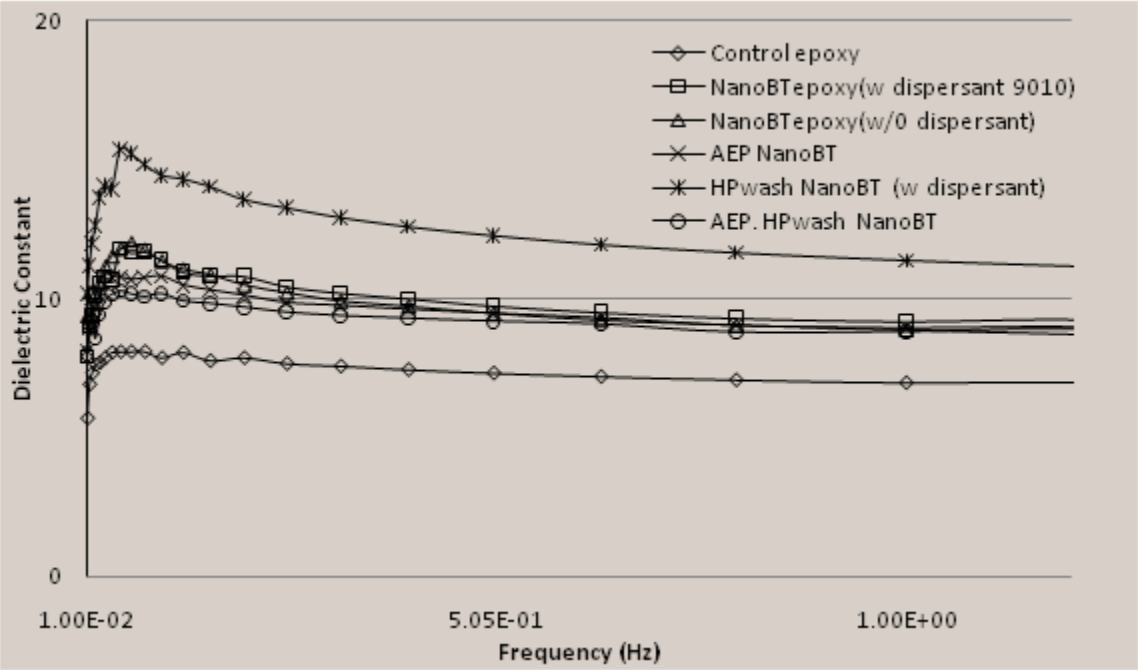

Figure 2. Frequency dependent dielectric constant of the epoxy polymer and 5 vol.-% nanoBT-epoxy dielectric composites, measured at 100 °C.

3. Table showing film thickness variation study of AEP HP NanoBT epoxy dielectric

Table I. Calculated energy densities as a function of the film thickness and breakdown strength of AEP HP nanoBT epoxy dielectric composites.

Thickness (μm)	Breakdown Strength(V/μm)	Energy Density(J/cm^3)
70	335	3.63
50	362	4.23
40	383	4.74
30	406	5.10

3. INTERFACE CONTROLLED HIGH ENERGY DENSITY POLYMER NANOCOMPOSITES

Sasidhar Siddabattuni,[a] *Thomas P. Schuman,*[a,*] *Fatih Dogan*[b]

[a] Missouri University of Science and Technology (formerly the University of Missouri-Rolla), Chemistry Department, 400 W. 11th Street, Rolla, MO 65409 (USA)
[b] Missouri University of Science and Technology, Materials Science and Engineering Department, 1400 N. Bishop Avenue, Rolla, MO 65409 (USA)
[*] Address all correspondence to tschuman@mst.edu

ABSTRACT Chemical bonding via covalent interface between polymer and particle in nanocomposite dielectric films improve resistance to flow of charge and dielectric breakdown. A bi-functional organophosphate coupling agent utilized to interact with the inorganic oxide particles surface not only assists in dispersion with thermosetting epoxy polymer matrix, but also covalently reacts with the polymer matrix upon curing. Interfacially coupled nanodielectric composite attains retention of native polymer glass transition temperature, reduced dielectric losses (including Maxwell-Wagner relaxation at very low frequencies) and improved dielectric breakdown resistance compared to nanocomposite dielectrics that lacked interfacial coupling. The energy density of an interfacially bonded 5 vol-% nano-sized barium titanate in epoxy composite was nearly thrice that of the pure polymer dielectric film. At higher volume concentration, 30 vol-%, a dielectric composite film of permittivity ~21.8 at 20μm film thickness achieved a calculated energy density of ~7.5 J/cm^3 with dielectric losses of less than 2.4% at 10 kHz.

KEYWORDS: covalent interface · organophosphate · dielectric breakdown · permittivity · energy density

INTRODUCTION

Dielectric materials are used to control and store electrical charges and electric energies that plays a key role in modern electronics and electric power systems.[1] The maximum energy density, (U_{max}), (energy stored per volume) in a linear dielectric material is limited to equation (1), where ε_r is the dielectric constant or permittivity of the material, ε_o (8.854×10^{-12} F/m) is the permittivity of free space and E_b is the breakdown strength. Both a larger permittivity and greater breakdown strength improve electric energy storage.[2]

$$U_{max} = \frac{1}{2}\varepsilon_o \varepsilon_r E_b^2 \quad (1)$$

Inorganic ceramic materials usually have large permittivity, but they are limited by their relatively small breakdown strengths, poor processability and mechanical properties due to high sintering temperature and porosity. On the other hand, polymers, which are usually organic have higher breakdown strength, excellent mechanical properties and processability but suffer from smaller permittivity.[2-4] Miniaturization and the current increasing need for high-power density, high voltage capacitors and power-storage devices have stimulated the use of polymer nanocomposites or nanocomposite dielectrics. By incorporating high permittivity inorganic nanoparticles into a polymer matrix with low dielectric loss and high breakdown strength, one may be able to develop new composite materials that have improved dielectric properties (dielectric strength, permittivity and dielectric losses) and retain the unique attributes of polymers.[5-10]

The most distinctive feature of polymer nanocomposites in comparison with conventional microcomposites, is the extremely high surface area between the

nanoparticles and the polymer matrix. Smaller the size of the embedded nanoparticles, larger is the surface area to volume ratio, which leads to larger interface regions.[11] Large interfacial areas in a nanocomposite could promote interfacial exchange coupling through a dipolar interface layer and lead to enhanced polarization and polarizability in polymer matrix near the interface.[12,13] The use of nano-sized particles makes it possible to reduce the thickness of the dielectric composite film. Enhanced polarization and reduced film thickness are beneficial for energy density.[14]

Control of interface is very important as the properties of polymer nanocomposites are often influenced by the interfacial region. Failure to control the interface results in aggregation or agglomeration of nanoparticles in polymer matrix, which leads into undesirable properties of resulting nanocomposites due to poor film quality and inhomogeneities.[7,15] In other words, interfaces that can conduct charge are created when dispersing high surface energy ceramic particles into a low surface energy polymer, which can produce low breakdown resistance and also make uniform dispersion of the particles problematic.[16]

Surface modification of nanoparticles can be obtained by using suitable surfactants that yields adsorptive interface or grafting organic groups on the surface of metal oxide nanoparticles using phosphates, phosphonates or silanes as coupling agents or dispersants which yields stable and complex organic oxide interface.[16,17] The addition of surfactants such as phosphate esters and organo-phosphonates improve dispersion and film quality that results in improved breakdown strengths compared to ceramic-particle composites without dispersants.[7,16] Examples include the embedding of high dielectric constant particles into poly(vinylidene difluoride) (PVDF) increasing the dielectric permittivity

but reducing the breakdown strength compared to PVDF, resulted in an energy density of about 6.1 J/cm^3 at 50 vol-% at a film thickness of about 3.84 μm. The energy density was greater than the current state-of-the-art biaxially oriented polypropylene high energy density capacitors (3.5 - 4 J/cm^3).[7]

In producing a surface modified particle, only one side of the interface was controlled by coupling leaving the remaining interface to be controlled by wetting and adsorption of the polymer chains, which is variable in structure.[18] In general, particulate inclusions of uncontrolled interfacial chemistry appear to decrease breakdown strength except for few exceptions: those composites typically involving high resistivity, low permittivity oxides like barium oxide, magnesium oxide, or silica/alumina nanoparticles.[2,5,16,19,20] A strongly bonded interface appears to be the key to enhancing resistance to dielectric breakdown via the filler interfaces.

In the present work, we report high energy density dielectric nanocomposites resulted from the surface functionalized barium titanate (BT) nanoparticles in epoxy polymer matrix. We applied a bi-functional coupling agent, 2-aminoethyl dihydrogen phosphate (AEP) to modify the surface of BT nanoparticles for dispersion and covalent reactivity with the epoxy polymer matrix to achieve high energy density nanocomposites. AEP not only bonds with particle surfaces, placing organic groups at the particle surface to assist with dispersion, but also reacts covalently with an epoxy polymer matrix upon curing. We anticipate that the AEP modified nanoBT may increase interfacial strength compared to native BT. However, commercial BT nanoparticles were found to be less reactive and difficult to manipulate their surface chemistry with organophosphates. We therefore synthesized surface hydroxyl groups on BT nanoparticles using aqueous hydrogen

peroxide (HP) solution[21] so as to improve the reactivity of BT nanoparticles towards a subsequent organophosphate treatment and composite interfacial strength against dielectric breakdown.

RESULTS AND DISCUSSION

Thermogravimetric analysis (TGA) measurements obtained for surface modified and unmodified powders showed significant organic layer weight loss (2.2%, onset 180 °C) only for AEP modified nano BT particles involving HP treatement (Fig. 1). TGA measurements of AEP modified HP treated BT particles showed surface group density of about 25 $Å^2$ per group calculated from mass loss (after removing mass losses assigned to HP treatment and adsorbed water) and particle surface area, which was similar to those previously reported for surface modification of metal oxides.[7,18,22-27] Poor reactivity of AEP ligand onto the surface of as received BT particles is clearly evident from weight loss data and strongly supports that high, robust surface coverage by AEP ligand is achieved only when HP treatment was involved before surface modification.

Generation of hydroxyl groups on the surface of BT nanoparticles was confirmed from the high resolution X-ray photoelectron spectroscopy (XPS) spectra of HP treated BT (See Supplementary Information in Appendix). XPS measurements indicated the introduction of phosphorous and nitrogen for AEP ligand modification (Table 3.1), which also gave evidence that the hydroxylation of BT improved the reactivity for organophosphate modification compared to as received BT. Theoretically, P(2p) spectra consists of doublet peaks with intensity ratio of 1.9:1.0, corresponding to $2p_{3/2}$ and $2p_{1/2}$ peaks , determined by spin-orbit splitting.[28-30] XPS characterization of AEP modified HP treated BT (AEP HP BT) (Fig. 2) powder shows the formation of AEP layers on the

surface of BT nanoparticles, clearly evident from P(2p) and N(1s) peaks. P(2p) peaks that were fitted as a spin-doublet at 133.6eV and 135.5eV corresponds to $2P_{3/2}$ and $2P_{1/2}$ peaks are in good agreement with the results previously reported.[28,31] AEP bonding to BT appears mostly bidentate, which was assessed through the observed oxygen peak area ratio (2.06) of O1s peaks at 530.0 eV to 531.8 eV (Fig. 2c). XPS scan of nitrogen group of pure AEP (Fig. 3) showed mostly protonated amine (85%, 401.7eV) with less free amine (15%, 400.0 eV). But the XPS scan of nitrogen group of AEP HP BT particles showed 58% protonated amine (400.7eV) and 42% free amine (399.5eV) (Fig. 2b). The free amine on the surface of AEP modified HP treated BT particles is expected to be reactive upon exposure to an epoxy group of the epoxy resin. An analogous free amine peak for AEP modified, as-received BT was not detectable.

Glass transition temperature (T_g), obtained by differential scanning calorimetry (DSC), is directly related to the free volume of polymer chains[32] which can quantitatively provide indirect information on the nanocomposite interface. The effect of T_g depends on the interaction strength between the polymer and nanoparticles.[33] With few exceptions,[33] generally polymer nanometer-sized particle composites typically show a decreased T_g, which can be caused by particle radius of curvature increasing the free volume of polymer chains.[16] For example, pure epoxy polymer showed a T_g of about 99 °C, while unmodified nanoparticle composites showed a depressed T_g inflection point, from about 92 to 95 °C (Table 3.2 and Fig. 4), a fairly large decrease. A decrease in T_g compared to pure epoxy could be due to particle curvature effects or, given the relatively large size of the particle compared to polymer radius of gyration and/or a surface-limited crosslinking reaction, could be a locally reduced crosslink density and broadened glass transition. A

weakly adsorbed interface could also explain an increased free volume[16,18] and would also reduce electromechanical strength.[32]

Free amino groups present on the surface of AEP modified HP treated BT particles, capable of covalently reacting with the epoxy polymer matrix, should be reactive to and crosslink into the polymer-particle interface upon curing resulting into stronger interface compared to adsorbed interface. Interfacial covalent bonding restricts interfacial chain motion, reducing free volume locally to be similar to bulk polymer free volume and, therefore, bulk T_g of the native epoxy polymer, which is evident by an increase in T_g to 97°C for AEP HP BT composite. Free volume has influence on the dielectric breakdown resistance and have previously evidenced that greater free volume for polymers reduces electrical breakdown resistance.[16,34,35] The T_g of AEP as-received BT (without HP surface activation) was similar to that of unmodified particle composites. XPS further supported the poor reactivity of as-received BT toward AEP by the relative absence of nitrogen or phosphate signals and, consequently, poorly reactive to the epoxy matrix.

Surface modification of BT particles using organophosphate also provided improved dispersion compared to unmodified BT particles with, without surfactant, evident from freeze fractured cross sectional Scanning electron microscopy (SEM) images of the nanocomposites at 5 vol % (see Supporting Information in Appendix). SEM images of unmodified BT particles exhibited cracks, pinhole defects and aggregates. In contrast, nanocomposites with organophosphate ligand with HP surface activation yielded uniform, improved dispersion quality even compared to AEP modified as-received BT composite.

Electrical properties of the pure polymer and their BT composites were studied by impedance spectroscopy. Frequency dependent permittivity and dielectric loss measurements obtained by impedance spectroscopy (Table 3.2), measured at room temperature, showed lower dielectric loss for covalent interface BT composites with surface activation possibly due to stronger interaction between polymer and particle compared to physically adsorbed interface composites. Dielectric constant values varied little for covalent interface compared to adsorbed interface composites, with slightly higher value for covalent interface AEP HP BT particle composites. Slightly higher dielectric constant of the AEP HP BT compared to unmodified or AEP as-received BT was attributed to the generation of hydroxyl groups on the surface of BT by HP treatment and better surface modification, through interfacial exchange coupling that leads to enhanced interfacial polarizability near the interface.[12,13]

Maxwell-Wagner relaxation (MW) loss at very low frequencies was of particular interest.[11,16] To be able to observe the MW loss trend in the composites comparatively, all samples were tested for dynamic impedance at higher temperature, 100 °C, to thermally enhance composite conductivity and thereby increase the signal to noise ratio (Fig. 5). The AEP HP BT particle composites showed lower dielectric loss compared to all other adsorbed interface composites, even less than that of pure polymer, at low polarization frequencies is attributed to the possible stronger covalent interactions at the interface. Unmodified particle composites showed higher dielectric losses at low polarization frequencies compared to the modified samples, which corresponds to a MW or free charge relaxation loss. Dielectric constant varied little as a function of temperature (See

Supplementary Information in Appendix) although samples displayed higher dielectric constant as a result of MW loss at near-D.C. polarization frequencies.

The results for dielectric breakdown voltages were obtained using high voltage generator by applying stepwise increasing DC polarization until failure. The dielectric breakdown strength (DBS) data obtained were analyzed using Weibull failure analysis method which has been frequently adopted for the investigation of dielectric breakdown of different materials systems.[36] Figure 6 shows the Weibull distributions of dielectric breakdown strengths of the composites at 5 vol.-%. The measurements were merged from multiple sample results and thus show a statistical E_o. Unmodified BT composites with dispersant alone showed improved breakdown resistance compared to without dispersant composite system signifying the effect of dispersion by surface modifying agents. From previous studies with nanometer sized BT composites for electrical insulation applications, DBS results from slight degradation to a significant improvement compared to unfilled polymer were reported.[15,36-38] Nanometer size BT filled epoxy composites with an added dispersant generated a DBS greater than pure epoxy (Table 3.2).

Large increase in Weibull E_o was resulted from the composites made from AEP HP BT particles, where a covalent interface between the polymer matrix and the AEP coupling agent is produced in comparison to both pure polymer and the composites with adsorbed interface. Nearly thrice the energy density of pure polymer was observed by chemically bonding the polymer to the particle surface using AEP as coupling agent in 5 vol.-% composites at 70μm film thickness (Table 3.2). The energy density of AEP as-received BT composites obtained was similar to that of pure polymer, which was attributed to the poor chemical reactivity of the AEP coupling agent to the as-received BT surface.

From equation (1), as the energy storage density in a linear dielectric is proportional to the square of the DBS, it is essential that the material has a reliable, high DBS.[39] Even though DBS is determined by both intrinsic and extrinsic factors, there is general consensus that, except for very thin films deposited on the substrate, the DBS in practical terms is limited by defects introduced during film manufacture. By varying film thickness (Fig. 7 and supplementary information in Appendix) to reduce film defects, we studied DBS that demonstrated further increases in breakdown strengths and thus energy densities for AEP HP BT composites in epoxy at 5 vol-% particle composite. Breakdown strength of 406 V/μm that resulted in calculated energy density of around 4.6 J/cm^3 was achieved at a dielectric film thickness of around 30μm (Table 3.2).

Increase in the dielectric constant by increasing the particle volume concentration in nanocomposite dielectric also results in increased energy storage density.[39] Previous studies suggest that the volume fraction of the high dielectric constant nanoparticles has to be increased to and above a certain threshold (usually 30%) to effectively increase nanocomposite dielectric constant while volume fractions greater than 50 vol.-% decreases the effective dielectric constant of the nanocomposite due to increased porosity [40]. At very high filler loadings, composite adhesion and film integrity also needs to be considered. Increasing volume fraction of the nanoparticles typically decreases the apparent DBS of the nanocomposite owing to the MW loss, conductivity, and a local enhancement of the electric field.[15,40-42] At higher filler loadings, one compromises in DBS to accommodate an increase in dielectric constant to optimize resulting energy density.[43] We summarize the dielectric properties obtained in our work for AEP HP BT composites in epoxy at different filler loadings in Table 3.3. At 30 volume fraction filler

loading and dielectric film thickness of ~20 microns, maximum energy density of ~7.5 $J \cdot cm^{-3}$ with dielectric loss of ~2.4 % was observed.

CONCLUSIONS

Interfacial coupling through covalent interface is an effective approach to improve interaction between polymer and particle in a nanocomposite dielectric film that resulted in improved dielectric properties compared to adsorbed interface and unmodified particle dispersions. Surface activation of nano-sized BT particles was utilized using HP treatment before surface modification to effectively improve the reactivity of BT particles towards organophosphate coupling agent compared to untreated particles. Surface modification of HP treated BT particle composites in epoxy yielded better quality of dispersion, raise in glass transition temperature, low MW loss, better dielectric constant and enhancement in DBS comparatively. Improvement in properties is mainly attributed to the stronger polymer-particle interaction due to covalent interface. The calculated energy storage density for a covalent interface composite was improved significantly compared to the polymer alone. A dielectric composite film of 30μm thickness achieved a calculated energy density of around 4.6 J/cm^3 at 5 vol-% BT filler concentration. When increased the filler loading to 30 vol.-% to increase dielectric constant, the interfacially bonded composite resulted in a dielectric film of permittivity ~21.8 at 20μm thickness that achieved a calculated energy density of 7.5 J/cm^3.

EXPERIMENTAL METHODS

In a typical surface modification reaction, nanoparticle BT (Sigma Aldrich, 30-50 nm particle size and 14 m^2/g average surface area) was dispersed in water (distilled and

deionized) and degassed by sonication while under aspirator-reduced pressure for 15 min. AEP (Acros Organics)(~ 2 wt.-% of particle mass) was added to the BT filler dispersion and magnetically stirred at reflux for 5 hr. The dispersion was then recovered by micro filtration followed by re-dispersion in fresh water and filtration, repeated twice. Surface activation of BT was achieved prior to surface modification by refluxing 10 g BT powder in 100 ml 30 wt.-% HP solution (Acros Organics) for 2 hours at 110 °C, which was cooled to 90 °C to add AEP and magnetically stirred for 2 hours. The dispersion was then recovered by filtration followed by re-dispersion in fresh water and filtration twice. Commercially available BYK-w-9010 (Byk-Chemie)(a proprietary copolymer mixture with acidic groups) was used as an adsorptive dispersant for comparison.

The powders, modified and unmodified, were analyzed by TGA and by XPS as described before.[16] Composite films were prepared and then characterized by SEM, DSC, electrical impedance and dielectric breakdown strength as described before.[16]

ACKNOWLEDGMENTS

This material is based upon work supported by the National Science Foundation, as part of the Pennsylvania State University-Missouri S&T I/UCRC for Dielectric Studies under Grant No. 0628817, Sub-Award No. 2164-UM-NSF-0812. The authors acknowledge the assistance of Jeffry Wight for XPS measurements and Eric Bohannan for TGA & DSC measurements obtained at the Materials Research Center at the Missouri University of Science and Technology.

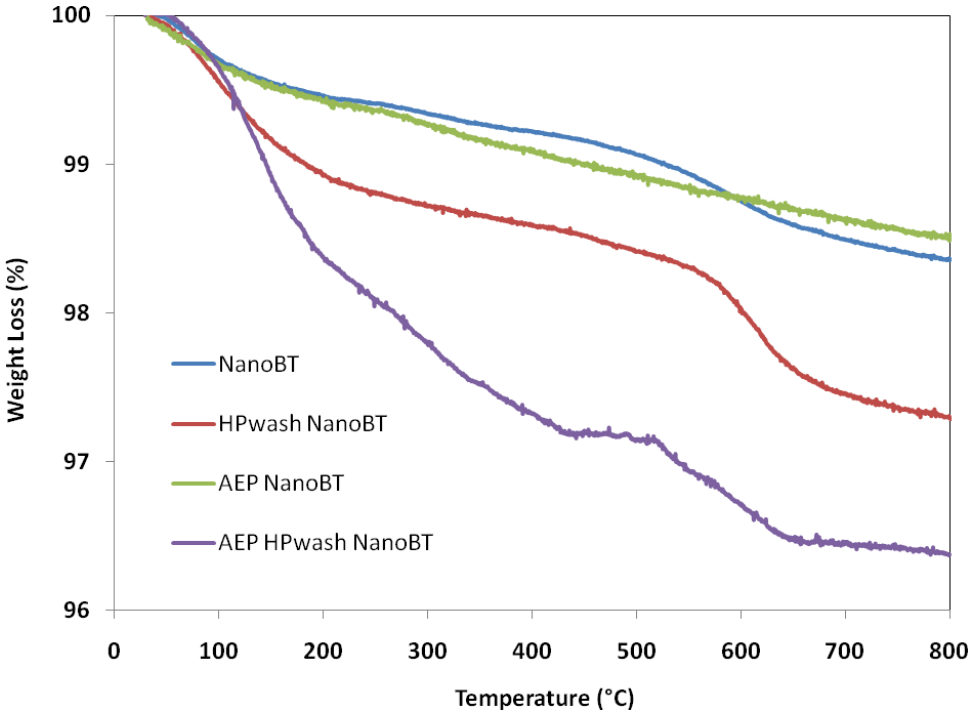

Figure 1. TGA analysis of surface modified and unmodified BT particles showing significant organic weight loss for only AEP modified HP treated BT particles compared to as-received BT particles.

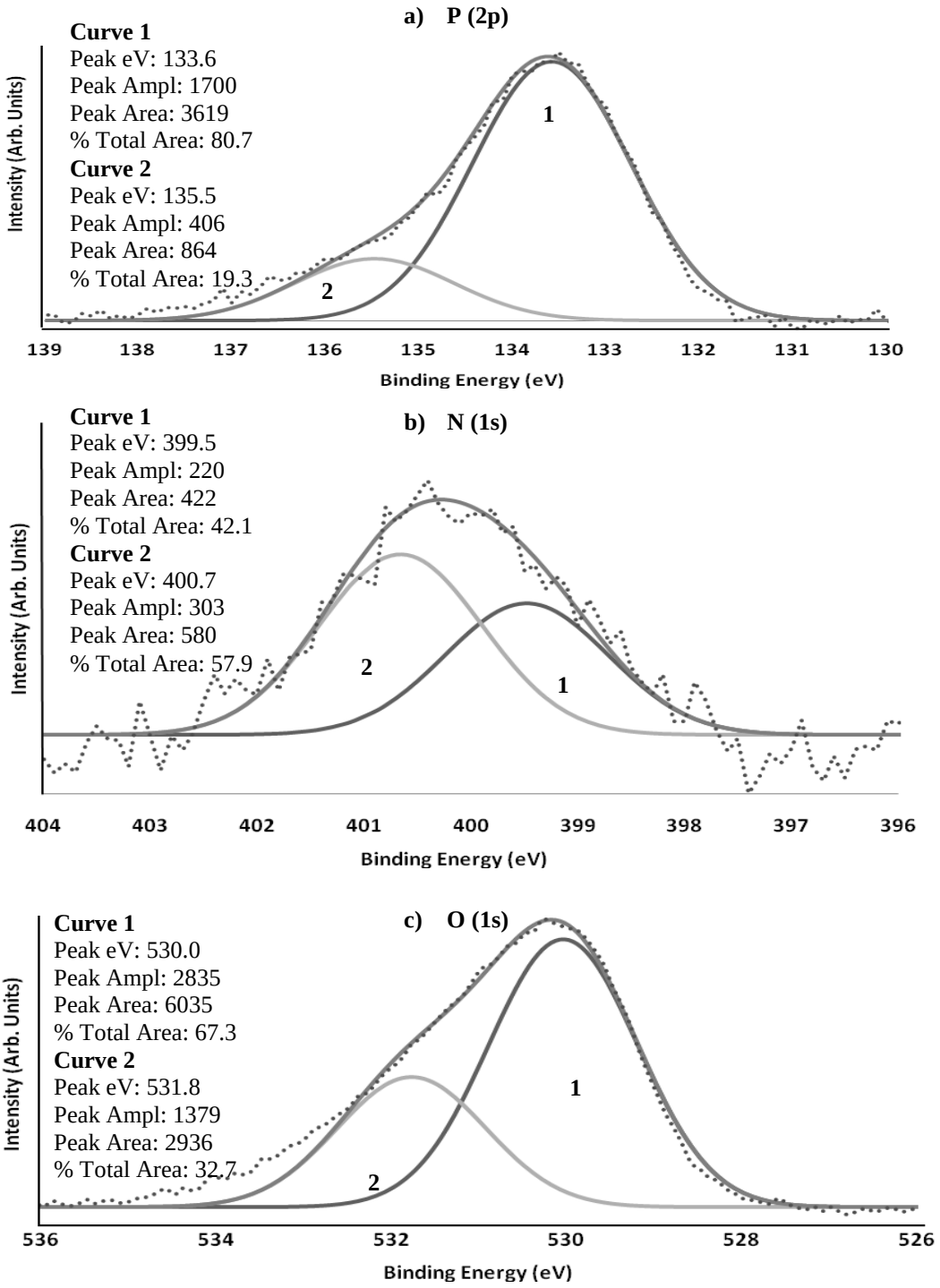

Figure 2. XPS spectra of: a) P(2p), b) N(1s) and c) O(1s) regions of AEP HP BT. Dotted line shows the raw data points that are plotted with continuous line deconvoluted and fitting summation curves.

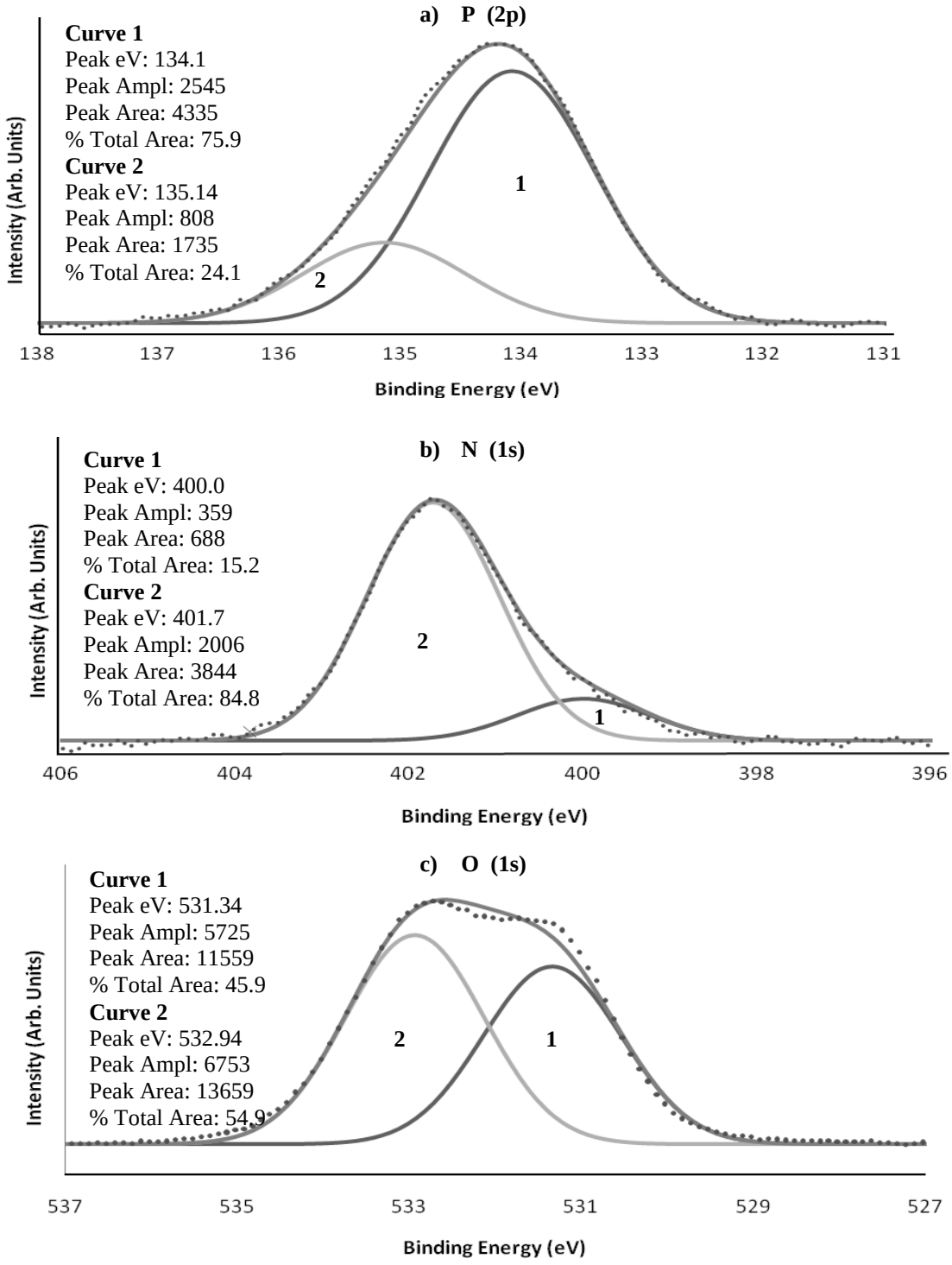

Figure 3. XPS spectra of: a) P(2p), b) N(1s) and c) O(1s) regions of pure AEP. Dotted line shows the raw data points that are plotted with continuous line deconvoluted and fitting summation curves.

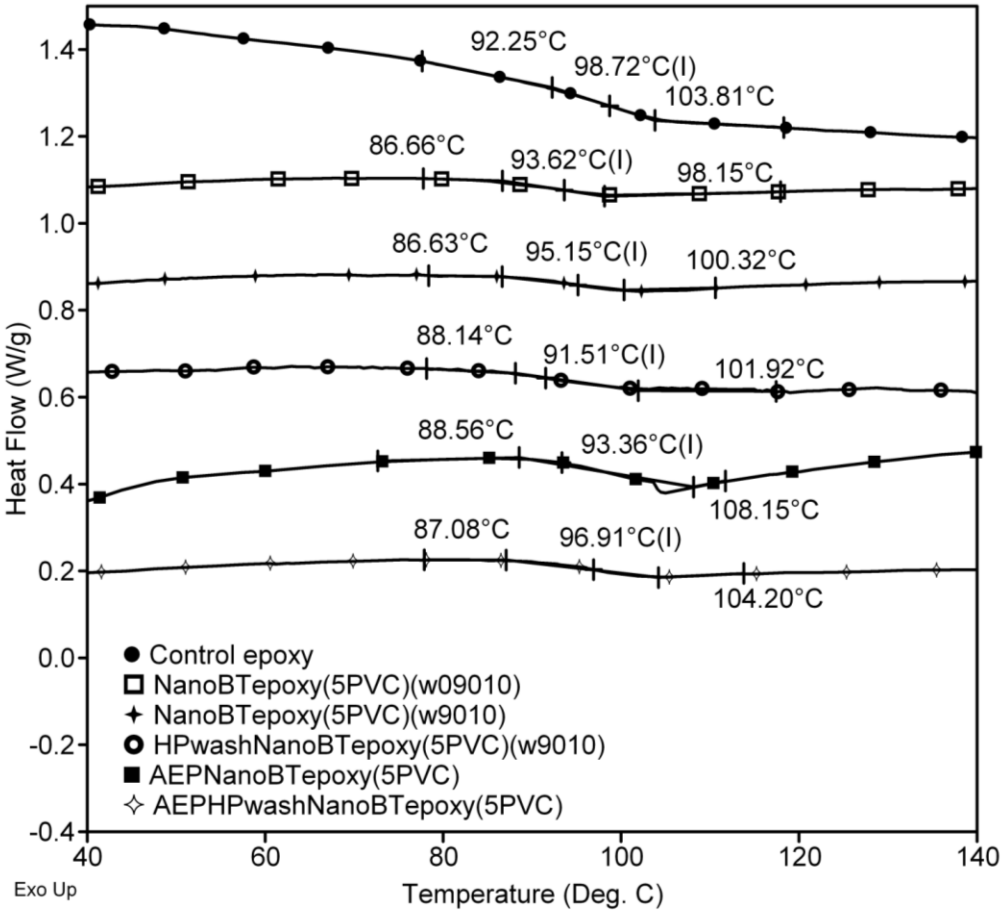

Figure 4. DSC plot of the epoxy polymer in comparison to the 5 vol.-% BT-epoxy composites. W/O9010 and W/9010 in the legend indicates BT composites synthesized in epoxy polymer without and with a dispersant, respectively.

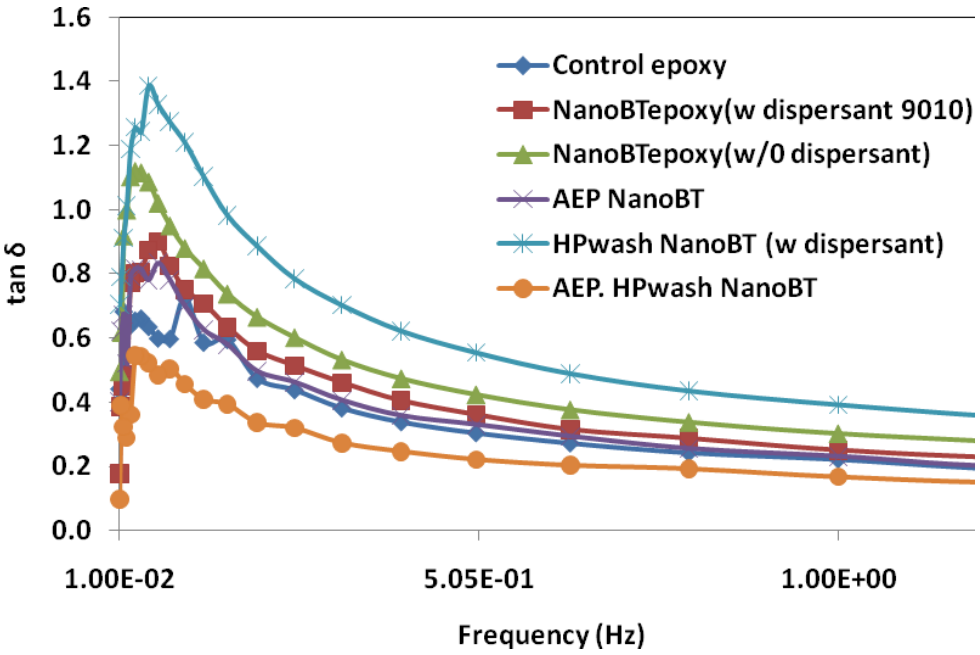

Figure 5. Frequency dependent dielectric loss response of pure polymer and 5 vol.-% BT-epoxy dielectric composites, measured at 100 °C.

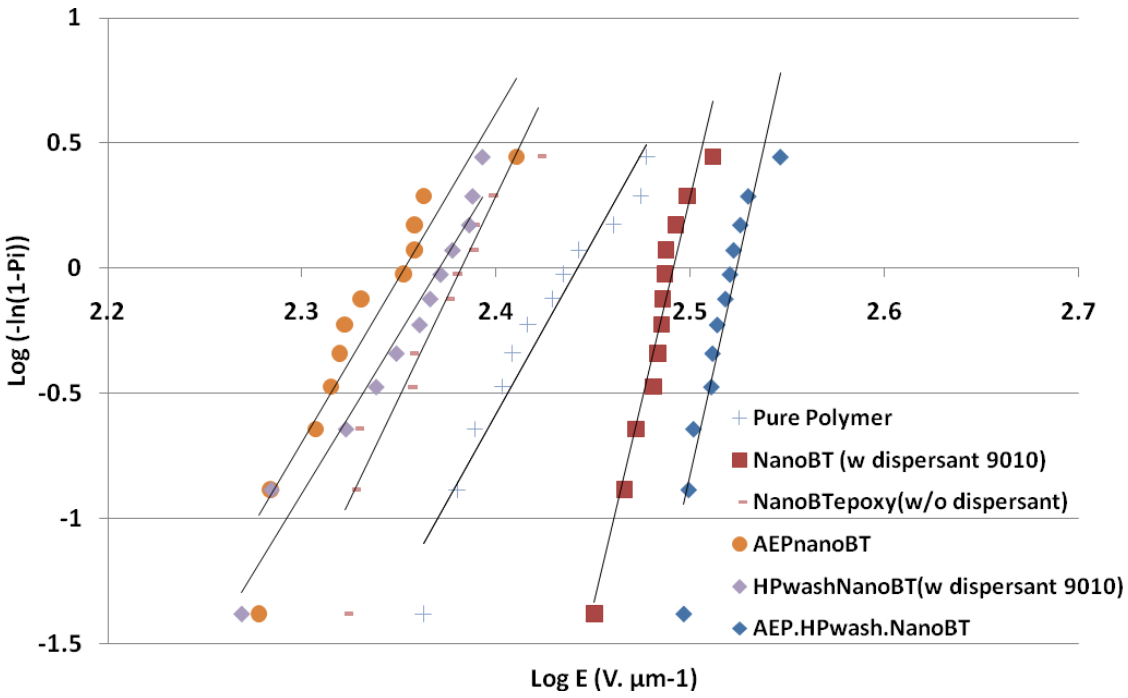

Figure 6. Weibull plot of DBS measurements for epoxy polymer 5 vol.-% BT composite dielectric films.

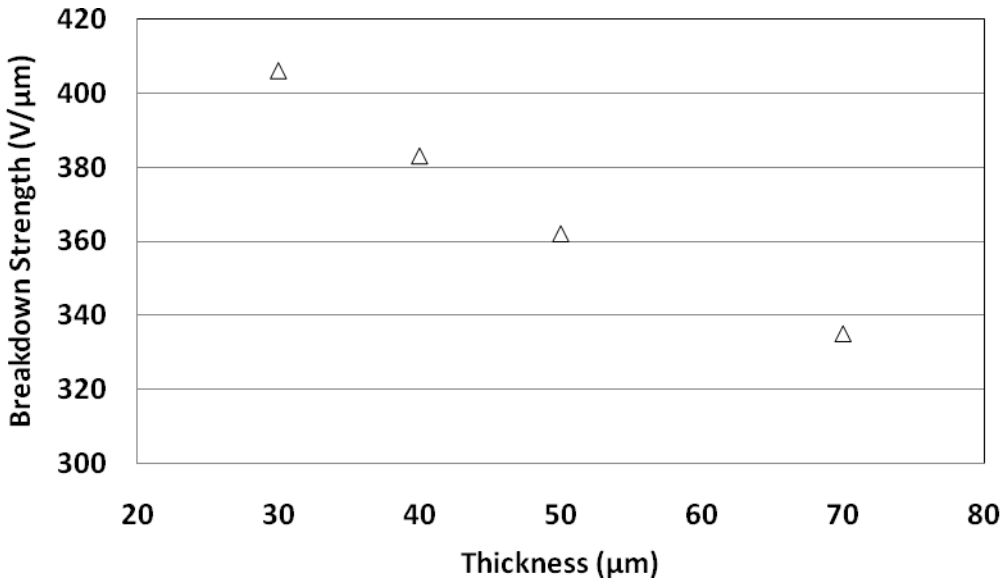

Figure 7. DBS measurements plotted as a function of film thickness measurements of AEP HP BT composite dielectric films.

Table 3.1. The characterization of atomic percent composition at the surface of modified BT powders as measured by XPS.

Sample	C (1s)	Ba (3d)	Ti (2p)	O (1s)	N (1s)	P (2p)
BT	28.48	8.5	13.18	46.35	3.5	0
HP treated BT	28.05	7.59	12.08	52.01	0	0
AEP.BT	24.57	7.49	11.98	51.81	0.55	3.59
AEP.HP treated BT	36.18	6.05	8.06	49.53	3.22	6.96

Table 3.2. DSC and Dielectric properties characterization data of 5 vol.-% BT polymer composites compared to pure polymer.

Dielectric film sample (~70 μm thickness)	T_g (°C)	ε_r at 10 kHz	Tan δ at 1 kHz	Tan δ at 10 kHz	E_b ($V \cdot \mu m^{-1}$)	U_{max} ($J \cdot cm^{-3}$)
Pure epoxy	99	3.9	<0.014	<0.022	277	1.3
BT (w/o dispersant)	94	6.1	<0.033	<0.034	240	1.6
BT (w/ dispersant)	95	6.8	<0.018	<0.026	310	2.9
HPwashBT (w/ dispersant)	92	6.9	<0.024	<0.043	235	1.7
AEP.BT	93	6.7	<0.017	<0.024	225	1.5
AEP.HPwash.BT	97	7.3	<0.014	<0.022	335	3.6
AEP.HPwash.BT (30 μm)	–	6.3	<0.017	<0.024	406	4.6

Table 3.3. Electrical characterization data of AEP HP BT polymer composites in epoxy polymer at varying filler concentration.

AEP HP BT composite (~30 μm thickness)	ε_r (at 10 kHz)	Tan δ (at 10 kHz)	E_b ($V \cdot \mu m^{-1}$)	U_{max} ($J \cdot cm^{-3}$)
5 vol.%	6.3	< 0.017	406	4.6
10 vol.%	8.0	< 0.016	356	4.5
15 vol.%	10.6	< 0.017	325	5.0
30 vol.%	22.9	< 0.023	255	6.6
30 vol.% (~20 μm)	21.8	< 0.024	279	7.5

REFERENCES

1. Chu, B.; Zhou, X.; Ren, K.; Neese, B.; Lin, M.; Wang, Q.; Bauer, F.; Zhang, Q. M. A Dielectric Polymer with High Electric Energy Density and Fast Discharge Speed. *Science* **2006**, *313*, 334-336.
2. Li, J. Y.; Zhang, L.; Ducharme, S. Electric energy density of dielectric nanocomposites. *Appl. Phys. Lett.* **2007**, *90*, 132901/1-132901/3.
3. Muralidhar, C. The Off-Valency Additive Effect and its Influence on the Curie Peak of the Barium Titanate ($BaTiO_3$)/Polyvinylidene Fluoride (PVDF) Composite. *Jpn. J. of Appl. Phys.* **1988**, *27*, 1349-1350.
4. Xiaojun, Y.; Zhimin, Y.; Changhui, M.; Jun, D. Dependence of Dielectric Properties of BT Particle Size in EP/BT Composites. *Rare Metals* **2006**, *25*, 250-254.
5. Cao, Y.; Irwin, P. C.; Younsi, K. The Future of Nanodielectrics in the Electrical Power Industry, *IEEE Trans. Dielectr. Electr. Insul.* **2004**, *11*, 797-807.
6. Ciuprina, F.; Plesa, I.; Notingher, P. V.; Tudorache, T.; Panaitescu, D. Dielectric Properties of Nanodielectrics with Inorganic Fillers. CEIDP Annual Report Conference on *Electrical Insulation and Dielectric Phenomena* **2008**, 682-685.
7. Kim, P.; Jones, S. C.; Hotchkiss, P. J.; Haddock, J. N.; Kippelen, B.; Marder, S. R.; Perry, J. W. Phosphonic acid-modified Barium Titanate Polymer Nanocomposites with High Permittivity and Dielectric Strength. *Adv. Mater.* **2007**, *19*, 1001-1005.
8. Ramesh, S.; Shutzberg, B. A.; Huang, C.; Gao, J.; Giannelis, E. P. Dielectric Nanocomposites for Integral Thin Film Capacitors: Materials Design, Fabrication and Integration Issues. *IEEE Trans. Adv. Packag.* **2003**, *26*, 17-24.

9. Bai, Y.; Cheng, Z.-Y.; Bharti, V.; Xu, H. S.; Zhang, Q. M. High-Dielectric-Constant Ceramic-Powder Polymer Composites. *Appl. Phys. Lett.* **2000**, *76*, 3804-3806.

10. Liang, S.; Chong, S. R.; Giannelis, E. P. Barium Titanate/Epoxy Composite Dielectric Materials for Integrated Thin Film Capacitors. In *Proceedings of 48th Electronic Components and Technology Conference* **1998**, 171.

11. Roy, M.; Nelson, J. K.; MacCrone, R. K.; Schadler, L. S.; Reed, C. W.; Keefe, R.; Zenger, W. Polymer Nanocomposite Dielectrics – The Role of the Interface. *IEEE Trans. Dielectr. Electr. Insul.* **2005**, *12*, 629-643.

12. Zhang, Q. M.; Li, H. F.; Poh, M.; Xia, F.; Cheng, Z. Y.; Xu, H. S.; Huang, C. An all-organic composite actuator material with a high dielectric constant. *Nature* **2002**, *419*, 284-287.

13. Li, J. Y. Exchange Coupling in P(VDF-TrFE) Copolymer Based All-Organic Composites with Giant Electrostriction. *Phys. Rev. Lett.* **2003**, *90*, 217601/1-217601/4.

14. Bune, A. V.; Fredkin, V. M.; Ducharme, S.; Blinov, L. M.; Palto, S. P.; Sorokin, A. V.; Yudin, S. G.; Zlatkin, A. Two-dimensional ferroelectric films. *Nature* **1998**, *391*, 874-877.

15. Gilbert, L. J.; Schuman, T. P.; Dogan, F. In Dielectric Powder/Polymer Composites for High Energy Density Capacitors. *Advances in Electronic and Electrochemical Ceramics*; Proceedings of the 107th Annual Meeting of the American Ceramic Society, Wiley, Baltimore, MD; Dogan, F., Kumta, P. M., Eds.; Wiley: Baltimore, MD, 2005.

16. Schuman, T. P.; Siddabattuni, S.; Cox, O.; Dogan, F. Improved Dielectric Breakdown Strength of Covalently-Bonded Interface Polymer-Particle Nanocomposites. *Composite Interfaces* **2010**, *17*, 719-731.
17. Hosokawa, M.; Nogi, K.; Naito, M.; Yokoyama, T. *Nanoparticle Technology Handbook*, Elvesier: Oxford, UK, 2007.
18. Blum, F. D.; Sinha, B. R.; Schwab, F. C. Density profile of terminally adsorbed polymers. *Macromolecules* **1990**, *23*, 3592-3598.
19. Smith, R. C.; Hui, L.; Nelson, J. K.; Schadler, L. S. Interfacial charge behavior in nanodielectrics. *IEEE Conference on Electrical Insulation and Dielectric Phenomena*, **2009**, 650-653.
20. Smith, R. C.; Liang, C.; Landry, M.; Nelson, J. K.; Schadler, L. S. The Mechanisms Leading to the Useful Electrical Properties of Polymer Nanodielectrics. *Trans. IEEE* **2008**, *DEI-15*, 187-196.
21. Chang, S. –J.; Liao, W. –S.; Ciou, C. –J.; Lee, J. –T.; Li, C. –C. An efficient approach to derive hydroxyl groups on the surface of barium titanate nanoparticles to improve its chemical modification ability. *J. Colloidal Interface Sci.* **2009**, *329*, 300-305.
22. Gao, W.; Dickinson, L.; Grozinger, C.; Morin, F. G.; Reven, L. Self-assembled monolayers of alkylphosphonic acids on metal oxides. *Langmuir* **1996**, *12*, 6429-6435.
23. Mutin, P. H.; Guerrero, G.; Vioux, A. Hybrid materials from organophosphorus coupling molecules. *J. Mater. Chem.* **2005**, *15*, 3761-3768.
24. Knobler, C. M.; Schwartz, D. K. Langmuir and self-assembled monolayers. *Curr. Opin. Colloid Interface Sci.* **1999**, *4*, 46-51.

25. Paik, U.; Hackley, V. A.; Choi. S. C.; Jung, Y. G. The effect of electrostatic repulsive forces on the stability of $BaTiO_3$ particles suspended in non-aqueous media. *Colloids and Surfaces A* **1998**, *135*, 77-88.

26. Rudolph, J.; Patzsch, Z.; Meyer, W. H. Interaction of acrylic diblock copolymers with aluminium oxide surfaces. *Colloids and Surfaces A* **1994**, *86*, 299-309.

27. Bhattacharjee, S.; Paria, M. K.; Maiti, S. H. Polyvinyl butyral as a dispersant for barium titanate in a non-aqueous suspension. *J. Mater. Sci.* **1993**, *28*, 6490-6495.

28. Chen, Y.; Guo, L. –R.; Chen, W.; Yang, X. –J.; Jin, B.; Zhang, L. –M.; Xia, X. -H. 3-mercaptopropylphophonic acid modified gold electrode for electrochemical detection of dopamine. *Bioelectrochemistry* **2009**, *75*, 26-31.

29. Tsai, M. Y.; Lin, J. C. Surface characterization and platelet adhesion studies of selfassembled monolayer with phosphonate ester and phosphonic acid functionalities. *J. Biomed. Mater. Res.* **2001**, *55*, 554-565.

30. Willey, T. M.; Vance, A. L.; Bostedt, C.; van Buuren, T.; Meulenberg, R. W.; Terminello, L. J.; Fadley, C. S. Surface structure and chemicalswitching of thioctic acid adsorbed onAu (111) as observed using near-edge X-ray absorption fine structure. *Langmuir* **2004**, *20*, 4939-4944.

31. Jespersen, M. L.; Inman, C. E.; Kearns, G. J.; Foster, E. W.; Hutchison, J. E. Alkanephosphonates on hafnium-modified gold: a new class of self-assembled organic monolayers. *J. Am. Chem. Soc.* **2007**, *129*, 2803-2807.

32. Grest, G. S.; Cohen, M. H. Liquids, glasses, and the glass transition: A free-volume approach. *Adv. Chem. Phys.* **1981**, *48*, 455-525.

33. Chen, H. M.; Lee, L. J.; Yang, J. T.; Gu, X.; Jean, J. C. Free volumes in polymer nanocomposites. *Materials Science Forum* **2009**, *607*, 177-179.

34. Barber, P.; Balasubramanian, S.; Anguchamy, Y.; Gong, S.; Wibowo, A.; Gao, H.; Ploehn, H. J.; Loye, H. C. Polymer composite and nanocomposite dielectric materials for pulse power energy storage. *Materials* **2009**, *2*, 1697-1733.

35. Ma, D.; Siegel, R. W.; Hong, J. I.; Schadler, L. S. Influence of nanoparticle surfaces on the electrical breakdown strength of nanoparticle-filled low-density polyethylene. *J. Mater. Res.* **2004**, *19*, 857-863.

36. Tuncer, E.; Sauers, I.; James, D. R.; Ellis, A. R.; Paranthaman, M. P.; Aytug, T.; Sathyamurthy, S.; More, K. L.; Li, J.; Goyal, A. Electrical properties of epoxy resin based nanocomposites, *Nanotechnology* **2007**, *18*, 25703-25708.

37. Tuncer, E.; Sauers, I.; James, D. R.; Ellis, A. R.; Duckworth, R. C. Nanodielectric System for Cryogenic Applications: Barium Titanate filled Polyvinyl Alcohol. *IEEE Trans. Dielectr. Electr. Insul.* **2008**, *15*, 236-242.

38. Nelson, J. K.; Hu, Y. Nanocomposite dielectric-properties and implications. *J. Phys. D: Appl. Phys.* **2005**, *38*, 213-222.

39. Stephen, D. An inside-out approach to storing electrostatic energy. *ACS Nano* **2009**, *3*, 2447-2450.

40. Kim, P.; Doss, N. M.; Tillotson, J. P.; Hotchkiss, P. J.; Pan, M. J.; Marder, S. R.; Li, J.; Calame, J. P.; Perry, J. W. High energy density nanocomposites based on surface modified $BaTiO_3$ and a ferroelectric polymer. *ACS Nano* **2009**, *3*, 2581-2592.

41. Huang, C.; Zhang, Q. Enhanced dielectric and electromechanical responses in high dielectric constant all-polymer percolative composites. *Adv. Funct. Mater.* **2004**, *14*, 501-506.

42. Shen, Y.; Lin, Y.; Nan, C. W. Interfacial effect on dielectric properties of polymer nanocomposites filled with core/shell-structured particles. *Adv. Funct. Mater.* **2007**, *17*, 2405-2410.

43. Blonkowski, S. Filamentary model of dielectric breakdown. *J. Appl. Phys.* **2010**, *107*, 084109.

APPENDIX

SUPPLEMENTARY INFORMATION

This document shows XPS comparison plots of as-received nanoBT and HP treated nanoBT (**Section 1**), SEM comparison images of 5 vol.-% BT nanocomposites (**Section 2**), dielectric constant versus frequency plot of dielectric nanocomposites measured at 100 °C (**Section 3**), and a table showing film thickness variation study of AEP HP NanoBT epoxy dielectric (**Section 4**).

1. High resolution XPS comparison plots of as-received nanoBT and HP treated nanoBT

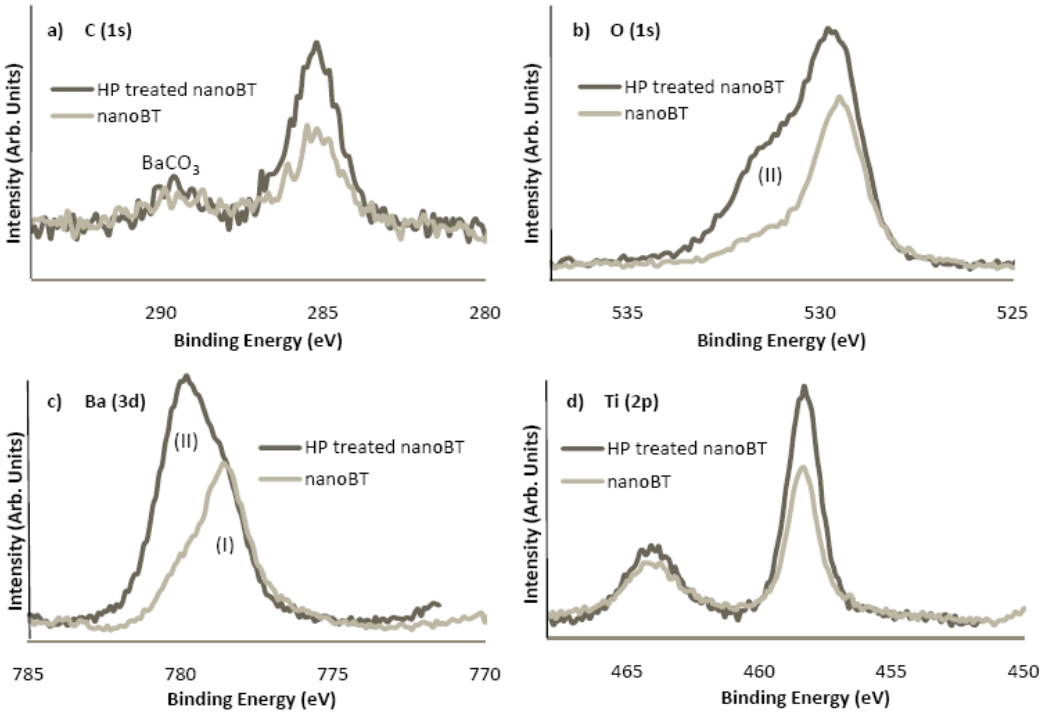

Figure 1. Comparative plots of the: a) C (1s), b) O (1s), c) Ba (3d) and d) Ti(2p) XPS spectra between hydrogen peroxide (HP) treated nanoBT and as-received nanoBT. The label 'I' was assigned to the perovskite structure while 'II' was assigned to surface oxide/hydroxide species. Assignment that shows a reduction of surface barium carbonate is labeled in the C(1s) spectrum.

Generation of hydroxyl groups by treating the surface of BT nanoparticles with aqueous hydrogen peroxide solution was evident from the XPS scan of the O(1s) region for HP treated nanoBT compared to as-received nanoBT. The main photoemission centered on 529.5 eV was assigned to oxygen in the $BaTiO_3$ lattice, which is in good agreement with the literature [1,2]. A broadened high binding energy shoulder associated with the main peak was assigned as hydroxyls or strongly chemisorbed H_2O (531.5 eV, Fig. 1b), which is in good agreement from previous studies [1] and XPS of bulk [3,4] and single crystal [5] $BaTiO_3$. The high resolution XPS spectra of the Ba(3d) region shows two components at 778.5 eV and 780 eV, which indicated the existence of barium in two different chemical environments [3]. The low energy component was assigned to the perovskite structure and the high energy emission that increased in intensity after peroxide treatment could be assigned as either $BaCO_3$ or $Ba(OH)_2$. While both $BaCO_3$ and $Ba(OH)_2$ environments possess binding energies of ~780.0 eV, we assigned the 780.0 eV emission to $Ba(OH)_2$ by corroborating the C(1s) region (C(1s) ~ 289.5 eV, see Fig. 1a) against the Ba(3d) region (Fig. 1c), which indicated a decrease in the $BaCO_3$ signal upon peroxide treatment. Thus, hydroxyl groups that were generated on the surface of nanoBT by HP treatment appear to be associated with surface barium rather than surface titanium groups since the high resolution XPS spectrum of the Ti(2p) region (Fig. 1d) appeared unchanged after HP treatment.

References:

1. Wegmann M, Watson L, Henry A. XPS analysis of submicrometer barium titanate powder. J Am Ceram Soc 2004; 87(3): 371-377.

2. Kumar S, Raju VS, Kutty TRN. Investigations on the chemical states of sintered barium titanate by X-ray photoelectron spectroscopy. Appl Surf Sci 2003; 206(1-4): 250-261.
3. Battye FL, Hochst H, Goldmann A. Photoelectron studies of the $BaTiO_3$ and $SrTiO_3$ valence states. Solid State Communications 1976; 19(3): 269-271.
4. Nakamatsu H, Adachi H, Ikeda S. Electronic structure of the valence band for perovskite-type titanium double oxides studied by XPS and DV-Xa cluster calculations. J Electron Spectrosc Relat Phenom 1981; 24(2): 149-159.
5. Pertosa P, Michel-Calendini F. X-Ray Photoelectron Spectra, Theoretical Band Structures, and Densities of States for $BaTiO_3$ and $KNbO_3$. Phys Rev B 1978; 17(4): 2011-2020.

2. SEM images of the freeze fractured cross sectional images of 5 vol.-% BT nanocomposites

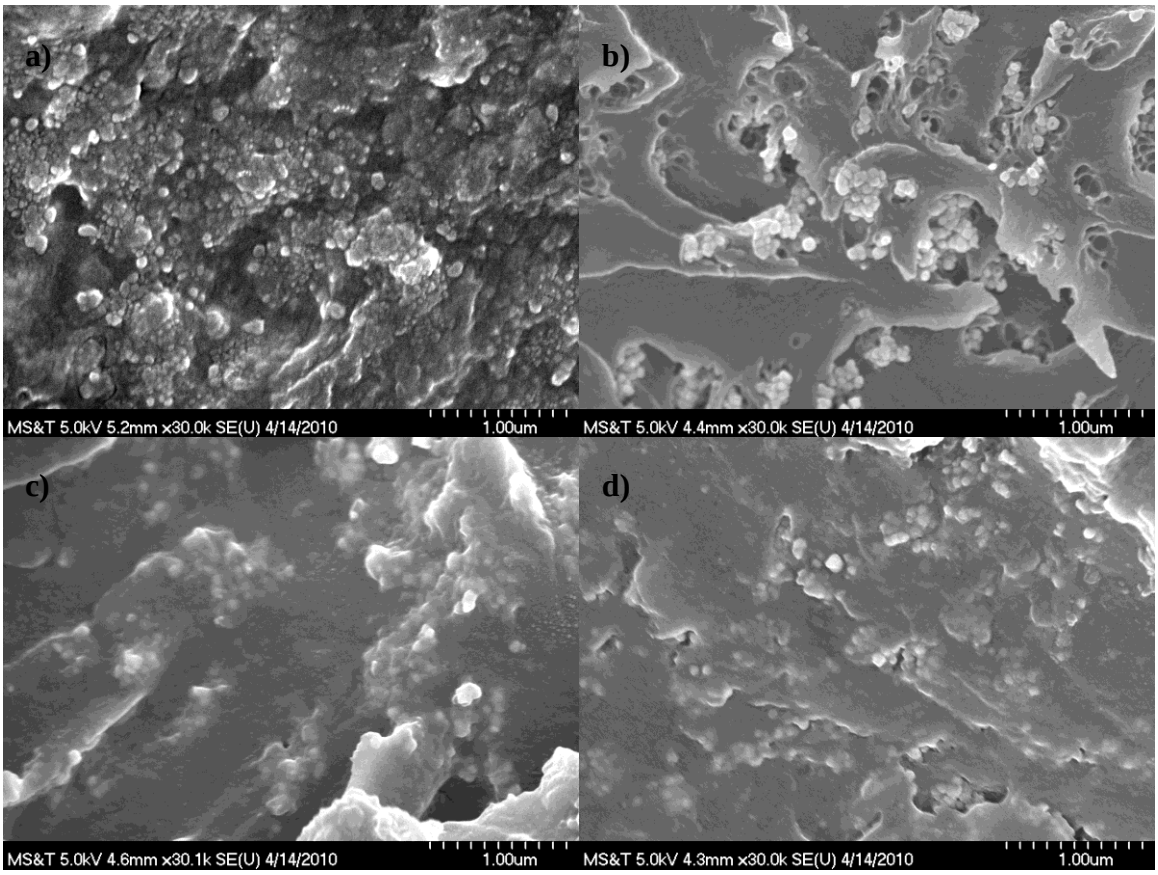

Figure 2. Freeze fractured cross sectional SEM images of 5 vol.-% nanocomposite dielectric films. a) Nano BT-epoxy(w surfactant, BYK-w-9010), (Note: adjusted brightness & contrast using ImageJ software) b) Nano BT-epoxy(wo surfactant), c) AEP modified as-received Nano BT-epoxy, d) AEP modified HP treated Nano BT-epoxy.

3. **Dielectric constant versus frequency plot of dielectric nanocomposites measured at 100 °C**

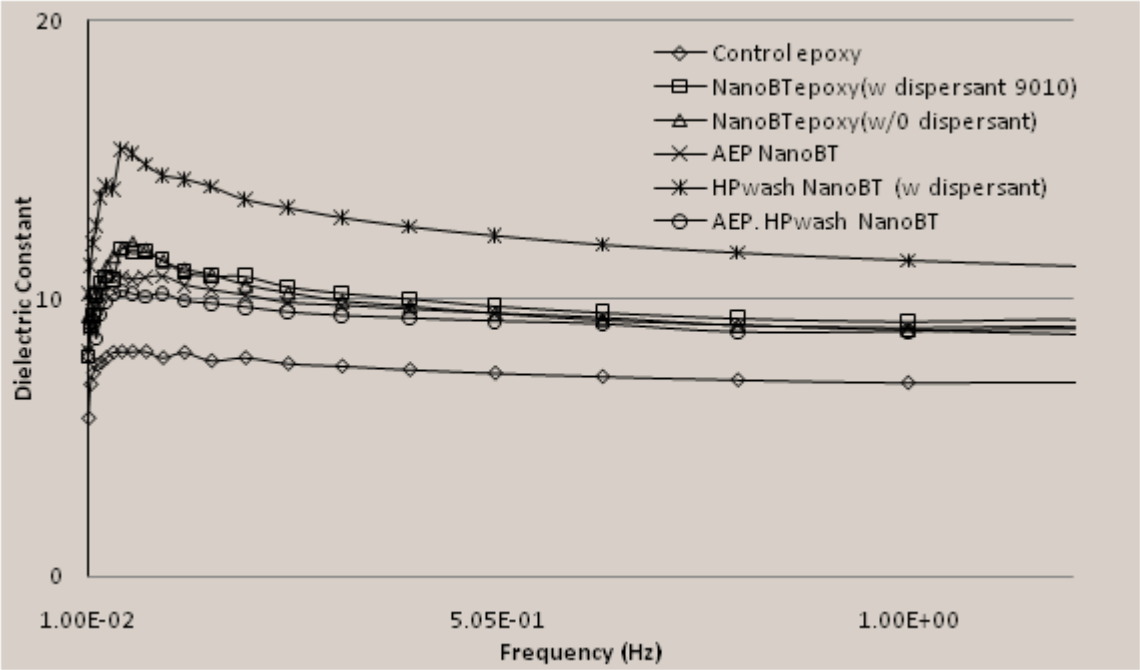

Figure 3. Frequency dependent dielectric constant of the epoxy polymer and the 5 vol.-% nanoBT-epoxy dielectric composites, measured at 100 °C.

4. **Table showing film thickness variation study of AEP HP NanoBT epoxy dielectric**

Table I. Calculated energy densities as a function of the film thickness and breakdown strength of AEP HP nanoBT epoxy dielectric composites.

Thickness (μm)	Breakdown Strength(V/μm)	Energy Density(J/cm^3)
70	335	3.63
50	362	3.95
40	383	4.10
30	406	4.60

4. INFLUENCE OF ELECTRONIC NATURE OF FILLER SURFACES ON DIELECTRIC PROPERTIES OF POLYMER-PARTICLE NANOCOMPOSITES

Sasidhar Siddabattuni,[a] *Thomas P. Schuman,*[a,*] *Fatih Dogan*[b]

[a] Missouri University of Science and Technology (formerly the University of Missouri-Rolla), Chemistry Department, 400 W. 11th Street, Rolla, MO 65409 (USA)
[b] Missouri University of Science and Technology, Materials Science and Engineering Department, 1400 N. Bishop Avenue, Rolla, MO 65409 (USA)
[*] Address all correspondence to tschuman@mst.edu

ABSTRACT Dielectric materials that are capable of efficiently storing large amounts of electrical energy are desirable for many electronic and power devices. Since the electrical energy density in a dielectric material is limited to $k\,E_b^2/2$, where k is the dielectric constant or permittivity of the material and E_b is the breakdown strength, increased permittivity and breakdown strength are required for large energy storage density. The presence of electron donating and electron accepting organophosphate coupling surface groups have the potential to influence dielectric properties, in particular the breakdown resistance, of polymer-particle nanocomposites in addition to improving the particle dispersion within the composite. Several functional organophosphates were used to modify the surface of titania nanofiller particles, which were analyzed by thermogravimetric analysis (TGA) and by X-ray photoelectron spectroscopy (XPS). The modified particles were then incorporated by dispersion into an epoxy thermosetting polymer matrix and applied as thin dielectric composite films onto copper plates. The composite films were analyzed by impedance spectroscopy and dielectric breakdown strength measurements. The data indicate that improved breakdown strengths and energy

densities resulted when electron-poor functional groups were located at the particle surfaces. At 30 vol-% particle concentration, dielectric composite films of permittivity ~14.4 at 15 micrometer thickness achieved a calculated energy density of ~8 J/cm^3. While the results were obtained using epoxy matrices, the methodology should be applicable to either thermoset, like epoxy, or thermoplastic matrices, like polyvinylidene fluoride (PVDF).

KEYWORDS: interface · organophosphate · dielectric breakdown · permittivity · energy density

INTRODUCTION

Numerous efforts have been ongoing to combine the polymers of high dielectric strength with nanoparticles of high permittivity to enhance the electric energy density of a resulting nanocomposite which are desirable for many electronic and electric systems.[1] While solid ferroelectric ceramic materials such as titania, barium titanate have large permittivity, they are limited by a relatively low breakdown resistance and poor processability of large parts due to high sintering temperature resulting in porosity defects and poor mechanical integrity. On the other hand, polymers usually have higher breakdown strengths, excellent mechanical properties and improved processability but suffer lower permittivity.[2]

$$U = k\, E_b^2/2 \qquad (1)$$

From equation (1), as electrical energy storage capacity or energy density (U) of a linear dielectric material is directly proportional to its dielectric constant (k) and directly proportional to square of the applied electric field (E_b), combination of large permittivity ceramic materials with polymers of high dielectric breakdown strength could lead to a

large energy storage capacity.[1,2] While most of the current research groups in the area of dielectric studies of polymer nanocomposites are focused on enhancement of dielectric constant, few researchers have investigated the dielectric properties and associated energy densities at high electric fields.[3]

The approach of using nano-sized ceramic particles in polymer matrix is appealing mainly for three reasons. Firstly, the small size of nanoparticles decreases the possibility of large local field enhancement.[4] Secondly, the use of nanoscale particles makes it possible to reduce the thickness of the dielectric composite film.[1,5] Thirdly, a higher surface area possessed by nanoparticles gives larger interfacial area, which can play a dominant role in determining dielectric performance compared to micrometer-sized particle composites.[4,6] However, interfaces that can conduct charge are created when dispersing high surface energy ceramic particles into a low surface energy polymer which also makes uniform dispersion of the particles problematic.

The addition of surfactants such as phosphate esters can improve dispersion and film quality that results in improved breakdown strengths compared to ceramic-particle composites without dispersants.[7] Surface complexation using phosphonate, sulfonate, silane, and carboxylate was recently tested by Schuman, et al. and other researchers.[7,8] Phosphonic acids have been reported to bond to TiO_2, ZrO_2, and In-Sn oxide surfaces and are thought to couple through heterocondensation with metal hydroxides or surface metal (crystal-defect) ions.[9-11]

Modification of the particle surfaces with organo-phosphonates has resulted in improved particle dispersion and breakdown strengths. Examples include the embedding of high dielectric constant particles into poly(vinylidene difluoride) (PVDF) that

increases the dielectric permittivity, but also reduces the breakdown strength compared to PVDF, resulted in an energy density of about 6.1 J/cm^3 at 50 vol-% at a film thickness of about 3.84 microns.[8] The energy density was greater than the current state-of-the-art biaxially oriented polypropylene high energy density capacitors (3.5-4 J/cm^3). The surface bond between the organophosphorous moiety and the metal oxide particle creates a stable, complexed organic oxide interface.[7-11] In producing a surface modified particle, only one side of the interface was controlled by coupling, leaving the remaining interface to be controlled by wetting and adsorption of the polymer chains, which is variable in structure.[12]

In the present work, we report high energy density dielectric nanocomposites resulted from the electronic nature of surface functionalized TiO_2 nanoparticles in epoxy polymer matrix. The electron donating and electron accepting functional groups were used as surface modifying reagents, attached via an organophosphate ligand on to the surface of TiO_2 filler particles. When the surface functionalized fillers were used as composites in polymer matrix, based on their electronic nature (i.e., electron donating or electron accepting), dielectric properties, in particular dielectric breakdown resistance and dielectric loss got affected.

A phosphate group is attached to a benzene ring in a typical aromatic organophosphate ligand. Delocalized π electrons that exists in the benzene ring as an electron cloud is the site of electron density. Figure 1 shows the set of organophosphate ligands that were examined as surface modifying agents or coupling agents, each aromatic or aliphatic and each bearing a terminal functional group, either electron donor (amine, NH_2) or electron scavenger (naphthalene/nitro (NO_2)) due to resonance effects except for phenyl

phosphate (PP) which does not bear any terminal functional group and was considered as reference or control organophosphate without any functional group on benzene ring. Distribution of the π electrons gets disturbed when a functional group is attached to the benzene ring. The electron cloud tends to be drawn towards the functional group when the connecting functional group is of electron-accepting/scavenging type. When the connecting functional group is of electron-donating type, electrons tend to be donated toward the cloud. Therefore, the energy conditions of the π electrons with the functional group are different from those of a benzene ring without functional group. Furthermore, an electric dipole will be induced when a functional group is attached to a benzene ring.[13]

RESULTS AND DISCUSSION

Thermogravimetric analysis (TGA) measurements (Fig. 2) of surface modified powders showed a significant weight loss for all organophosphate ligands that corresponds to a surface coverage somewhat greater (a factor of 1.2x to 1.8x) than a theoretical monolayer.[14] TGA measurements strongly supports high and robust surface coverage by organophosphate ligands onto the surface of titania nano filler particles after surface modification. The surface densities correlated with X-ray photoelectron spectroscopy (XPS) measurements (Table 4.1) indicated the introduction of phosphorus groups in approximately equal amounts of around 2 atomic percent for all surface modified samples, indicating uniform and consistent surface modification for all organophosphate ligands on the surface of nano TiO_2.

Glass transition temperature (T_g) is related to the free volume of polymer chains.[15] Polymer nanometer-sized particle composites typically show a decreased glass transition temperature, which may be related to the curvature of the particles increasing the free

volume of polymer chains. For example, pure epoxy polymer showed a glass transition temperature of about 99°C, while unmodified nanoparticle composites with surfactant show a depressed T_g, about 85°C at 5 vol % particle concentration (Table 4.2). Bare TiO_2 particles with adsorbed polymer molecules of surfactant in the composite are also observed to increase the free volume of the interfacial polymer chains as shown by a depressed T_g. Either bare particles or those dispersed with adsorbent surfactant molecules, observed to increase the free volume of the interfacial polymer chains, would also reduce electromechanical strength,[7, 16] which is evident from decrease in DBS of the unmodified TiO_2 polymer composites (Table 4.2). An increased free volume of the chains at the interface may be similar in effect as increased crystallinity, which increases the mean free path length of an accelerated electron and decreases breakdown strength despite the polymer matrix being non-crystalline.[17] Unlike adsorbed interfaces, increased T_g values of organophosphate ligand modified TiO_2 composites indicates the formation of stable, complexed organic oxide interfaces that comparatively reduce chain mobility of interfacial polymer chains.

Surface modification using organophosphates also provided improved dispersion compared to unmodified TiO_2 particles with surfactant, evident from freeze fractured cross sectional SEM images of the nanocomposites at 5 vol % (see Supporting Information in Appendix). SEM images of unmodified TiO_2 particles with surfactant exhibited cracks, pinhole defects and aggregates. In contrast, nanocomposites with organophosphate ligands yielded uniform, improved dispersion quality.

Surface modification and its relevance to dispersion quality and dielectric properties, in particular breakdown strength were studied previously,[4, 8, 16, 18] but not much

experimental work has been performed to study the electronic nature of filler surfaces required to optimize the dielectric properties in polymer-ceramic nanocomposites. In this work, we summarize the dielectric properties of the nanocomposite films at 5 vol % particle concentration in Table 4.2 that comprises the use of various organophosphate coupling agents based on their electronic nature. From dielectric breakdown strength (DBS) electron accepting organic functional group containing organophosphate coupling agents, NPP and NP, used to modify the surface of TiO_2 showed significantly higher breakdown resistance compared to pure polymer, unmodified TiO_2 composite or electron donating organic functional group coupling agent. DBS data in Table 4.2 were obtained using Weibull failure analysis method which has been frequently adopted for the investigation of dielectric breakdown of different materials systems.[19] Figure 3 shows the Weibull distributions of dielectric breakdown strengths of the composites at 5 vol.-%. The measurements were merged from multiple sample results and thus show a statistical E_o. Unmodified TiO_2 composite (though with commercial surfactant BYK-w-9010) showed breakdown resistance lower than the pure epoxy polymer, which is in agreement with previous results[7] and indicates the importance of surface modification of filler surfaces for improved dielectric properties, especially breakdown strength.

Dielectric constants obtained using surface modified TiO_2 nanocomposites were comparable to those of unmodified TiO_2 particle nanocomposites. However, dielectric loss measurements, including Maxwell-Wagner (MW) relaxation losses at lower frequencies measured at 100 °C to enhance composite conductivity signal and reduce low frequency signal noise (Figure 4), indicated electron accepting organic functional group containing organophosphate coupling agents, NPP and NP, used to modify the surface of

TiO_2 showed significantly lower dielectric losses across all frequencies compared to pure polymer, unmodified TiO_2 composite or electron donating organic functional group coupling agent.

Breakdown resistance results obtained were in agreement with previous studies[20, 21] where electrical breakdown strength of thermoplastic polymers were improved by adding additives containing halogen and aromatic chemical structures. Halobenzenes are inductive electron scavengers that overweigh the weaker electron donating resonance effect have been shown as potential electron trapping and scattering sites for the conduction electrons by X-ray induced thermally stimulated current (TSC) measurements.[20]

The surface of TiO_2 particles after modifying with organophosphate ligands containing electron scavenging functional groups, nitro or naphthyl, which have the ability to create electron trapping sites based on the chemical structure, are thought to be responsible for the observed improvement in breakdown strengths and minimal dielectric loss. Furthermore, electrostatic potential maps of benzene and several substituted benzenes suggest that electron withdrawing groups will induce the ring to be more positive,[13] making the ring an effective electron trap or scavenger.

Improved energy density values (Table 4.2) observed for composite systems of electron scavenging interfaces also support the above arguments. DBS in practical terms is limited by current promoting defects introduced during film manufacture.[22] Our study of DBS for varied thickness (see Supporting Information in Appendix) to reduce film defects demonstrates further increases in dielectric breakdown resistance and calculated energy densities for NPP modified nano TiO_2 in epoxy composites at 5 vol-% particle

centration. At a film thickness of ~15 microns, maximum energy density of ~5 $J \cdot cm^{-3}$ was observed for dielectric films.

Previous studies suggest that the volume fraction of the high dielectric constant nanoparticles has to be increased above a certain threshold (usually 30%) to effectively increase nanocomposite dielectric constant while volume fractions greater than 50 vol.-% typically decreases the effective dielectric constant of the nanocomposite due to increased porosity.[22] However, an increasing volume fraction of the nanoparticles typically decreases the apparent DBS of the nanocomposite owing to the MW conductive loss, conductivity, and a local enhancement of the electric field.[23-26] Volume concentrations greater than 50 vol.-% also reduce the composite adhesion and flexibility. At higher filler loadings, one compromises in DBS to accommodate an increase in dielectric constant to optimize resulting energy density.[27] We summarize the dielectric properties obtained in our work for highest DBS NPP modified nano TiO_2 composites in epoxy at different filler loadings in Table 4.3. At 30 volume fraction filler loading and dielectric film thickness of ~15 microns, maximum energy density of ~8 $J \cdot cm^{-3}$ with dielectric loss of ~2.1% was observed (see Supporting Information in Appendix for SEM images of different filler loaded composites).

CONCLUSIONS

In conclusion, we demonstrate that the electronic nature of surface modified nano TiO_2 filler particles influences the DBS and energy density of a dielectric particle film epoxy nanocomposite. An aromatic electron withdrawing/accepting nature filler surface is recommended to obtain significant enhancement in dielectric properties that result in high energy storage parallel plate capacitors via a remarkable increase in dielectric breakdown

resistance with minimal dielectric loss. As this surface modification methodology is straightforward and can be easily adaptable to different range of materials with suitable choice of electron accepting functional group, both thermoplastic and thermoset polymer systems can be employed to yield higher energy storage capacity polymer nanocomposites.

EXPERIMENTAL METHODS

In a typical surface modification reaction, a sample of each ligand, approximately 2 wt.-% of particle mass was mixed with TiO_2 nanoparticles (30-40 nm in diameter) in water and stirred at reflux conditions followed by extensive washing with water and centrifugation to remove any excess and/or physisorbed ligand. The treated TiO_2 nanoparticles were dried thoroughly and characterized by X-ray photoelectron spectroscopy (XPS) and thermogravimetric analysis (TGA) (see Supporting Information in Appendix C for detailed experimental procedure and characterizing data).

Composites were made by dispersing surface modified particles into the curing agent resin portion of the epoxy polymer without use of additional surfactant, except for unmodified particles. The dispersion was then combined with base epoxy resin, mixed well before applying on to the surface of freshly exposed, polished copper substrate and heated above the projected glass transition temperature (T_g) for a week to allow complete curing and solvent volatilization. The composite films were characterized by differential scanning calorimetry (DSC) for their T_g, scanning electron microscopy (SEM) of freeze fractured film cross sections for examining quality of dispersion, impedance spectroscopy (IS) for electrical properties, and dielectric breakdown strength (DBS) by stepwise-

increasing DC voltage using a Spellman SL 30 high voltage generator (see Supporting Information in Appendix C for details).

ACKNOWLEDGMENTS

This material is based upon work supported by the National Science Foundation, as part of the Pennsylvania State University-Missouri S&T I/UCRC for Dielectric Studies under Grant No. 0628817, Sub-Award No. 2164-UM-NSF-0812. The authors acknowledge the assistance of Jeffry Wight for XPS measurements and Eric Bohannan for TGA & DSC measurements obtained at the Materials Research Center at the Missouri University of Science and Technology.

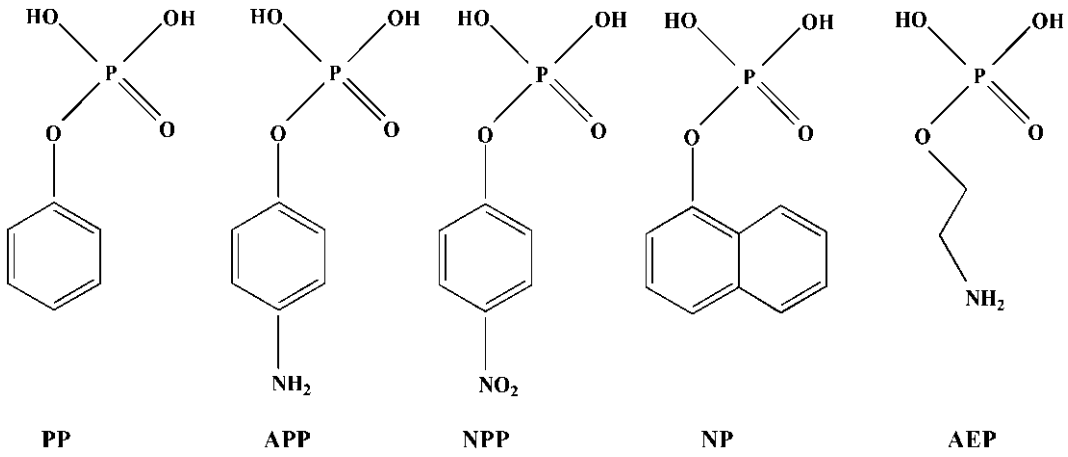

Figure 1. Molecular structures of organophosphate ligands: phenyl phosphate (PP), aminophenyl phosphate (APP), nitrophenyl phosphate (NPP), napthyl phosphate (NP) and aminoethyl phosphate (AEP) used to modify the surface of TiO_2 before dispersing in polymer. For unmodified TiO_2, BYK-w-9010 surfactant was used while dispersing in polymer.

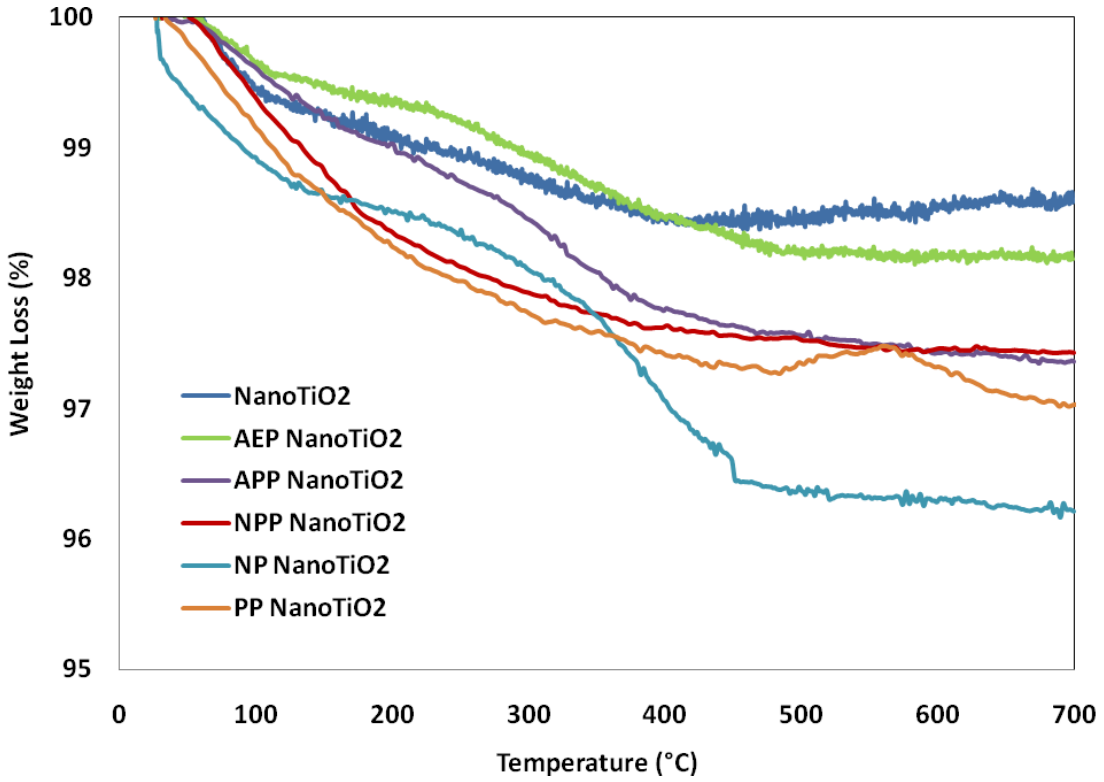

Figure 2. Thermogravimetric analyses (TGA) of surface modified and unmodified TiO_2 nanoparticles.

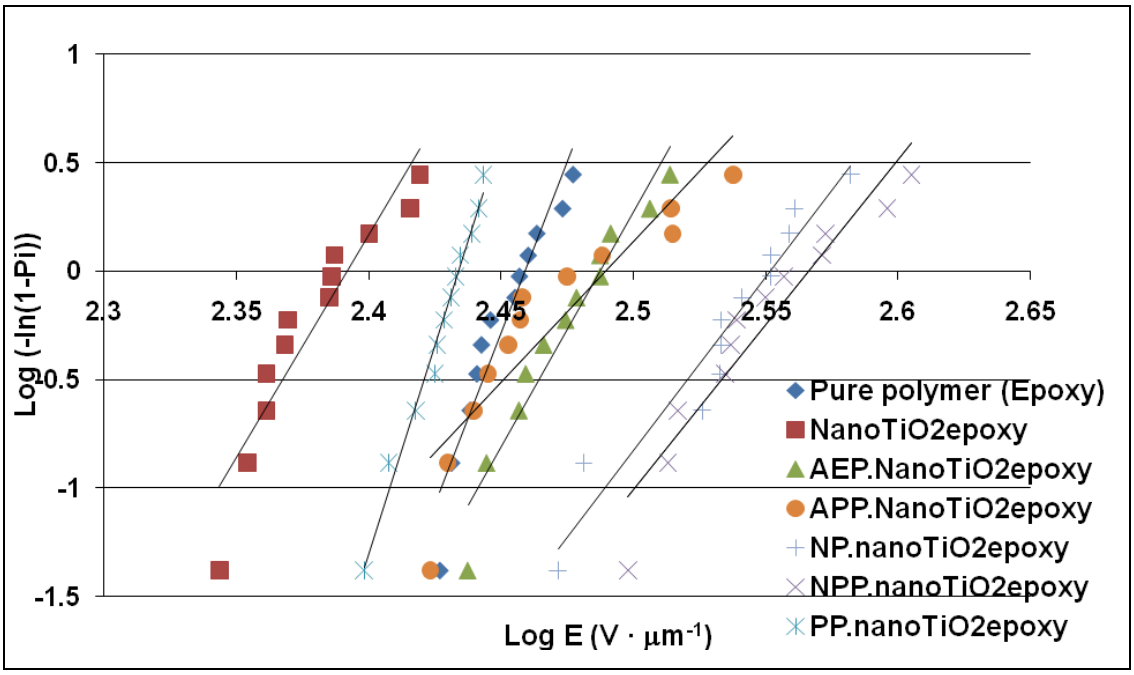

Figure 3. Weibull plot of dielectric breakdown strength measurements of 5 vol % nanoTiO_2 epoxy dielectric composite films

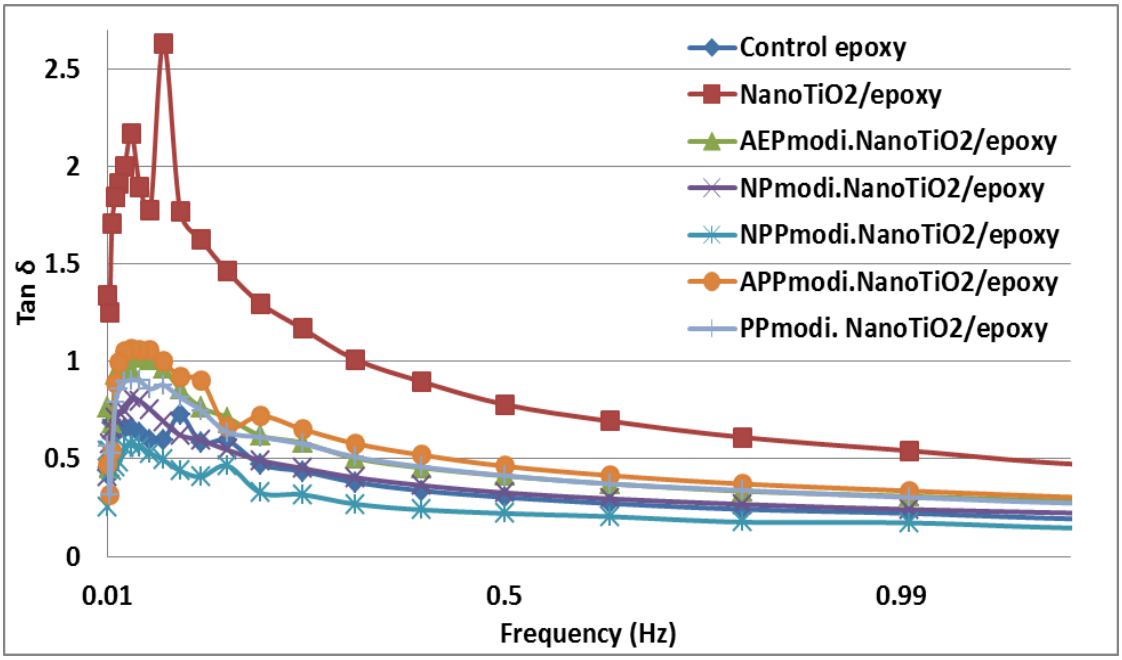

Figure 4. Frequency dependent dielectric loss response of pure polymer and 5 vol % TiO_2 epoxy dielectric composites at lower frequencies that shows MW relaxation loss, measured at 100 °C.

Table 4.1. XPS measurement data of surface modified and unmodified TiO_2 nanoparticles.

Powder	XPS (atomic percent)				
	C1s	Ti2p	O1s	N1s	P2p
TiO_2	47.99	12.32	39.69	0.0	0.0
NPP modi. TiO_2	19.73	21.45	56.22	0.71	1.90
APP modi. TiO_2	26.93	18.20	48.79	1.62	4.19
NP modi. TiO_2	24.65	22.33	51.02	0.0	1.99
PP modi. TiO_2	35.18	14.33	47.73	0.86	1.90
AEP modi. TiO_2	21.07	21.23	54.53	1.16	2.02

Table 4.2. DSC and Dielectric properties characterization data of 5 vol.-% TiO_2 polymer composites compared to pure polymer.

Dielectric Film (~60μm thickness)	Tg (°C)	Dielectric Strength ($V \cdot \mu m^{-1}$)	Dielectric Constant at 10k Hz	Dielectric loss at 10k Hz	Dielectric loss at 1k Hz	Energy Density[b] ($J \cdot cm^{-3}$)
Pure polymer (Epoxy)	99	288	3.9	< 0.022	< 0.014	1.4
NanoTiO_2epoxy[a]	85	247	5.8	< 0.024	< 0.015	1.6
AEPnanoTiO_2epoxy[a]	97	307	6.4	< 0.024	< 0.015	2.7
APPnanoTiO_2epoxy[a]	95	309	5.5	< 0.021	< 0.012	2.3
NPnanoTiO_2epoxy[a]	100.5	355	5.4	< 0.019	< 0.011	3.0
NPPmodi.nanoTiO_2epoxy[a]	100	368	5.3	< 0.020	< 0.012	3.2
PPmodi.nanoTiO_2epoxy[a]	96.5	271	5.3	< 0.018	< 0.012	1.7

[a] TiO_2 nanoparticles were 30–40 nm in diameter. [b] Energy density was calculated using average relative permittivity measured at 10 kHz and breakdown strength using Weibull distribution intercept (E_o).

Table 4.3. Dielectric properties at various volume fractions of NPP modified nanoTiO_2 epoxy composites

Dielectric Film (~15μm thickness)	Dielectric Strength ($V \cdot \mu m^{-1}$)	Dielectric Constant at 10k Hz	Dielectric loss at 10k Hz	Dielectric loss at 1k Hz	Maximum Energy Density ($J \cdot cm^{-3}$)
NPPmodi.nanoTiO_2epoxy (5 Vol.-%)	460	5.3	< 0.020	< 0.012	5.0
NPPmodi.nanoTiO_2epoxy (15 Vol.-%)	425	7.1	< 0.022	< 0.019	5.7
NPPmodi.nanoTiO_2epoxy (30 Vol.-%)	355	14.4	< 0.021	< 0.021	8.0

REFERENCES

1. Li, J. Y.; Zhang, L.; Ducharme, S. Electric energy density of dielectric nanocomposites. Appl. Phys. Lett. 2007, 90, 132901/1-132901/3.
2. Xiaojun, Y.; Zhimin, Y.; Changhui, M.; Jun, D. Dependence of Dielectric Properties of BT Particle Size in EP/BT Composites. Rare Metals 2006, 25, 250-254.
3. Li, J.; Seok, S.; Chu, B.; Dogan, F.; Zhang, Q.; Wang, Q. Nanocomposites of ferroelectric polymers with TiO2 nanoparticles exhibiting significantly enhanced electrical energy density. Adv. Mater. 2009, 21, 217-221.
4. Ma, D.; Hugener, T. A.; Siegel, R. W.; Christenson, A.; Martensson, E.; Onneby, C.; Schadler, L. S. Influence of nanoparticle surface modification on the electrical behaviour of polyethylene nanocomposites. Nanotechnology 2005, 16, 724-731.

5. Bune, A. V.; Fredkin, V. M.; Ducharme, S.; Blinov, L. M.; Palto, S. P.; Sorokin, A. V.; Yudin, S. G.; Zlatkin, A. Two-dimensional ferroelectric films. Nature 1998, 391, 874-877.
6. Lewis, T. J. Interfaces: nanometric dielectrics. J. Phys. D: Appl. Phys. 2005, 38, 202-212.
7. Schuman, T. P.; Siddabattuni, S.; Cox, O.; Dogan, F. Improved Dielectric Breakdown Strength of Covalently-Bonded Interface Polymer-Particle Nanocomposites. Composite Interfaces 2010, 17, 719-731.
8. Kim, P.; Jones, S. C.; Hotchkiss, P. J.; Haddock, J. N.; Kippelen, B.; Marder, S. R.; Perry, J. W. Phosphonic acid-modified Barium Titanate Polymer Nanocomposites with High Permittivity and Dielectric Strength. Adv. Mater. 2007, 19, 1001-1005.
9. Gao, W.; Dickinson, L.; Grozinger, C.; Morin, F. G.; Reven, L. Self-assembled monolayers of alkylphosphonic acids on metal oxides. Langmuir 1996, 12, 6429-6435.
10. Mutin, P. H.; Guerrero, G.; Vioux, A. Hybrid materials from organophosphorus coupling molecules. J. Mater. Chem. 2005, 15, 3761-3768.
11. Knobler, C. M.; Schwartz, D. K. Langmuir and self-assembled monolayers. Curr. Opin. Colloid Interface Sci. 1999, 4, 46-51.
12. Blum, F. D.; Sinha, B. R.; Schwab, F. C. Density profile of terminally adsorbed polymers. Macromolecules 1990, 23, 3592-3598.
13. McMurry, J. in Organic Chemistry, 5th Edition, Brooks/Cole, CA, USA 2000, Ch. 16.

14. Helmy, R.; Fadeev, A. Y. Self-Assembled Monolayers Supported on TiO2: Comparison of C18H37SiX3 (X = H, Cl, OCH3), C18H37Si(CH3)2Cl, and C18H37PO(OH)2. Langmuir 2002, 18, 8924-8928.
15. Grest, G. S.; Cohen, M. H. Liquids, glasses, and the glass transition: A free-volume approach. Adv. Chem. Phys. 1981, 48, 455-525.
16. Siddabattuni, S.; Schuman, T. P.; Dogan, F. Dielectric Properties of Interface Controlled Polymer Composites (submitted).
17. Tanaka, Y.; Ohnuma, N.; Katsunami, K.; Ohki, Y. Effects of crystallinity and electron mean-free-path on dielectric strength of low density polyethylene. IEEE Transactions on Electrical Insulation 1991, 26, 258-265.
18. Ma, D.; Siegel, R. W.; Hong, J. I.; Schadler, L. S. Influence of nanoparticle surfaces on the electrical breakdown strength of nanoparticle-filled low-density polyethylene. J. Mater. Res. 2004, 19, 857-863.
19. Tuncer, E.; Sauers, I.; James, D. R.; Ellis, A. R.; Paranthaman, M. P.; Aytug, T.; Sathyamurthy, S.; More, K. L.; Li, J.; Goyal, A. Electrical properties of epoxy resin based nanocomposites, Nanotechnology 2007, 18, 25703-25708
20. Ishino, I.; Hikita, M.; Suzuoki, Y.; Mizutani, T.; Ieda, M. High-field conduction and carrier traps in polyethylene copolymerized with various monomers. Electrical Engineering in Japan 1992, 112, 1-9.
21. Yamano, Y.; Endoh, H. Increase in breakdown strength of PE film by additives of azocompounds. IEEE Transactions on Dielectrics and Electrical Insulation 1998, 5, 270-275.

22. Stephen, D. An inside-out approach to storing electrostatic energy. ACS Nano 2009, 3, 2447-2450.

23. Kim, P.; Doss, N. M.; Tillotson, J. P.; Hotchkiss, P. J.; Pan, M. J.; Marder, S. R.; Li, J.; Calame, J. P.; Perry, J. W. High energy density nanocomposites based on surface modified BaTiO3 and a ferroelectric polymer. ACS Nano 2009, 3, 2581-2592.

24. Gilbert, L. J.; Schuman, T. P.; Dogan, F. In Dielectric Powder/Polymer Composites for High Energy Density Capacitors. Advances in Electronic and Electrochemical Ceramics; Proceedings of the 107th Annual Meeting of the American Ceramic Society, Wiley, Baltimore, MD; Dogan, F., Kumta, P. M., Eds.; Wiley: Baltimore, MD, 2005.

25. Huang, C.; Zhang, Q. Enhanced dielectric and electromechanical responses in high dielectric constant all-polymer percolative composites. Adv. Funct. Mater. 2004, 14, 501-506.

26. Shen, Y.; Lin, Y.; Nan, C. W. Interfacial effect on dielectric properties of polymer nanocomposites filled with core/shell-structured particles. Adv. Funct. Mater. 2007, 17, 2405-2410.

27. Blonkowski, S. Filamentary model of dielectric breakdown. J. Appl. Phys. 2010, 107, 084109.

APPENDIX
SUPPLEMENTARY INFORMATION

Experimental Procedure

The chemicals and reagents were obtained from the following sources and were used without further purification. Titanium dioxide, anatase in structure, of average particle size 32nm and surface area of 45 $m^2.g^{-1}$ was obtained from Alfa Aesar. The surfactant BYK-w-9010 (a proprietary copolymer mixture with acidic groups) was provided by Byk-Chimie. 2-aminoethyl phosphate and 1-napthyl phosphate were obtained from Sigma Aldrich. Phenyl phosphate was obtained from Acros Organics. 4-nitrophenyl phosphate was obtained from Chem Impex International. Aminophenyl phosphate was synthesized in lab as mentioned in reference[1]. Water was distilled-deionized and of 1MΩ-cm^{-1} resistance. Epoxy resin Epon 828 was obtained from Hexion. The polyamide resin used was a moderately low molecular weight, liquid, blend of the commercial Ancamide 2353 and Ancamine 2205 at a 3:1 ratio and activated with 5 vol.-% Ancamine K-54. Ancamide 2353, Ancamine 2205 and K-54 were obtained from Air Products. Mirror-polished copper sheet (Electronic grade 110 alloy, 0.8125mm thick, #8 finish) was purchased from McMaster Carr that was protected by vinyl peel ply and cut to a 5x5cm size upon receipt. The ply was removed prior to film application onto the polished copper surface.

In a typical surface modification reaction, the titanium dioxide was dispersed in water and degassed by sonication while under aspirator-reduced pressure for 15 minutes. The organophosphate was added to the titanium oxide dispersion and well-stirred at reflux for 24 hr. The dispersion was then recovered by filtration using centrifugation

followed by re-dispersion in fresh water and filtration several times before drying in vacuum oven.

Characterization of the powders, modified and unmodified, were by thermogravimetric analysis (TGA) and by X-ray photoelectron spectroscopy (XPS). Thermogravometric analysis (TGA, Netzsch STA409) was used to measure the weight of organophosphate incorporated on the surface ofparticles and then used with surface area per weight of unmodified particles to calculate the number of groups per square area. Weight loss was measured from ambient to 700°C at 10°C/min in air. X-ray photoelectron spectroscopy (XPS) (KRATOS model AXIS 165 XPS spectrometer) was utilized for determining the chemical composition of the particle surfaces. A Mg Kα anode with a photon energy of hν= 1253.6eV was operated at 225 watts. Adventitious carbon for the C 1s orbital at a binding energy of 285.2eV was used to correct for charging. The system pressure during XPS analysis was ca. 1 x 10^{-9} Torr. The Cu $2p^{3/2}$ (932.7eV) and Au $4f^{7/2}$ (84.0eV) orbitals were employed as standards from sputter-cleaned foils to calibrate the XPS binding energy (BE) range. XPS scans were performed on powder samples of 1 cm^2 mounted onto copper stubs with double-sided conductive adhesive tape and introduced into the UHV via a turbo-pumped antechamber.

Composite films were made by dispersing particles into polyamide resin in a silica jar with Teflon sealed lid via 0.635cm polished zirconia cylinders as a ball-mill process overnight (~16-18hr). The dispersion was sieved through a coarse stainless steel screen to remove ball media into a clean, pre-weighed jar. The stoichiometric amount of epoxy resin was added to the dispersion and the wet composite mixed well for 5 minutes using high speed shear mixing. The composite films were applied to copper plate whose

protective plastic film was removed just prior to composite film application. Composites were initially dried overnight in a dust-free vented cabinet, followed by baking in a forced-air conventional oven 24 hours at 80 °C, and finally baked at 100 °C for 6 days.

Composites were characterized by differential scanning calorimetry (DSC), scanning electron microscopy of the freeze fractured cross section interfaces, electrical impedance and dielectric breakdown strength. Film thicknesses were measured with a Mitutoyo 0293-340 micrometer and subtracting the measured thickness of the copper sheet. Glass transition temperatures were assessed in a Perkin Elmer DSC after an anneal stage (10°C/min, ambient to 100°C, quenched to ambient using liquid nitrogen) by scanning from ambient to 150°C versus an air-sealed pan. Glass transition temperatures reported are using the inflection point of the transition. Electron microscopy images were collected on a field emission Hitachi 4700. Samples were sectioned by freeze fracturing in liquid nitrogen, mounted using conductive tape and sputtered with gold-palladium.

Parallel-plate capacitors were fabricated by depositing circular (31.67mm^2) silver (Pelco® colloidal silver liquid, Ted Pella Inc.) top electrodes onto the nanocomposite thin films. Frequency-dependent capacitance was measured on a Solartron 1260 impedance analyzer connected with a Solartron 1296 dielectric interface (Solartron Analytical, Hampshire, England) at frequency range of 1 Hz to 1 MHz at 22°C and from 0.01 Hz to 1 MHz at 100°C with voltage amplitude of 1V and analyzed by Zview® software. Reported relative dielectric constant was calculated according to capacitance measured at 10kHz.

Dielectric breakdown strength measurements were made by applying D.C. voltage across the films using a Spellman SL 30 high voltage generator (Spellman High

Voltage Electronics Corporation, New York, USA), with a fixed ramp rate of 200V/second until the point of catastrophic device failure observed. A pin electrode was applied by spring tension to the surface of the composite, which served as the electrical ground. The Spellman electrode was connected beneath the copper substrate and the sample immersed in Fluorinert FC-40 (Acros Scientific) to displace air.

[1]. J. E. Frew, N. C. Foulds, J. M. Wilshere, N. J. Forrow, M. J. Green, *J. Electrochem. Interfacial Electrochem.* **1989**, 266, 309.

Characterization Data

Table 1. Influence of dielectric film thickness on dielectric breakdown strength and overall energy density of 5 vol % NPPmodi.NanoTiO_2 epoxy composites.

Thickness (μm)	Breakdown Strength (V/μm)	Maximum Energy Density (J/cm^3)
57	368.1	3.2
46	396.1	3.7
15	460.2	5.0

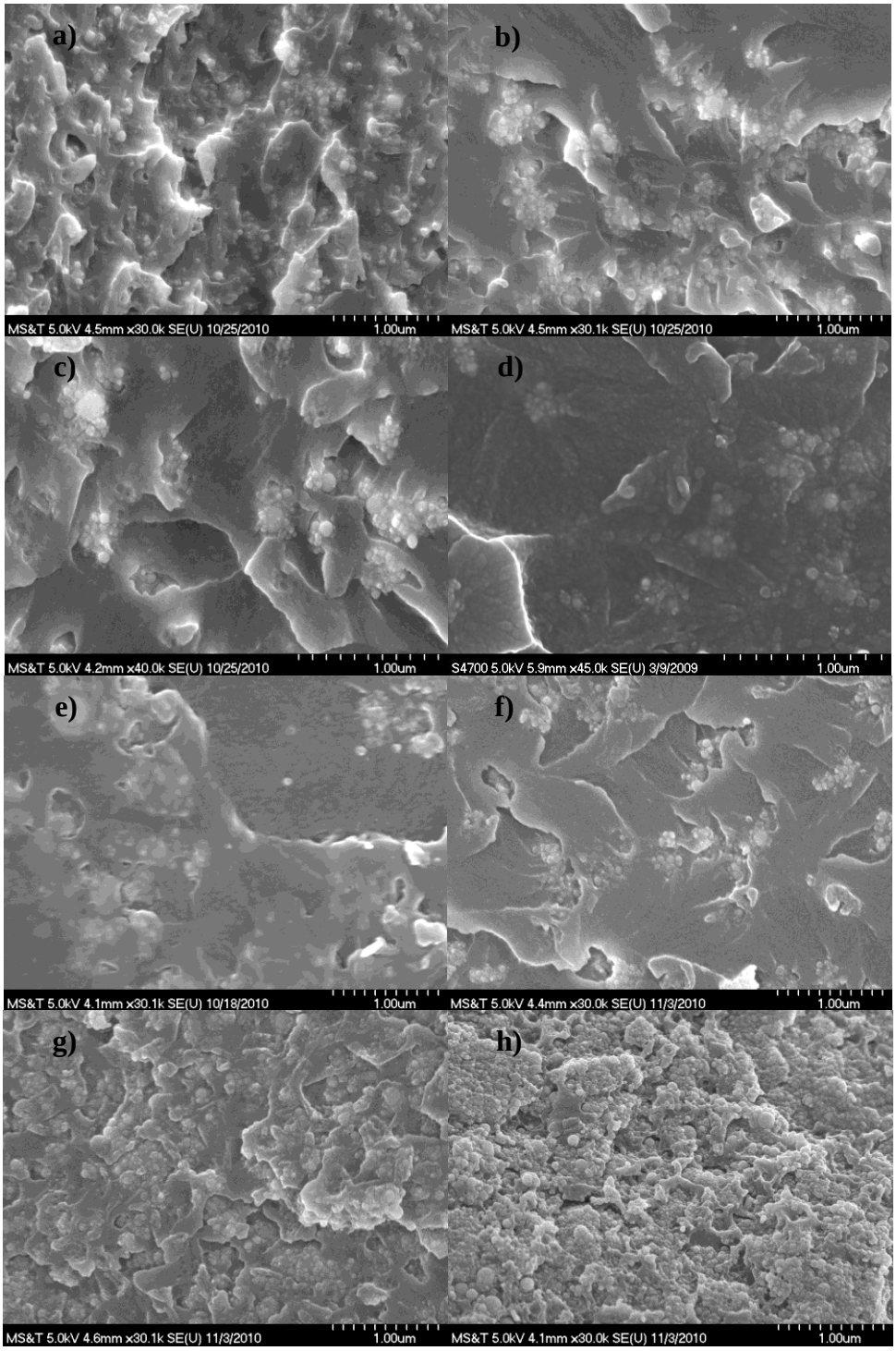

Figure 1. Freeze fractured cross section SEM images of nanocomposite dielectric films. a) NanoTiO_2epoxy(with surfactant, BYK-w-9010), b) PPmodi.NanoTiO_2epoxy, c)APPmodi.NanoTiO_2epoxy, d) AEPmodi.NanoTiO_2epoxy, e) NPmodi.NanoTiO_2epoxy, f) NPPmodi.NanoTiO_2epoxy, g) and h) are 15 vol% and 30 vol% images of NPPmodi.NanoTiO_2epoxy.

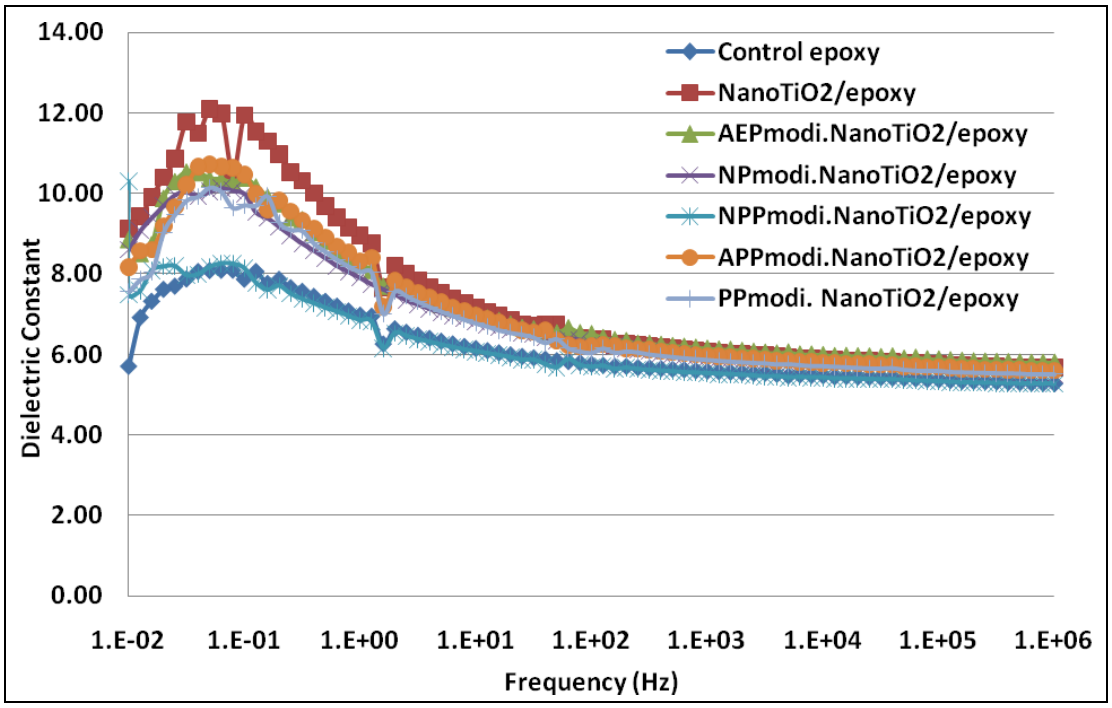

Figure 2. Frequency dependent dielectric constant of pure polymer and 5 vol % TiO_2 epoxy dielectric composites, measured at 100 °C.

5. ELECTRON DONATING NATURE OF FILLER SURFACES FOR HIGH ENERGY DENSITY POLYMER-PARTICLE NANODIELECTRICS

Sasidhar Siddabattuni,[†] Thomas P. Schuman,[,†] and Fatih Dogan[‡]*

[†]Department of Chemistry. Missouri University of Science and Technology, 400 W. 11th Street, Rolla, Missouri 65409, United States, and [‡]Department of Materials Science and Engineering, Missouri University of Science and Technology, 1400 N. Bishop, Rolla, Missouri 65409, United States.

[*]Corresponding Author. Email: tschuman@mst.edu, Tel: (001)573-341-6236

Conventional inorganic ceramic materials which are usually used as dielectric materials have large permittivity, but they are limited by their relatively small breakdown strengths, poor processability and mechanical properties due to high sintering temperature and porosity.[1,2] On the other hand, polymers, which are organic in nature usually have higher breakdown strength, excellent mechanical properties and processability but suffer from smaller permittivity.[2-4] Numerous efforts have been ongoing to combine the polymers of high dielectric strength with nanoparticles of high permittivity to enhance the electric energy storage density of a resulting nanocomposites which are desirable for many electronic and electric systems, such as pulsed-power and power capacitors.[5,6] Dielectric properties of polymer nanocomposites are found to be enhanced in comparison to conventional microcomposites and neat polymer.[7,8] Various proposed models with some experimental evidence have attributed the dielectric properties enhancement of polymer nanocomposites to the interfacial effects related to filler-polymer interactions.[7-10]

Interfaces that can conduct charge are created when dispersing high surface energy ceramic particles into a low surface energy polymer which makes uniform dispersion of particles problematic. Surfactants or surface modifying agents such as phosphate esters or

organo-phosphates are used to improve dispersion and film quality that results in improved dielectric breakdown strengths compared to composites without dispersants.[11,12] The surface bond between the organophosphorous moiety and the metal oxide particles create a stable, complexed organic oxide interface.[11] Examples include the embedding of organo-phosphonate modified high permittivity barium titanate(BT) particles in poly(vinylidene difluoride) (PVDF) resulted in an energy density of about 6.1 J/cm^3 at 50 vol-% at a film thickness of about 3.84 μm. The energy density was greater than the current state-of-the-art biaxially oriented polypropylene capacitors (3.5-4 J/cm^3).[12]

In the present work, we report high energy density dielectric nanocomposites, resulted from the electron accepting/with-drawing/scavenging nature of surface functionalized BT nanoparticles in thermosetting epoxy polymer matrix. We choose aromatic organophosphate, 4-nitrophenyl phosphate (NPP) as a surface modifying agent. Commercial BT nanoparticles were found to be less reactive and difficult to manipulate their surface chemistry by organophosphate. We therefore synthesized hydroxyl groups on the surface of BT nanoparticles using aqueous hydrogen peroxide (HP) solution[13] so as to improve the reactivity of BT nanoparticles towards a subsequent organophosphate treatment.

A typical aromatic organophosphate consists of a benzene ring attached to a phosphate group. A cloud of delocalized π (pi) electrons exists in the benzene ring, which is a site of electron density. When a functional group is present on the benzene ring, distribution of π electrons will be disturbed. When the connecting functional group is of electron accepting/scavenging type, the electron cloud tends to be drawn towards the functional

group. When the connecting functional group is of electron-donating type, electrons tend to be donated toward the cloud. Therefore, the energy conditions of the π electrons with the functional group are different from those of benzene group without functional group. Futhermore, an electric dipole will be induced when a functional group is attached to a benzene ring.[14]

Surface modified BT nanoparticles were synthesized by refluxing 10g of BT nanoparticles in 100ml 30 wt.-% HP solution for 2 hours at 110 °C prior to the addition of NPP(~ 2 wt.-% of particle mass) at 90 °C and magnetically stirred for 2 hours at reflux conditions. The dispersion was then recovered by micro-filtration followed by re-dispersion in fresh water and filtration 4 times. Surface modified filler particles were characterized by thermogravimetric analysis (TGA) and X-ray photoelectron spectroscopy (XPS) as described before.[11] The surfactant BYK-w-9010 (a proprietary copolymer mixture with acidic groups) was used for comparison purpose.

TGA measurements showed a significant weight loss (Figure 1) for NPP modified BT nanoparticles that corresponds to organophosphate ligand surface coverage somewhat greater (a factor of 1.4 times) than a theoretical monolayer.[15] TGA results provide strong evidence that high and robust surface coverage of BT particles is achieved by NPP ligand. The surface densities correlated with XPS characterization (See supporting information in Appendix) that indicated the introduction of phosphorous groups also supports the surface functionalization of NPP ligand on the surface of BT nanoparticles. High resolution XPS spectra of HP treated nano BT indicated the generation of hydroxyl groups on the surface of BT particles, which helped in reactivity of organophosphate ligand onto the surface of BT (See supporting information in Appendix).

Composites were made by dispersing surface modified particles into the curing agent resin portion of the epoxy polymer without the use of additional surfactant, except for unmodified particles using zirconia media ball milling method. The dispersion was then combined with base epoxy resin, mixed well and degassed before applying on to the surface of freshly exposed, polished copper substrate and heated above the projected glass transition temperature for a week to allow complete curing and solvent volatization. The composite films were characterized by impedance spectroscopy (IS) for electrical properties and dielectric breakdown strength (DBS) by stepwise-increasing DC voltage using a Spellman SL 30 high voltage generator as described before.[11]

Surface modification and its relevance to dielectric properties, in particular breakdown strength were studied previously,[11,12,16,17] but not much experimental work has been performed to study the electronic nature of filler surfaces required to optimize the dielectric properties in polymer-ceramic nanocomposites. Our recent work[18] of polymer nanocomposites using titania particles suggested that the presence of electron accepting nature of filler surfaces over electron donating nature of filler surfaces is required for significant improvement in dielectric properties. In the current work, we summarize the dielectric properties of the nanoBT composites in epoxy polymer at 5 vol.-% particle concentration in Table 5.1. From DBS and dielectric loss measurements, including the Maxwell-Wagner (MW) relaxation losses at lower frequencies measured at 100 °C to enhance composite conductivity signal and reduce low frequency signal noise (Figure 2), NPP modified nanoBT composites showed significantly higher breakdown resistance (Figure 3) and lower dielectric loss across all frequencies compared to pure polymer, unmodified and physically adsorbed nanoBT composites obtained by using commercial

surfactant. We attribute the enhancement in dielectric properties to the electron accepting nature of functional group of NPP modified nanoBT. Dielectric constant obtained for surface modified nanoBT composite was comparable to unmodified BT nanocomposites.

Significant improvement in dielectric breakdown resistance results for electron scavenging nature of NPP modified nanoBT composites obtained were in agreement with previous studies,[19,20] where electrical breakdown strength of thermoplastic polymers were improved by adding additives containing halogen and aromatic chemical structures. Halobenzenes are inductive electron scavengers that overweigh the weaker electron donating resonance effect have been shown as potential electron trapping and scattering sites for the conduction electrons by X-ray induced thermally stimulated current (TSC) measurements.[19] The surface of nanoBT particles after modifying with organophosphate ligand containing electron scavenging nitro functional group have the ability to create electron trapping sites based on the chemical structure, is thought to be responsible for the observed improvement in breakdown strengths. Furthermore, electrostatic potential maps of benzene and several substituted benzenes suggest that electron withdrawing groups will induce the ring to be more positive,[14] making the ring an effective electron trap or scavenger. Improvement in the energy storage density values (Table 5.1) for composite systems of electron scavenging interface also support the above arguments.

Previous studies suggests that the volume fraction of the high dielectric constant nanoparticles has to be increased above a certain threshold (usually 30%) to effectively increase nanocomposite dielectric constant while volume fractions greater than 50vol.% typically decreases the effective dielectric constant of the nanocomposite due to increased porosity.[21] However, an increasing volume fraction of the nanoparticles typically

decreases the apparent DBS of the nanocomposite owing to the MW conductive loss, conductivity, and a local enhancement of the electric field.[21-24] Volume fractions greater than 50 vol.-% also reduces the composite adhesion and flexibility. At higher filler loadings, one compromise decrease in DBS to accommodate increase in dielectric constant to optimize resulting energy density.[25] DBS in practical terms is limited by current promoting defects introduced during film manufacture,[26] and hence lower film thickness is favored. At 30 vol.-% filler loading of NPP modified nanoBT particles in epoxy at dielectric film thickness of ~20μm, maximum energy storage density of ~8.3 $J.cm^{-3}$ with dielectric loss of around 2.4% was observed (Table 5.1).

In summary, electronic nature of filler surface influences the DBS and energy storage density of a dielectric particle film polymer nanocomposite. An aromatic electron withdrawing/scavenging nature of filler surface is recommended to obtain significant enhancement in dielectric properties that result in high energy storage parallel plate capacitors via a remarkable increase in dielectric breakdown resistance with comparatively minimal dielectric loss. As this surface modification methodology is straightforward and can be easily adaptable to different range of materials with suitable choice of electron accepting functional group, both thermoplastic and thermoset polymer systems can be employed to yield higher energy storage capacity polymer nanocomposites.

ACKNOWLEDGEMENTS.

This material is based upon the work supported by the National Science Foundation, as part of the Pennsylvania State University-Missouri S&T I/UCRC for Dielectric Studies

under Grant No. 0628817, Sub-Award No. 2164-UM-NSF-0812. The authors acknowledge the assistance of Jeff Wight and Brian Porter for XPS measurements and Eric Bohannan for TGA measurements obtained at the Materials Research Center at the Missouri University of Science and Technology.

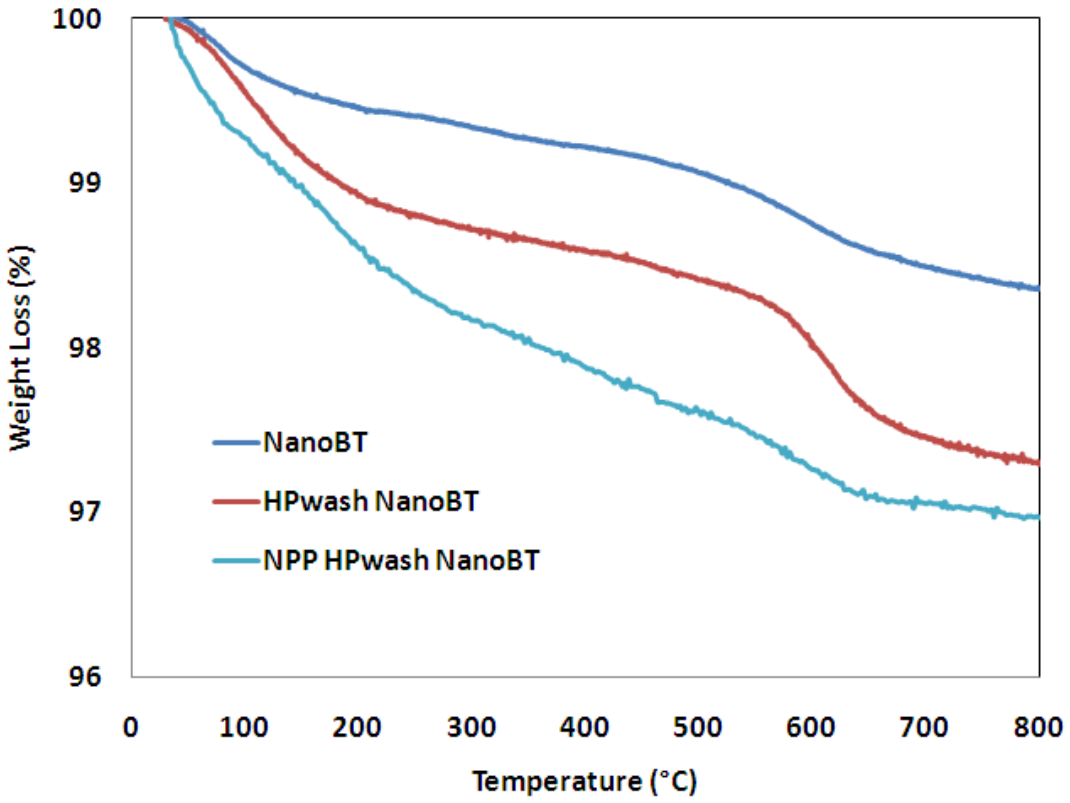

Figure 1. Thermogravimetric analysis of NPP modified and unmodified BT nanoparticles.

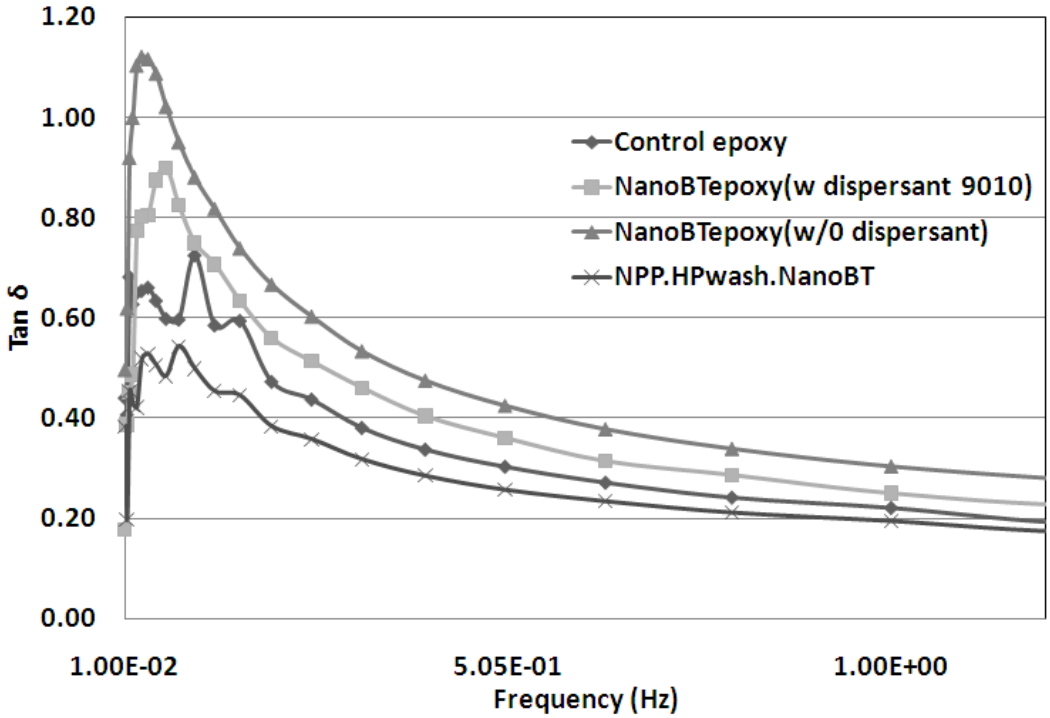

Figure 2. Frequency dependent dielectric loss of pure polymer and 5 vol.-% nanoBT – Epoxy dielectric composites, measured at 100 °C.

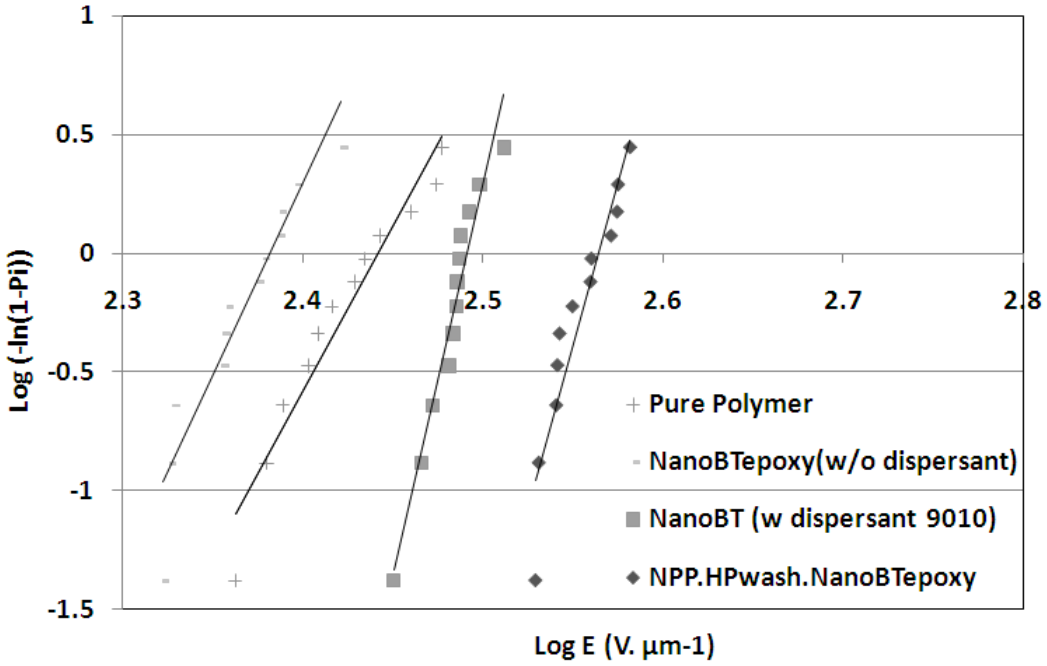

Figure 3. Weibull plot of dielectric breakdown strength measurements of 5 vol.-% nanoBT –Epoxy dielectric composites compared to pure polymer.

Table 5.1. Dielectric properties of nanoBT-epoxy composites

Particle Concentration	Dielectric film sample (~70 µm thickness)	Dielectric Permittivity ε_r [b]	Dielectric Loss Tan δ [b]	Dielectric breakdown strength [c] ($V \cdot \mu m^{-1}$)	Energy Density ($J \cdot cm^{-3}$)
5 Vol.-%	Pure epoxy	3.9	< 0.022	277	1.3
	BT (w/o dispersant) [a]	6.1	< 0.034	240	1.6
	BT (w/ dispersant) [a]	6.8	< 0.026	310	2.9
	NPP.HPwash.BT [a]	6.5	< 0.019	367	3.9
30 Vol.-%	NPP.HPwash.BT [a](20 µm)	21.3	< 0.024	296	8.3

[a] BT nanoparticles were 30-50 nm in diameter. [b] Average relative permittivity and dissipation factors measured at 10 kHz. [c] Weibull distribution intercepts (E_o) were used for breakdown strengths.

REFERENCES

1. Polotai, A. V.; Yang, G. Y.; Dickey, E. C.; Randall, C. A. *J. Am. Ceram. Soc.* **2007**, *90*, 3811.
2. Xiaojun, Y.; Zhimin, Y.; Changhui, M.; Jun, D. *Rare Metals* **2006**, *25*, 250.
3. Michalczyk, P.; Bramoulle, M. *IEEE Trans. Magn.* **2003**, *39*, 362.
4. Rabuffi, M.; Picci, G. *IEEE Trans. Plasma Sci.* **2002**, *30*, 1939.
5. Li, J. Y.; Zhang, L.; Ducharme, S. *Appl. Phys. Lett.* **2007**, *90*, 132901.
6. Li, Z.; Fredin, L. A.; Tewari, P.; Dibenedetto, S. A.; Lanagan, M. T.; Ratner, M. A.; Marks, T. J. *Chem. Mater.* **2010**, *22*, 5154.
7. Roy, M.; Nelson, J. K.; MacCrone, R. K.; Schadler, L. S.; Reed, C. W.; Keefe, R.; Zenger, W. *IEEE Transactions on Dielectrics and Electrical Insulation* **2005**, *12*, 629.
8. Smith, R. C.; Liang, C.; Landry, M.; Nelson, J. K.; Schadler, L. S. *IEEE Transactions on Dielectrics and Electrical Insulation* **2008**, *15*, 187.
9. Tanaka, T.; Kozako, M.; Fuse, N.; Ohki, Y. IEEE Transactions on Dielectrics and Electrical Insulation 2005, 12, 669.
10. Nelson, J. K. *IEEE Electrical Insulation Conference and Electrical Manufacturing Expo* **2007**, 229.
11. Schuman, T. P.; Siddabattuni, S.; Cox, O.; Dogan, F. *Composite Interfaces* **2010**, *17*, 719.
12. Kim, P.; Jones, S. C.; Hotchkiss, P. J.; Haddock, J. N.; Kippelen, B.; Marder, S. R.; Perry, J. W. *Adv. Mater.* **2007**, *19*, 1001.

13. Chang, S.-Li.; Liao, W.-S.; Ciou, C.-J.; Li, C.-C. *J. Colloidal Interface Sci*. **2009**, *329*, 300.

14. McMurry, J. *Organic Chemistry*; 5th Ed.; Ch. 16; Brooks/Cole: CA, USA, 2000.

15. Helmy, R.; Fadeev, A. Y. *Langmuir* **2002**, *18*, 8924.

16. Ma, D.; Hugener, T. A.; Siegel, R. W.; Christensen, A.; Martensson, E.; Onneby, C.; Schadler, L. S. *Nanotechnology* **2005**, *16*, 724.

17. Ma, D. Siegel, R. W.; Hong, J.-I.; Schadler, L. S.; Martenssen, E.; Onneby, C. *J. Mater. Res. Soc.* **2004**, *19*, 857.

18. Siddabattuni, S.; Schuman, T. P.; Dogan, F. *Midwest Regional Meeting of the American Chemical Society*, Abstract 93, Wichita, KS, October 27-30, 2010.

19. Ishino, I.; Hikita, M.; Suzuoki, Y.; Mizutani, T.; Ieda, M. *Electrical Engineering in Japan* **1992**, *112*, 1.

20. Yamano, Y.; Endoh, H. *IEEE Transactions on Dielectrics and Electrical Insulation* **1998**, *5*, 270.

21. Kim, P.; Doss, N. M.; Tillotson, J. P.; Hotchkiss, P. J.; Pan, M. J.; Marder, S. R.; Li, J.; Calame, J. P.; Perry, J. W. *ACS Nano* **2009**, *3*, 2581.

22. Gilbert, L. J.; Schuman, T. P.; Dogan, F. in *Ceramic Transactions (Advances in Electronic and Electrochemical Ceramics)* (Eds. Dogan, F.; Kumta, P. N.), Wiley: NY, **2006**, *179*, 17.

23. Huang, C.; Zhang, Q. *Adv. Funct. Mater.* **2004**, *14*, 501.

24. Shen, Y.; Lin, Y.; Nan, C. W. *Adv. Funct. Mater.* **2007**, *17*, 2405.

25. Blonkowski, S. *J. Appl. Phys.* **2010**, *107*, 084109.

26. Stephen, D. *ACS Nano* **2009**, *3*, 2447.

APPENDIX

SUPPLEMENTARY INFORMATION

This document shows XPS data of modified and unmodified nanoBT filler particles (**Section 1**), XPS comparison plots of as-received nanoBT versus HP treated nanoBT (**Section 2**).

1. XPS characterization data of modified and unmodified nanoBT powders.

Table I. The characterization of atomic percent composition at the surface of modified BT powders as measured by XPS.

Powder	XPS (atomic percent)					
	C (1s)	Ba (3d)	Ti (2p)	O (1s)	N (1s)	P (2p)
BT	28.48	8.5	13.18	46.35	3.5	0
HPwashBT	28.05	7.59	12.08	52.01	0	0
NPP.HPwash.BT	10.34	9.62	9.62	63.23	0.77	6.42

2. High resolution XPS comparison plots of as-received nanoBT and HP treated nanoBT

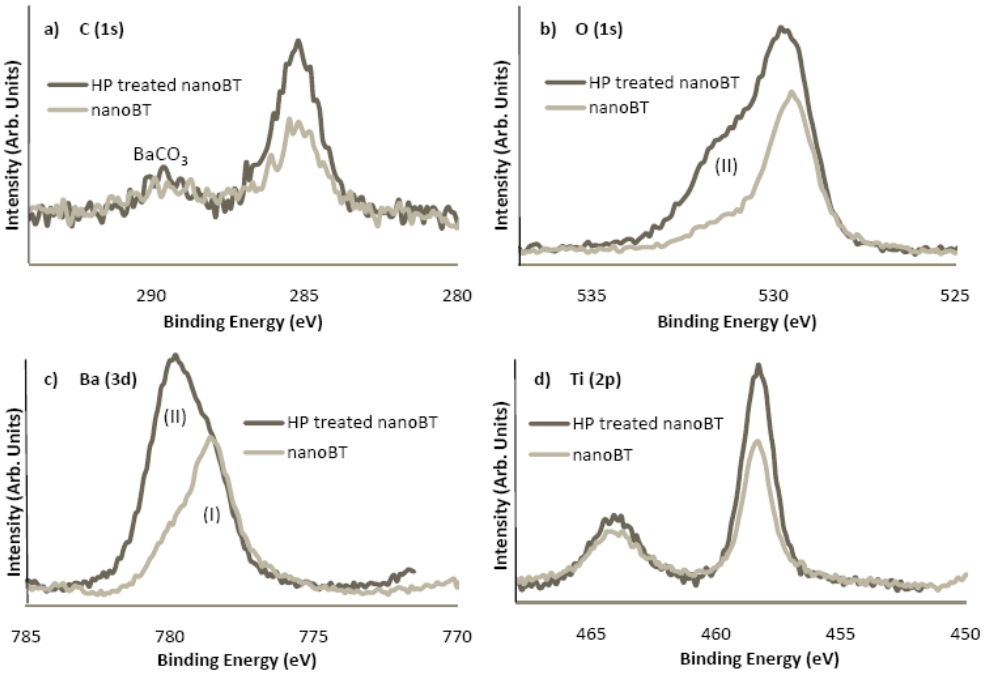

Figure 1. Comparative plots of the: a) C (1s), b) O (1s), c) Ba (3d) and d) Ti(2p) XPS spectra between hydrogen peroxide (HP) treated nanoBT and as-received nanoBT. The label 'I' was assigned to the perovskite structure while 'II' was assigned to surface oxide/hydroxide species. Assignment that shows a reduction of surface barium carbonate is labeled in the C(1s) spectrum.

Generation of hydroxyl groups by treating the surface of BT nanoparticles with aqueous hydrogen peroxide solution was evident from the XPS scan of the O(1s) region for HP treated nanoBT compared to as-received nanoBT. The main photoemission centered on 529.5 eV was assigned to oxygen in the $BaTiO_3$ lattice, which is in good agreement with the literature [1,2]. A broadened high binding energy shoulder associated with the main peak was assigned as hydroxyls or strongly chemisorbed H_2O (531.5 eV, Fig. 1b), which is in good agreement from previous studies [1] and XPS of bulk [3,4] and

single crystal [5] $BaTiO_3$. The high resolution XPS spectra of the Ba(3d) region shows two components at 778.5 eV and 780 eV, which indicated the existence of barium in two different chemical environments [3]. The low energy component was assigned to the perovskite structure and the high energy emission that increased in intensity after peroxide treatment could be assigned as either $BaCO_3$ or $Ba(OH)_2$. While both $BaCO_3$ and $Ba(OH)_2$ environments possess binding energies of ~780.0 eV, we assigned the 780.0 eV emission to $Ba(OH)_2$ by corroborating the C(1s) region (C(1s) ~ 289.5 eV, see Fig. 1a) against the Ba(3d) region (Fig. 1c), which indicated a decrease in the $BaCO_3$ signal upon peroxide treatment. Thus, hydroxyl groups that were generated on the surface of nanoBT by HP treatment appear to be associated with surface barium rather than surface titanium groups since the high resolution XPS spectrum of the Ti(2p) region (Fig. 1d) appeared unchanged after HP treatment.

References:

1. Wegmann M, Watson L, Henry A. XPS analysis of submicrometer barium titanate powder. J Am Ceram Soc 2004; 87(3): 371-377.

2. Kumar S, Raju VS, Kutty TRN. Investigations on the chemical states of sintered barium titanate by X-ray photoelectron spectroscopy. Appl Surf Sci 2003; 206(1-4): 250-261.

3. Battye FL, Hochst H, Goldmann A. Photoelectron studies of the $BaTiO_3$ and $SrTiO_3$ valence states. Solid State Communications 1976; 19(3): 269-271.

4. Nakamatsu H, Adachi H, Ikeda S. Electronic structure of the valence band for perovskite-type titanium double oxides studied by XPS and DV-Xa cluster calculations. J Electron Spectrosc Relat Phenom 1981; 24(2): 149-159.

5. Pertosa P, Michel-Calendini F. X-Ray Photoelectron Spectra, Theoretical Band Structures, and Densities of States for $BaTiO_3$ and $KNbO_3$. Phys Rev B 1978; 17(4): 2011-2020.

SECTION

2. SUMMARY

Nanocomposite dielectrics comprising of high permittivity oxide particles dispersed in high breakdown strength polymer matrix are considered as a potential high energy storage density materials for capacitor applications. As large interfacial volume is generated due to introduction of nano fillers in polymer matrix, the work carried out during the course of this research work is to study the interfacial effects on the dielectric properties, especially dielectric breakdown resistance of polymer-particle nanocomposites. A novel approach of surface modification of oxide particles was developed that exhibited remarkable enhancement in breakdown resistance compared to pure polymer and unmodified particle-polymer composites.

Various functional organophosphates were utilized to modify the surface of nano-sized titania and barium titanate oxide particles that produced robust surface modification, evidenced from thermogravimetric analysis and X-ray photoelectron spectroscopy characterization results. The surface modification using electron accepting functional aromatic organophosphate, p-nitrophenyl phosphate (NPP), which was used to engineer the surface of oxide particles, remarkably enhanced the dielectric properties in the epoxy polymer host material, especially breakdown resistance, evidenced from the results of dielectric breakdown strength measurements and impedance spectroscopy results comparatively. Although the dielectric breakdown resistance results of electron donating functional aromatic organophosphate modified particle-polymer composites, including those that resulted in covalent interface, were lesser than NPP modified

nanocomposite dielectric properties, their breakdown resistance results were better than pure polymer and physically adsorbed interface particle-polymer composites.

Improved quality of dispersion, reduction in dielectric losses including Maxwell-Wagner relaxation losses at lower frequencies, raise in matrix glass temperature was also resulted from surface modification, including that of NPP modification, compared to unmodified or physically adsorbed particle-polymer composites. Dielectric constant values of modified and unmodified particle-polymer nanocomposites were comparable. Since, the dielectric breakdown resistance is limited by current promoting defects introduced during film manufacturing, low dielectric film thickness study to reduce film defects of NPP modified nano titania and barium titanate composites in epoxy matrix yielded energy storage densities of ~ 8 J/cm^3 and ~8.3 J/cm^3 at 15µm and 20µm film thicknesses respectively using 30 vol.-% filler loadings.

Since the surface modification methodology used in the study is straightforward and can be easily adaptable to different range of materials, with suitable choice of electron accepting functional group organophosphate, both thermoplastic and thermoset polymer systems can be employed to yield higher energy storage capacity polymer nanocomposite dielectrics.

VITA

Sasidhar Veeranjaneyulu Siddabattuni was born on August 20, 1985 in Desaipet, India. Sasidhar obtained his primary and secondary education in Chirala, India and received his Bachelor of Paint Technology degree in May 2006, First Class with Distinction from University of Mumbai – Institute of Chemical Technology (formerly University Department of Chemical Technology, UDCT). From June 2006 to June 2007, he worked with Asian Paints Limited as an Officer II in Mumbai, India. He enrolled as a PhD student in the Department of Chemistry at Missouri University of Science and Technology in Fall 2007 and began his doctoral studies under the guidance of Dr. Thomas P. Schuman. The degree of Doctorate in Philosophy, in chemistry was awarded to Sasidhar V. Siddabattuni in May 2011 from Missouri University of Science and Technology.